

Wilfrid Laurier University

Scholars Commons @ Laurier

Theses and Dissertations (Comprehensive)

2010

Controls on Terrestrial Evapotranspiration from a Forest-Wetland Complex in the Western Boreal Plain, Alberta, Canada

Scott M. Brown
Wilfrid Laurier University

Follow this and additional works at: <https://scholars.wlu.ca/etd>



Part of the [Physical and Environmental Geography Commons](#)

Recommended Citation

Brown, Scott M., "Controls on Terrestrial Evapotranspiration from a Forest-Wetland Complex in the Western Boreal Plain, Alberta, Canada" (2010). *Theses and Dissertations (Comprehensive)*. 970.
<https://scholars.wlu.ca/etd/970>

This Thesis is brought to you for free and open access by Scholars Commons @ Laurier. It has been accepted for inclusion in Theses and Dissertations (Comprehensive) by an authorized administrator of Scholars Commons @ Laurier. For more information, please contact scholarscommons@wlu.ca.

NOTE TO USERS

This reproduction is the best copy available.

UMI[®]





Library and Archives
Canada

Bibliothèque et
Archives Canada

Published Heritage
Branch

Direction du
Patrimoine de l'édition

395 Wellington Street
Ottawa ON K1A 0N4
Canada

395, rue Wellington
Ottawa ON K1A 0N4
Canada

Your file *Votre référence*
ISBN: 978-0-494-64360-0
Our file *Notre référence*
ISBN: 978-0-494-64360-0

NOTICE:

The author has granted a non-exclusive license allowing Library and Archives Canada to reproduce, publish, archive, preserve, conserve, communicate to the public by telecommunication or on the Internet, loan, distribute and sell theses worldwide, for commercial or non-commercial purposes, in microform, paper, electronic and/or any other formats.

The author retains copyright ownership and moral rights in this thesis. Neither the thesis nor substantial extracts from it may be printed or otherwise reproduced without the author's permission.

AVIS:

L'auteur a accordé une licence non exclusive permettant à la Bibliothèque et Archives Canada de reproduire, publier, archiver, sauvegarder, conserver, transmettre au public par télécommunication ou par l'Internet, prêter, distribuer et vendre des thèses partout dans le monde, à des fins commerciales ou autres, sur support microforme, papier, électronique et/ou autres formats.

L'auteur conserve la propriété du droit d'auteur et des droits moraux qui protègent cette thèse. Ni la thèse ni des extraits substantiels de celle-ci ne doivent être imprimés ou autrement reproduits sans son autorisation.

In compliance with the Canadian Privacy Act some supporting forms may have been removed from this thesis.

Conformément à la loi canadienne sur la protection de la vie privée, quelques formulaires secondaires ont été enlevés de cette thèse.

While these forms may be included in the document page count, their removal does not represent any loss of content from the thesis.

Bien que ces formulaires aient inclus dans la pagination, il n'y aura aucun contenu manquant.


Canada

**Controls on Terrestrial Evapotranspiration from a
Forest - Wetland Complex in the Western Boreal Plain,
Alberta, Canada.**

By

Scott M. Brown
Honours B.A., Wilfrid Laurier University, 2005

THESIS

Submitted to the Department of Geography and Environmental Studies
in partial fulfillment of the requirements for
Degree in Masters of Science

Wilfrid Laurier University, 2010

© Scott Brown
2010

ABSTRACT

The Western Boreal Plain (WBP) of North Central Alberta consists of a mosaic of wetlands and aspen (*Populus tremuloides*) dominated uplands. This region operates within a moisture deficit regime where precipitation (P) and evapotranspiration (ET) are the dominant hydrologic fluxes. As such these systems are extremely susceptible to the slightest climatic variability that may upset the balance between P and ET. Vegetation composition is the dominant control on wetland ET, and itself is extremely dynamic within these wetland environments, which can be attributed to varying moisture regimes along with micrometeorological variations. To address this variability in moisture regimes ET was examined in a typical moraine wetland of the WBP during the 2005 and 2006 snow-free seasons. Closed dynamic chamber measurements were used to gather data on plant community scale actual evapotranspiration (ET) for an undisturbed natural bog with varying degrees of canopy cover surrounding a shallow groundwater fed pond. For the purposes of scaling plant community ET contributions to that of the wetland, potential ET (PET_{EQ}) was measured using a Priestley-Taylor energy balance approach at three separate wetland sites with varying aspects surrounding the central pond, along with actual ET using a roving eddy covariance (EC) tower. Growing season peak ET rates ranged from 0.2 mm hr^{-1} to 0.6 mm hr^{-1} depending on location, vegetation composition and time period. *Sphagnum* contributions were the greatest early in the growing season reaching peaks of 0.6 mm hr^{-1} , while lichen sites exhibited the greatest late season rates at 0.4 mm hr^{-1} . Thus, *Sphagnum* and other non-vascular wetland plant species control ET differently throughout the growing season and as such should be considered an integral part of the moisture and water balances within wetland environments at the sub-landcover unit scale.

Upland ET was characterized over three scales during the 2005 and 2006 snow-free seasons. Above canopy (ET_C) and within canopy (ET_B) were examined using the EC technique situated at 25.5 m (7.5 m above crown) and 4.0 m above the ground surface respectively. Soil evaporation (E_S) was examined using a closed dynamic chamber system to gather data on surface evaporation for upland soils. ET_C and ET_B were controlled primarily through atmospheric demand (VPD) while E_S was controlled by soil moisture (θ). During the green periods ET_C averaged 3.08 mm d^{-1} and 3.45 mm d^{-1} in 2005 and 2006 respectively while ET_B averaged 1.56 mm d^{-1} and 1.95 mm d^{-1} . E_S was consistent across both snow-free seasons and averaged 0.28 mm hr^{-1} in 2005 and 0.31 mm hr^{-1} in 2006. The nature of *Populus tremuloides* canopies permits ample energy availability within the canopy during the early season early green periods which promotes the development of a lush understory consisting of *Rosa acicularis* and *Viburnum edule*. ET_B fluxes were equal to or greater than the ET_C fluxes once understory development had occurred. Upon crown growth ET_B fluxes were reduced as a reduction in available energy existed. ET_B fluxes ranged from 42 to 56% of ET_C fluxes over the remainder of the snow-free seasons. Vapour pressure deficit (VPD) and soil moisture (θ) displayed strong controls on both ET_C and ET_B fluxes. ET_C fluxes responded to precipitation events as the developed crown intercepted and held available water which contributed to peak ET_C fluxes following precipitation events $>10 \text{ mm}$. This indicates the importance of interception in aspen dominated forest canopies of the WBF.

ACKNOWLEDGEMENTS

There are numerous individuals and groups that provided great assistance that lead to the completion of this thesis. First, I must thank my supervisor, Dr. Richard Petrone for not only providing me with the opportunity to conduct research in an outstanding and critical region of Canada but also having the confidence in me to shape the research project the way I found most appropriate. Additional thanks must go to Dr. Kevin Devito, who pushed me to better myself as a researcher and really ask the critical questions when they needed to be asked. In addition, I would like to thank Dr. Carl Mendoza for his comments on chapter two and Dr. Laura Chasmer for her assistance and comments on chapter three.

I am also grateful for the HEAD 2 NSERC – CRD Program (Devito, and others), NSERC – Discovery Program (Petrone), NSERC – RTI Program (Petrone), CFI (Schindler and Devito), Northern Scientific Training Program, Ducks Unlimited Canada, and Sustainable Forest Management Network for providing financial assistance that made this research possible.

For laboratory and field assistance I would like to thank Steve Kaufman, J.R. Van Haarlem, Todd Redding, Danielle Solondz, Jason Leach, Scott Ketcheson, Megan Mclean, and anyone else who assisted in the smallest of jobs along the way. Friends outside of the research community including Peter Hertz and Amy Mallett who provided a floor (with air mattress) in Chateau Brun while in Edmonton. Chesher, Robbie and Scandy all provided their utmost support over this long process from start to finish.

The support of my parents and brother has been undeniable. Their constant questions about what it is I actually do, along with their unyielding encouragement cannot go unmentioned. This thesis is done, the research continues but the constant questions of when this thesis will be finished have finally come to its conclusion.

Finally, this research and even more so, the completion of the written thesis would not have occurred if it wasn't for the ongoing and critical support of my best friend and wife, Karen. There have been an abundance of obstacles throughout this process, all of which could not have been tackled without your constant encouragement and your desire to see me finish what has taken a significant portion of our life together to complete. Without your support, I wouldn't be where I am today, and for that I thank you from the bottom of my heart.

Table of Contents

Abstract	i
Acknowledgments	ii
Table of Contents	iii
List of Figures	vi
List of Tables	xi
<i>Chapter 1 Introduction</i>	1
1.1 Western Boreal Forest	1
1.2 Evapotranspiration in the Western Boreal Forest	3
1.3 Thesis Objective and Format	8
1.4 Utikuma Region Study Area	9
<i>Chapter 2 Surface vegetation controls on evapotranspiration from a sub-humid Western Boreal Plain wetland</i>	13
2.0 Introduction	13
2.1 Study Objectives	15
2.2 Study Area	16
2.2.1 Utikuma Region Study Area	16
2.2.2 Study Catchment	17
2.3 Methods	21
2.3.1 Wetland Energy Balance	21
2.3.2 Potential Evapotranspiration	22
2.3.3 Eddy Covariance Theory	23
2.3.4 Eddy Covariance Measurements of ET	25
2.3.5 Community-Scale Measurements of Evapotranspiration.....	27
2.3.6 Chamber Flux Calculations	29
2.4 Results	30
2.4.1 Climate	30
2.4.2 Wetland Energy and Mass Exchange Processes	32

2.4.2.1 Energy Flux Densities	32
2.4.2.2 Atmosphere-Surface Interactions	35
2.4.3 Vegetation Controls on ET	38
2.4.4 Microtopographical Controls on Wetland ET	43
2.4.5 Regulation of Wetland ET by Persistent Seasonal Ground Frost.....	46
2.5 Discussion	49
2.5.1 Vegetation Controls on Wetland Evapotranspiration.....	49
2.5.2 Vegetation and Ground Thermal Influences on Wetland Evapotranspiration ..	52
2.6 Conclusions	53

Chapter 3 Evapotranspiration from above and within a Western Boreal Plain aspen

<i>forest</i>	55
3.0 Introduction	55
3.1 Study Objectives	58
3.2 Study Site	59
3.2.1 Utikuma Region Study Area	59
3.2.2 Study Catchment	61
3.3 Methods	62
3.3.1 Above and Below Canopy Eddy Covariance Measurements.....	62
3.3.2 EC Data Filtering and Gap Filling.....	64
3.3.3 Chamber Measurements of Surface Evaporation	67
3.3.4 Chamber Flux Calculations	68
3.3.5 LAI Measurements	69
3.4 Results and Discussion	70
3.4.1 Climate and Environmental Conditions	70
3.4.2 Flux Footprint Analysis.....	73
3.4.3 Temporal Dynamics of the Energy Balance.....	77
3.4.4 Overstory and Understory Flux Partitioning	82
3.4.5 Seasonal and Diurnal Partitioning of Evapotranspiration	84
3.4.6 Soil Moisture (θ), Soil Suction (ψ) and Evapotranspiration	89

3.4.7 Atmospheric Controls on Evapotranspiration	94
3.4.8 Interaction Between Atmospheric Demand and θ	97
3.5 Conclusions	103
<i>Chapter 4 Summary and Management Implications</i>	105
4.1 Spatial and temporal variability in evapotranspiration within a forested wetland complex	105
4.1.1 Wetland Evapotranspiration	105
4.1.2 Aspen Upland Evapotranspiration.....	106
4.2 Implications for Watershed Management	107
4.2.1 Forest Harvesting Impacts on Evapotranspiration	108
4.2.2 Impacts of Oil and Gas Development on Evapotranspiration	109
4.3 Conclusion.....	110
<i>Chapter 5 References.....</i>	112
<i>Chapter 6 Appendices</i>	123
6.1 Water Vapour Absorption by IRGA.....	123
6.2 Eddy Covariance Pre-Analysis	124

List of Figures

Figure 1.1: Schematic diagram of the Utikuma Region Study Area (URSA) regional surficial geology and location of “Pond 40” research study site within the Western Boreal Plain region of North Central Alberta, Canada.....	10
Figure 1.2: Schematic diagram of the Utikuma Region Study Area (URSA) (Pond 40) study site and location within the Western Boreal Plain region of North Central Alberta, Canada. The distribution of the landcover units comprising the study catchment are illustrated.....	12
Figure 2.1: Schematic diagram of the Utikuma Region Study Area (URSA) (Pond 40) study site and location within the Western Boreal Plain region of North Central Alberta, Canada. The distribution of the landcover units comprising the study catchment and the location of measurement sites are illustrated.....	19
Figure 2.2: Daily precipitation (bars) and daily averaged air temperature (lines) over the (a) 2005 and (b) 2006 snow-free seasons, Pond 40, Utikuma Region Study Area (URSA), Alberta, Canada.....	31
Figure 2.3: Seasonal daily averaged wetland energy flux densities for the 2005 and 2006 snow-free seasons, Pond 40, Utikuma Region Study Area (URSA), Alberta, Canada.....	33
Figure 2.4: Period averages composed of Early Green, Green and Late Green for a) Vapour Pressure Deficit (VPD), b) Available Energy (Q^*-Q_G), c) Peatland Evapotranspiration (ET) calculated using the combined methods of eddy covariance and Priestley-Taylor model, and d) Soil Moisture (θ) ($m^3 m^{-3}$) over the 2005 and 2006 snow-free seasons, Pond 40, Utikuma Region Study Area (URSA), Alberta, Canada. Bars denote standard error (SE) of variables.	37
Figure 2.5: Daily chamber evapotranspiration (ET) as a function of a) Vapour Pressure Deficit (VPD) and b) Soil Moisture (θ) ($m^3 m^{-3}$) for each dominant wetland vegetation community for the 2005 and 2006 snow-free seasons, Pond 40, Utikuma Region Study Area (URSA), Alberta, Canada.	39

Figure 2.6: Period averaged data of a) Chamber Evapotranspiration (ET), b) Soil Moisture (θ) ($\text{m}^3 \text{m}^{-3}$) and c) Ground Temperatures (at 5 cm below ground) grouped by vegetation composition for both the 2005 and 2006 snow-free seasons, Pond 40, Utikuma Region Study Area (URSA), Alberta, Canada. Bars denote standard error (SE) of measurement variables.....42

Figure 2.7: Period averaged a) Chamber Evapotranspiration (ET), b) Soil Moisture (θ) ($\text{m}^3 \text{m}^{-3}$), and c) Ground Temperatures (at 5 cm below ground) (T_g) for microtopography (lawns and depressions) over 2005 and 2006 snow-free seasons, Pond 40, Utikuma Region Study Area (URSA), Alberta, Canada. Bars denote standard error (SE) of measurement variables.....45

Figure 2.8: Daily averaged a) Cummulative Wetland Evapotranspiration (ET), b) Depth of Frost Table (cm below ground surface), c) Depth of Water Table (WT) (cm below ground surface) and d) Soil Moisture (θ) ($\text{m}^3 \text{m}^{-3}$) of the upper 20 cm of peat soil for both the 2005 and 2006 snow-free seasons, Pond 40, Utikuma Region Study Area (URSA), Alberta, Canada.....48

Figure 3.1: Schematic diagram of the research catchment, location of the instrumentation and dominant vegetation landcover units comprising the catchment, Pond 40, Utikuma Region Study Area (URSA), Alberta, Canada.....61

Figure 3.2: Daily Averaged a) Air Temperature ($^{\circ}\text{C}$), b) Photosynthetic Active Radiation (PAR) (W m^{-2}), c) 2005 Soil Moisture (θ) ($\text{m}^3 \text{m}^{-3}$) of the rooting zone (0-50cm depth) and daily precipitation, d) 2006 Soil Moisture (θ) ($\text{m}^3 \text{m}^{-3}$) of the rooting zone (0-50cm depth) and daily precipitation and e) Vapour Pressure Deficits (VPD) (kPa) for the 2005 and 2006 snow-free seasons, Pond 40, Utikuma Region Study Area (URSA), Alberta, Canada.....72

Figure 3.3: Histogram of daily averaged above canopy wind direction frequency as classified in 45° intervals for the 2005 and 2006 snow-free seasons, Pond 40, Utikuma Region Study Area (URSA), Alberta, Canada.....77

Figure 3.4: Daily averaged above canopy energy flux densities for the a) 2005 and b) 2006 snow-free seasons, Pond 40, Utikuma Region Study Area (URSA), Alberta, Canada. Transitions between defined growth periods are denoted by vertical lines.79

Figure 3.5: Period averaged diurnal above canopy energy flux densities for a) Early Green period 2006, b) 2005 Green/Late Green Period, c) 2006 Green/Late Green Period, d) Senescence 2005 and e) Senescence 2006, Pond 40, Utikuma Region Study Area (URSA), Alberta, Canada.81

Figure 3.6: Daily averaged energy flux densities of a) Net Radiation (Q^*) ($W m^{-2}$), b) Latent Heat Flux (Q_E) ($W m^{-2}$) and c) Sensible Heat Flux (Q_H) ($W m^{-2}$) for both above and within canopy measurements during the 2005 and 2006 snow-free seasons, Pond 40, Utikuma Region Study Area (URSA), Alberta, Canada. Transitions between defined growth periods are denoted by vertical lines. EG represents early green period, G represents green period, LG represents the late green period and S represents senescence.83

Figure 3.7: Daily averaged a) rooting zone Soil Moisture (θ) ($m^3 m^{-3}$) (0-50cm) and daily precipitation (mm), b) above canopy ET (mm) and c) within canopy ET (mm) for the 2005 and 2006 snow-free seasons, Pond 40, Utikuma Region Study Area (URSA), Alberta, Canada. Transitions between defined growth periods are denoted by vertical lines. EG represents early green period, G represents green period, LG represents the late green period and S represents senescence.86

Figure 3.8: Precipitation free 4 day periods for the green (G), late green (LG) and senescence (S) periods of rooting zone Soil Moisture (θ) ($m^3 m^{-3}$) (solid blue line), rooting zone soil tension (ψ) (kPa) (dashed red line) and above canopy ET (ET_C) (mm) for the 2005 snow-free season, Pond 40, Utikuma Region Study Area (URSA), Alberta, Canada.90

Figure 3.9: Precipitation free 4 day periods for the early green (EG), green (G), late green (LG) and senescence (S) periods of rooting zone Soil Moisture (θ) ($m^3 m^{-3}$) (solid blue line), rooting zone soil tension (ψ) (kPa) (dashed red line) and above canopy ET (ET_C) (mm) for the 2006 snow-free season, Pond 40, Utikuma Region Study Area (URSA), Alberta, Canada.93

Figure 3.10: Above (ACEC) and within canopy (BCEC) period averaged diurnal comparisons of a) Evapotranspiration (ET) (mm hr^{-1}), b) Vapour Pressure Deficits (VPD) (kPa) and c) Photosynthetic Active Radiation (PAR) (W m^{-2}) Pond 40, Utikuma Region Study Area (URSA), Alberta, Canada.....96

Figure 3.11: Relationship between above canopy ET (ET_C) (mm hr^{-1}) and VPD (kPa) based on VPD_O thresholds of a) VPD_O LOW < 0.05 kPa, b) VPD_O MID > 0.05 kPa and < 0.15 kPa and c) VPD_O HIGH > 0.15 kPa, Pond 40, Utikuma Region Study Area (URSA), Alberta, Canada.98

Figure 3.12: Relationship between daily maximum ET (mm hr^{-1}) and VPD_O (kPa) for above and within canopy layers of the forest canopy during defined green periods of the 2005 and 2006 snow-free seasons, Pond 40, Utikuma Region Study Area (URSA), Alberta, Canada.....100

Figure 3.13: Relationship between above canopy ET (ET_C) (mm hr^{-1}) and VPD (kPa) for periods during the 2005 and 2006 peak growth periods when Soil Moisture (θ) become limited and approaches the wilting point ($0.15 \text{ m}^3 \text{ m}^{-3}$) (Saxton et al, 1986), Pond 40, Utikuma Region Study Area (URSA), Alberta, Canada.....103

Figure 6.1 Power spectral density function of vertical windspeed using Welch's method. Data for spectral analysis was taken on August 18, 2005. Pond 40, Utikuma Region Study Area (URSA), Alberta, Canada.....126

Figure 6.2 Blanford and Gay correction factor relative to horizontal windspeed for Pond 40, Utikuma Region Study Area (URSA), Alberta, Canada. Values are based on mean sensible heat flux and horizontal wind speed values from the 2005 and 2006 above canopy.127

Figure 6.3 Wetland friction velocity (u^*) (m s^{-1}) thresholds plotted against energy balance closure for a) 2005 and b) 2006 for Pond 40, Utikuma Region Study Area (URSA), Alberta, Canada. Crosshairs in plots indicate the inferred threshold values. All fluxes were then filtered using the inferred thresholds (0.23 m s^{-1}).130

Figure 6.4 Aspen upland friction velocity (u^*) (m s^{-1}) thresholds plotted against energy balance closure for a) 2005 and b) 2006 for Pond 40, Utikuma Region Study Area (URSA), Alberta, Canada. Crosshairs in plots indicate the inferred threshold values. All fluxes were then filtered using the inferred thresholds (0.1 m s^{-1}).131

Figure 6.5 Within canopy upland friction velocity (u^*) (m s^{-1}) thresholds plotted against energy balance closure combined for the 2005 and 2006 snow-free seasons for Pond 40, Utikuma Region Study Area (URSA), Alberta, Canada. Crosshairs in plots indicate the inferred threshold values. All fluxes were then filtered using the inferred thresholds (0.29 m s^{-1}).132

List of Tables

Table 1.1: Summary of monthly growing season evapotranspiration results (mm d^{-1}) from various studies within similar vegetation compositions as compared to the Utikuma Region of North Central Alberta, Canada.....7

Table 2.1: Dominant vegetation present at examined sites (% cover), microtopography description (% per 10 m^2 area) with a description of maximum relief (cm) and estimated canopy closure (%) for all examined peatland sites, Utikuma Region Study Area (URSA), Alberta, Canada. Values within parentheses are standard errors (SE). Vascular vegetation comprising the % cover at each site were *Ledum groenlandicum*, *Vaccinium oxycoccos* and *Rubus chamemorus*.20

Table 2.2: Alpha (α) values calculated from the comparison of PET values and AET from eddy covariance measurements at all three peatland sites of the 2005 and 2006 snow-free seasons where (n/a) denotes time periods where measurements did not occur. Period measurements were delineated into Early Green (EG) (DOY 121 to DOY 158), Green (G) (DOY 158 to DOY 218) and Late Green (LG) (DOY 219 to DOY 260) periods and reported as arithmetic averages over the periods, Pond 40, Utikuma Region Study Area (URSA), Alberta, Canada. Values in parentheses are standard error (SE) of measurements.....34

Table 3.1: Summary table of catchment forest characteristics for the upland aspen dominated forest situated at “Pond 40”, Utikuma Region, Alberta Canada. Measurements consisted of three $15 \text{ m} \times 15 \text{ m}$ plots situated on the south facing slope (SFS) of the catchment within the calculated footprint of the EC tower. Values in parentheses are standard errors (SE) of measurement variables.70

Table 3.2: Snow-free season period averaged flux footprint characteristics of maximum flux contribution ($x \text{ max}$) (m), fractional flux source at 80% of flux contribution ($x \text{ frac}$) (m), mean wind speed (u) (m s^{-1}), wind direction (degrees) and friction velocity (u^*) (m s^{-1}) for a) Above canopy EC tower (ACEC) and b) Below Canopy EC Tower (BCEC), Pond 40, Utikuma Region Study Area (URSA), Alberta, Canada.75

Table 3.3: Period averaged daily maximum (defined as between 1100MST and 1500MST) scalar catchment flux partitioning of above canopy ET (ET_C) (mm hr^{-1}), within canopy ET (ET_B) (mm hr^{-1}) and surface evaporation (E_S) (mm hr^{-1}) for the 2005 and 2006 snow-free seasons, Pond 40, Utikuma Region Study Area (URSA), Alberta, Canada. As E_S was examined as spot measurements, fluxes from both ET_C and ET_B were matched to the closest half hour interval when E_S was sampled. The data was then grouped and averaged by defined growth periods. Values in parentheses are standard errors (SE) of measurements.....88

Table 3.4: Soil texture properties for the rooting zone (0-50 cm) of this silty clay loam soil below the litter fall horizon based on soil cores and taken during installation (May 2005), soil texture classifications and soil moisture properties based on Saxton et al, 1986.....102

Chapter One

Introduction

1.1 Western Boreal Forest

The Western Boreal Forest (WBF) is a large ecosystem covering 35% of Canada (Canadian Forest Service, 2006) and contains nearly one quarter of the world's undeveloped forested area (Bryant et al., 1997). This forest region represents an extremely important ecosystem for fresh water resources and carbon storage crucial for global climate regulation (Metcalf and Buttle, 1999). A large portion of the WBF is comprised of the Western Boreal Plain (WBP) ecozone (Devito et al., 2005a). The WBP supports a variety of landcover units (upland forest, shallow lakes, peatlands, and ponds) on three common landforms including coarse-grained glaciofluvial outwash deposits, fine-grained disintegration moraines and low-lying glaciolacustrine plains (Devito et al., 2005a). This ecozone extends across the provinces of Alberta, Saskatchewan, and Manitoba in west-central Canada (National Wetlands Working Group, 1988), and is currently subject to the potential impacts from rapid development and the proliferation of natural resource based industries (Alberta Environmental Protection, 1998). Recent hydrologic research completed in the WBP has shown that temporal climate patterns and geology control hydrologic processes driving wetland sustainability, vegetation patterns, and regional groundwater recharge (Ferone and Devito, 2004; Devito et al., 2005b; Smerdon et al., 2005; Petrone et al., 2007; Smerdon et al., 2007). Quantifying impacts caused by anthropogenic development in the area requires a detailed understanding of the natural variability of hydrologic processes and water cycling unique to this region, under past, present, and future climatic conditions.

The WBP has many physical characteristics that necessitate different hydrologic analyses than other Boreal ecozones (Winter, 2001; Devito et al., 2005a; Smerdon et al., 2007). The combination of the sub-humid climate (i.e., precipitation (P) is exceeded by potential evapotranspiration (PET); Winter and Woo, 1990), low relief, deep glacial sediments (20 to 240 m thick; Klassen, 1989; Pawlowicz and Fenton, 2002), and its location south of the discontinuous permafrost zone (Woo and Winter, 1993) creates a unique hydrologic environment that has achieved a temporal and volumetric balance of atmospheric water fluxes, vegetative water demand, and soil water storage that differs from other ecozones (Smerdon et al., 2005). The wetland-upland mosaic in the WBP is sustained by infrequent wet years within periods of drought where PET exceeds P on a 10–15 year cycle (Marshall et al., 1999; Devito et al., 2005a). Thus, the wetlands and uplands within this region are vulnerable to any climatic change that may alter patterns of P and actual evapotranspiration (AET) (Petroni et al., 2007). Further, several industries are currently developing vast areas of the WBP, with major disturbances from the forestry and conventional oil/gas industries, as well the development of oil sands resources (Ducks Unlimited Canada, 2006). This rapid development of the WBP presents challenges in preserving its ecological characteristics for storing fresh water (in wetlands) and carbon, and for providing habitat for millions of waterfowl and songbirds (Blancher and Wells, 2005). A disconnect exists between the intrinsic, economic and ecologic values of the WBP, requiring development of a standard conservation methodology that considers the diversity and complex hydrology of the landscape.

To further investigate this hydrologic environment, a research area within the Boreal Plain ecozone has been established called the Utikuma Region Study Area

(URSA), which encompasses the spectrum of physiographic landforms commonly found in the region and the WBP. Current multidisciplinary research at the URSA includes concurrent characterization of atmospheric flux patterns, surface water-groundwater interaction, recharge characteristics, vegetative controls, and soil water storage. The determination of the influence of climatic and geologic characteristics on the ecohydrology of several wetland/upland complexes located across the geologic and physiographic gradients observed in the Boreal Plain will improve our ability to scale-up hydrologic responses to natural variability and disturbances.

Current research ongoing in the WBP is divergent from the model of topographically driven flow systems and the fundamental hydrologic landscape unit (FHLU) concept as described by Winter (2001). Completing process based research at plot and catchment scales allows the development of hydrologic response unit (HRU; Devito et al., 2005a) characteristics for a variety of land features in this environment. These characteristics will guide generalizations implemented within larger-scale hydrologic modeling, while improving our ability to predict hydrologic responses and natural variability at the landscape scale. Ultimately, this approach is intended to improve sustainable development of the Boreal Plains.

1.2 Evapotranspiration in the Western Boreal Forest

ET is the dominant hydrologic flux in this landscape however research into the nature and seasonal variability of ET within the Boreal regions of northern Canada is difficult to quantify (Amiro et al, 2006; Blanken et al., 2001) and represents a significant challenge towards the characterization of ET within the WBP hydrologic cycle (Balocchi et al.,

1997). Examining the controls on ET within the context of landcover units through a focus on both the wetland and aspen dominated uplands will provide an insight into the nature and scope of this integral aspect of the hydrologic cycle within a sub-humid climatic setting, where water use efficiency is of growing concern (Peterson and Peterson, 1992). Other studies (Blanken et al., 2001; Nijssen and Lettenmaier, 2002; Amiro et al., 2006) have outlined differing controls on ET within Boreal forests, however limited work has been done covering different scales of research that encompasses both wetland and forested upland landcover units within the WBP region of North Central Alberta.

Vegetation plays a significant role in the contributions of ET within Boreal landscapes (Nijssen and Lettenmaier, 2002) in both the wetland and forested upland landcover units, and is dependent on the nature of the forest cover and underlying surface vegetation and soil composition (Cuenca et al., 1997; Grelle et al., 1997). Landcover unit vegetation composition has been identified as a significant driver of energy exchange within *Sphagnum* dominated wetland environments (Heijmans et al., 2004) and aspen dominated forests (Blanken et al., 1997). Within wetland environments vegetation controls on ET in general, whether dominated by vascular plants or bryophytes, are an integral part of the seasonal energy balance for wetlands of the WBP. When present, a dense canopy of vascular plants will dominate the exchange processes with the atmosphere, and the resultant energy partitioning will largely depend on the transpiration capacity of the canopy (Heijmans et al., 2004). Whereas, feathermoss species rely on the occurrence of precipitation and dew formation, critical hydrological events, which provides the single most important source of moisture (Busby et al., 1978; Longton and

Greene, 1979; Skre et al., 1983; Vitt, 1990; Bisbee et al., 2001). In addition, the presence of frost (Amiro et al., 2006), limited soil moisture content (Moore et al., 2000) and a late development of leaf area index (LAI) inhibit the rates of ET originating from boreal wetlands (Nijssen and Lettenmaier, 2002).

Aspen dominated upland vegetation exerts a strong control on ET processes, because of their ability to access, transport, and evaporate water that would otherwise be detached from terrestrial water cycles (Calder 1998; Noretto et al. 2005). The deciduous nature of aspen in addition to their clonal root systems has an especially important effect on the water and energy exchanges from these southern boreal portions of the boreal forest (Blanken et al., 2001). The sparse and trembling nature of aspen crowns often allows a sufficient amount of light penetration and the proliferation of understory species such as *Rosa acicularis* and *Viburnum edule*, which also contributes to the canopy energy and mass exchanges (Blanken et al., 1998). Studies have shown that much of the variation in aspen upland ET can be explained by variation in vapour pressure deficit (VPD) (Kurpius et al., 2003; Hogg et al., 2000; Hogg et al., 1997; Hogg and Hurdle, 1997).

Determining the rates of ET from boreal wetlands and forested uplands must incorporate the above mentioned aspects in order to properly quantify the spatial and temporal (seasonal) variability that is present within this system. Accurately identifying the drivers of ET within the WBP will lead to a more concise description of the factors that act to control ET from within Boreal Forest catchments, inside and outside the WBP, ultimately leading to better conceptual understanding of the processes and more

acceptable model predictions. A summary of the role of vegetation within Boreal regions is summarized in Table 1.1 along with the seasonal contributions of ET during the growing season.

Vegetation Description	Study Site Location	May (mm d ⁻¹)	June (mm d ⁻¹)	July (mm d ⁻¹)	August (mm d ⁻¹)	September (mm d ⁻¹)
Aspen (Amiro et al., 2006)	BOREAS SOA, Prince Albert SK.	1.0	2.0	3.0	2.0	1.0
Aspen (Blanken et al., 2001)	BOREAS SSA, Prince Albert SK.	1.5	3.0	3.0	3.0	2.0
Pine (Amiro et al., 2006)	BOREAS SOJP, Prince Albert SK.	0.5	1.0	2.0	1.0	0.5
Pine (Baldocchi et al., 1997)	BOREAS SOJP, Prince Albert SK.	1.0	1.5	2.0	1.5	1.0
Pine (Cuenca et al., 1997)	BOREAS NOJP, Thompson MB.	2.4	3.0	3.5	n/a	n/a
Pine & Spruce (Cienciala et al., 1998)	NOPEX, Sweden	1.5	2.0	2.5	1.0	0.5
Pine & Spruce (Grelle et al., 1997)	NOPEX, Sweden	2.0	2.5	3.0	2.0	1.0

SOA is defined as an old growth aspen forest (>80 yrs)

SSA is defined as a young aspen forest (< 40 yrs)

SOJP/NOJP is defined as an old jack pine forest (> 80 yrs)

Table 1.1: Summary of monthly growing season evapotranspiration results (mm d⁻¹) from various studies within similar vegetation compositions as compared to the Utikuma Region of North Central Alberta, Canada.

1.3 Thesis objective and format

The objective of this thesis is to understand the processes and controls on evapotranspiration from a typical wetland-forested upland complex within the Western Boreal Plain region of North Central Alberta, Canada. A small moraine landscape catchment typical of the WBP (Devito et al, 2005a) referred to as “Pond 40” was utilized for this study with a detailed analysis of two distinct landcover units within the catchment (wetland and aspen dominated upland). This thesis addresses the following research questions:

- 1) What is the role that surface vegetation (especially the extensive moss covers) play in moderating soil and atmospheric controls on ET within a wetland of the sub-humid WBP?
- 2) What are the roles of surface and atmospheric conditions when characterizing the dynamics of the energy balance and ET from above and within an aspen dominated upland in the sub-humid WBP?

This thesis follows a paper based format and has been organized into four chapters including this introduction, which provides a brief overview of the Western Boreal forest, the role of evapotranspiration within the WBP and the study rationale. The field research element of the thesis, including independent measurements and interpretation on the controls on evapotranspiration is summarized in chapter two and three. Chapter two is focused on the role of wetland vegetation in controlling evapotranspiration rates within the WBP and as such is designed to address question 1 posed above. This chapter examines the role of differing moss and vascular plant cover found within the WBP, their role in controlling ET along with near surface hydrological

linkages which act in parallel to typical hydrological function of these wetland landcover units. Chapter three is focused on the nature and seasonal distribution of evapotranspiration from above and within an aspen dominated forest HRU of the WBP and as such is organized to address question 2. Both the role of vegetation (above and within canopy) distribution coupled with atmospheric demands at both scales are key aspects of the analysis. Finally, Chapter four provides a summary of the two main data chapters focusing on the controls on ET within two distinct landcover units within the WBP and elaborates on the applicability of this research to evolving water resource management practices, and landscape reclamation approaches currently ongoing in the region.

1.4 Utikuma Region Study Area

The wetland-forested upland complex studied is located 370 km north of Edmonton AB, Canada (56°6N, 116°32W) at the URSA. The URSA is located in the Mixed-wood Boreal Plains ecoregion and lies approximately 150 km south of the discontinuous permafrost zone (National Wetlands Working Group, 1988; Woo and Winter, 1993). The climate is characterized by seasonally variable average monthly air temperatures ranging from -14.6 °C in January to 15.6 °C in July (Environment Canada, 2003), and is considered sub-humid with normal annual precipitation (481 mm; Environment Canada, 2003) which is exceeded by annual potential evapotranspiration (517 mm; Bothe and Abraham, 1993). This net deficit in atmospheric fluxes is typical of most years, with atmospheric surpluses occurring approximately every 10 to 15 years, resulting from a combination of cool summer temperatures and greater than normal annual precipitation (Devito *et al.*, 2005b). Most precipitation (~ 70%) generally falls in the summer months

(June, July, and August), and snow typically accounts for <25% (<100 mm) of the average total annual precipitation (Devito *et al.*, 2005a). The surficial geology of the URSA is composed of glacial derived sediments including glaciofluvial, moraine, and glaciolacustrine deposits that vary in thickness from 20 to 240 m (see Figure 1.1) (Pawlowicz and Fenton, 2002).

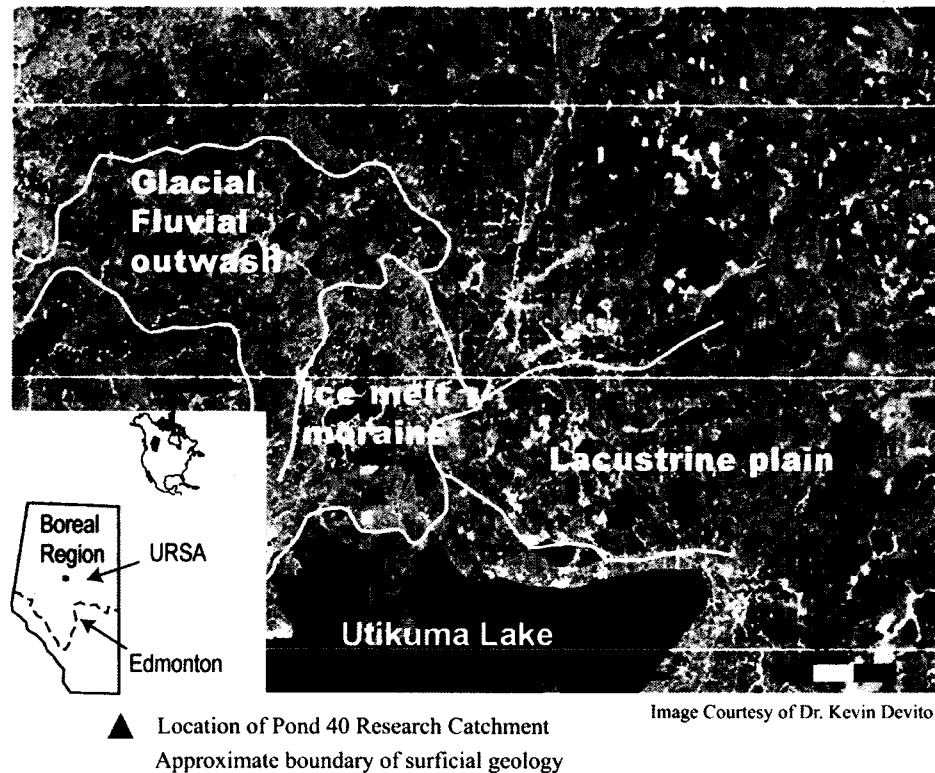


Figure 1.1: Schematic diagram of the Utikuma Region Study Area (URSA) regional surficial geology and location of “Pond 40” research study site within the Western Boreal Plain region of North Central Alberta, Canada.

This research was conducted within a small (~1 km²) moraine landscape catchment, the central feature of which is a shallow (1 m deep) pond with an area of 175 m² ringed by a well defined black spruce dominated wetland (Figure 1.2). The overstory canopy of the study catchment is predominantly trembling aspen (*Populus tremuloides*), with minor amounts of black poplar (*Populus balsamifera*) in depressions and ephemeral draws (Figure 1.2). Forested uplands consisting of Gray Luvisolic soils (Soil Classification Working Group, 1998) developed from disintegration moraine deposits, which are typically silt-rich but spatially heterogeneous, with zones of high clay or sand contents (Redding and Devito, 2008; Fenton et al., 2003).

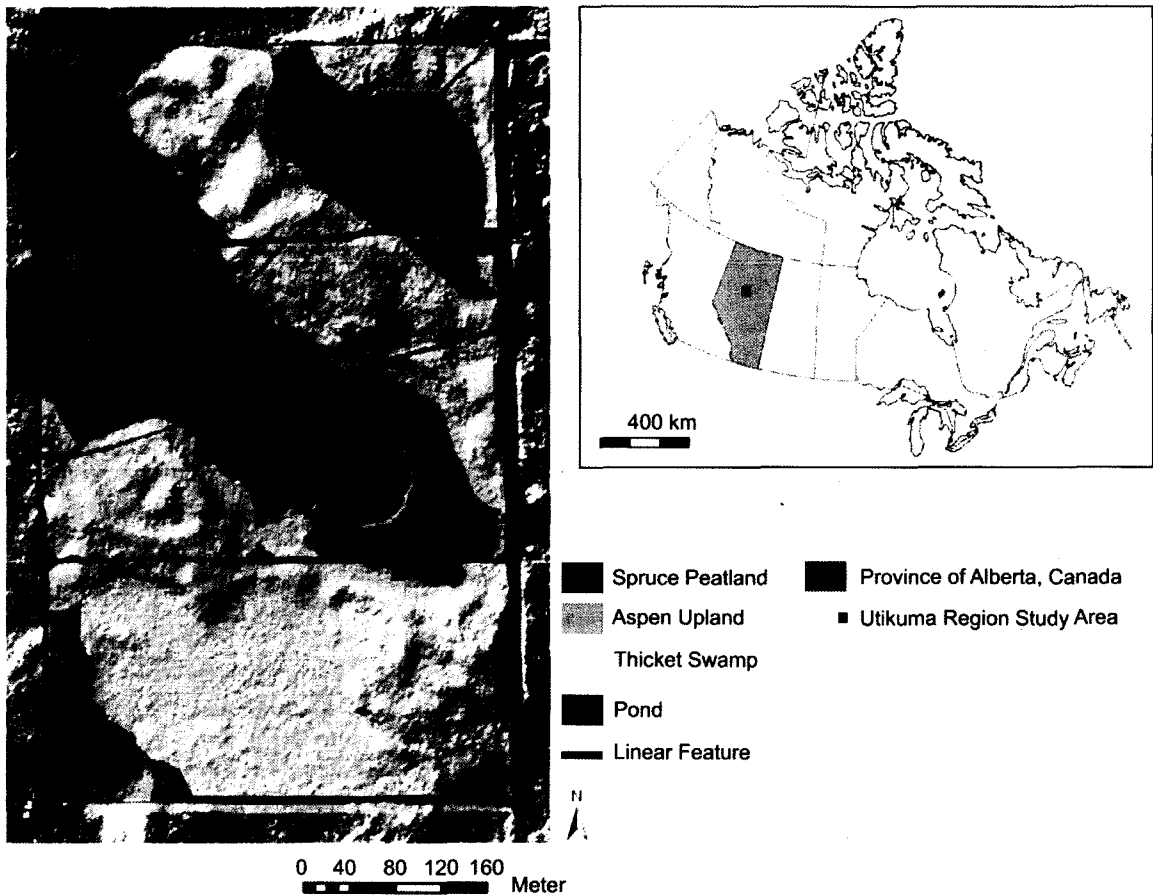


Figure 1.2: Schematic diagram of the Utikuma Region Study Area (URSA) (Pond 40) study site and location within the Western Boreal Plain region of North Central Alberta, Canada. The distribution of the landcover units comprising the study catchment are illustrated.

Chapter Two

Surface vegetation controls on evapotranspiration from a sub-humid Western Boreal Plain wetland

2.0 Introduction

Wetlands comprise approximately 50% of the Western Boreal Plain (WBP) (Vitt et al., 2000). These wetlands exist although annual precipitation (P) inputs are less than annual potential evapotranspiration (PET) (Hogg et al., 1994; Devito et al., 2005b; Petrone et al., 2006; Redding and Devito, 2008). Low surface runoff is common (Devito et al., 2005b) and hydrologic contributions to low lying areas (i.e.; wetlands) may not be controlled by topography, but rather climate patterns and regional surficial geology (Devito et al., 2005a). The water budgets of low-lying pond-wetland complexes are dominated by vertical fluxes (Smerdon et al., 2005). Furthermore, at the local scale the exchange of water between ponds and wetlands is dynamic and can shift direction during intra-annual wet and dry periods (Ferone and Devito, 2004). Evapotranspiration (ET) is a significant aspect of the water balance for this region and the mechanisms by which these wetlands retain and exchange water with the atmosphere is important to the overall maintenance of these common ecosystems within the WBP.

Peatland ecosystems dominated by black spruce are the most widespread boreal forest type in North America (Viereck et al., 1986). Boreal black spruce cover is relatively open due to the narrow structure and low density of trees (Heijmans et al., 2004). This results in a large portion of solar radiation received at the surface, creating a significant role for understory/surface vegetation species dominated by *Sphagnum*, feathermoss and lichen (spp) with regards to energy exchange (Baldocchi et al., 2000;

Heijmans et al., 2004). The ground surface within these open black spruce systems is often dominated by *Sphagnum* and feathermoss, which can account for a significant fraction of the water exchange between the terrestrial biosphere and atmosphere (Williams and Flanagan, 1996). Lafleur and Schreder (1994) demonstrated that from a sub-arctic forest *Sphagnum* and feathermoss surface cover can account for as much as 65% of the total water loss from the ecosystem. As *Sphagnum* mosses act to insulate the soil, intercept atmospheric nutrients, and decompose slowly resulting in lower soil temperatures and rates of nutrient supply (Heijmans et al., 2004) they should be considered significant with regards to their role in surface energy exchange within the WBP.

Vegetation controls on ET in general, whether dominated by vascular plants or bryophytes, are an integral part of the seasonal energy balance for wetlands of the WBP. When present, a dense canopy of vascular plants will dominate the exchange processes with the atmosphere, and the resultant energy partitioning will largely depend on the transpiration capacity of the canopy (Heijmans et al., 2004). As vascular plants have extensive root systems, they are seldom restricted by water supply (Lafleur, 1990). However, many northern wetlands, especially those in the WBP, are covered by a sparse canopy because of a low trophic status (Schipperget and Rydin, 1998). Since water supply in these systems is primarily by rainwater, rather than by groundwater from surrounding areas, the peat substrate is acidic and mineral-poor in bogs (totally rain-fed) and poor fens (to some extent supplied by groundwater but still acid and mineral-poor). The ground surface then is often dominated by *Sphagnum* mosses, which unlike vascular plants, do not have roots or internal water conducting tissues but depend on capillary

transport from underlying layers (Price et al., 2002). Therefore, the evaporative capacity should largely depend on peat wetness. Little is known about the variation of peat wetness and its influence on the total ET, though peat wetness seems to be crucial for some types of wetlands (Price, 1991), it is probable that the impact of surface wetness varies seasonally with the development of vascular plants (Kim and Verma, 1996). Thus, in order to quantify and predict the ET regime from WBP wetlands and how they may respond to climate variability requires an understanding of how these vegetation groups interact with each other along with soil moisture patterns over a season.

Feathermoss species, also present in these systems, have a significantly different physiological and structural design compared to *Sphagnum*. The occurrence of precipitation and dew formation are critical hydrological events and provide the single most important sources of moisture (Busby et al., 1978; Longton and Greene, 1979; Skre et al., 1983; Vitt, 1990; Bisbee et al., 2001). Feathermoss species commonly occur within environments where incident shortwave radiation and evaporative demand are low (Bisbee et al., 2001). Skre et al. (1983) suggest water loss from feathermoss species occur at greater rates in open, more exposed locations as a result of the increased exposure to precipitation when coupled with a greater exposure to incident radiation and wind.

2.1 Study Objectives

The objective of this study is to examine the role that surface vegetation (especially the extensive moss covers) plays in moderating soil and atmospheric controls on ET within a wetland of the sub-humid WBP. It is hypothesized that wetland scale ET will be

controlled primarily by the vegetation communities present. Consequently, these controls were characterized temporally throughout the 2005 and 2006 snow free seasons (May 1 to Sept 30). Environmental factors including water table (WT), soil moisture (θ), photosynthetic active radiation (PAR) and ground temperatures (T_g) were also examined at the vegetation scale to determine the relationships between variables coupled with the vegetation controls on ET. It is also hypothesized that ground thermal conditions, especially the depth of ice, will impact ET (especially early in the season) more so than soil moisture within these wetland environments, and thus, the depth of ice is also considered within this study to characterize the roles of wetlands within a broader representation of ET at the catchment scale.

2.2 Study Area

2.2.1 Utikuma Region Study Area

The wetland studied here is located within the Utikuma Region Study Area (URSA), 370 km north of Edmonton, Alberta, Canada (56° 4' N, 115° 28' W) (Figure 2.1). URSA is situated approximately 150 km south of the discontinuous permafrost zone (Woo and Winter, 1993) within the Plains region of the Western Boreal forest. Climate within URSA can be characterized by cold winters and warm summers with average temperatures of -14.6 to 15.6 °C, respectively over the past 30 years (Environment Canada, 2003). Annual PET (517 mm, Bothe and Abraham, 1993) is slightly higher than the average annual P (481 mm, Environment Canada, 2003) at URSA over this same period, with snowfall averaging less than 100 mm yr⁻¹ (less than 25% of the total annual precipitation for the region) (Marshall et al., 1999; Devito et al, 2005). Devito et al.

(2005) report that within the sub-humid boreal plains region, a water deficit exists during most years, and that only on an average cycle of 10 to 15 years, will annual P surpass ET. Furthermore, 70 % of annual P occurs between June and August, coinciding with peak vegetation growth and maximum ET demand, and is followed by a relatively dry period during fall (Ferone and Devito, 2004; Devito et al, 2005; Petrone et al, 2006).

2.2.2 Study Catchment

This research was conducted within a small (~1 km²) moraine landscape catchment, the central feature of which is a shallow (1 m deep) pond with an area of 7500 m² ringed by a well defined black spruce dominated wetland (Figure 2.1). Six sites were selected for community scale measurements of ET based on aspect, dominant vegetation species (ie; vascular vs. non-vascular), microtopography (i.e. lawn vs. depression) and canopy closure (i.e. covered vs. uncovered) and represent the range of vegetation within the wetland. As the controls of vegetation coverage on snow-free season ET was the primary goal of this research, experimental plots were assigned in an attempt to characterize the vegetation distribution within the wetland (Table 2.1). Overlain on top of this distribution of six sites were three energy balance towers with varying aspects surrounding the central pond, among which a roving eddy covariance system was relocated every 2 weeks.

Microtopography and vegetation distribution among the three main sites were highly dynamic depending on location and moisture conditions (Table 2.1). Microtopographical relief ranged from 35 cm (± 6 (SE)) to 76 cm (± 10 (SE)), with the smallest ratio of lawn to depression areas in the northern portion of the system, and the largest ratio in the southern area (Table 2.1). Overstory species throughout the wetland

consisted of black spruce (*Picea mariana*), white spruce (*Picea glauca*), paper birch (*Betula papyrifera*) and willow (*salix sp*). Canopy closure ranged from 80% in the northwestern portion to ~30% in the southern portion of the wetland (Table 2.1). The surface cover vegetation distribution within the wetland had lichen species (*Cladina mitis*) largely on the lawns (90%) within the southern portion, and in both the lawn and depression sites in the northern portion of the wetland (Table 2.1). *Sphagnum* species (*Sphagnum fuscum*, *Sphagnum cappifolium*) were dominant (60 – 90%) in both lawns and depressions in northern and southern sides of the pond. While feathermoss species (*Pleurozium schreberi* and *Hylocomium splendens*) were located primarily at the northwestern end of the wetland with 97% on lawns and 95% in depressions (Table 2.1). Vascular plants (*Ledum groenlandicum*, *Vaccinium oxycoccos*, *Rubus chamaemorus*) were present as well throughout the entire wetland (Table 2.1).

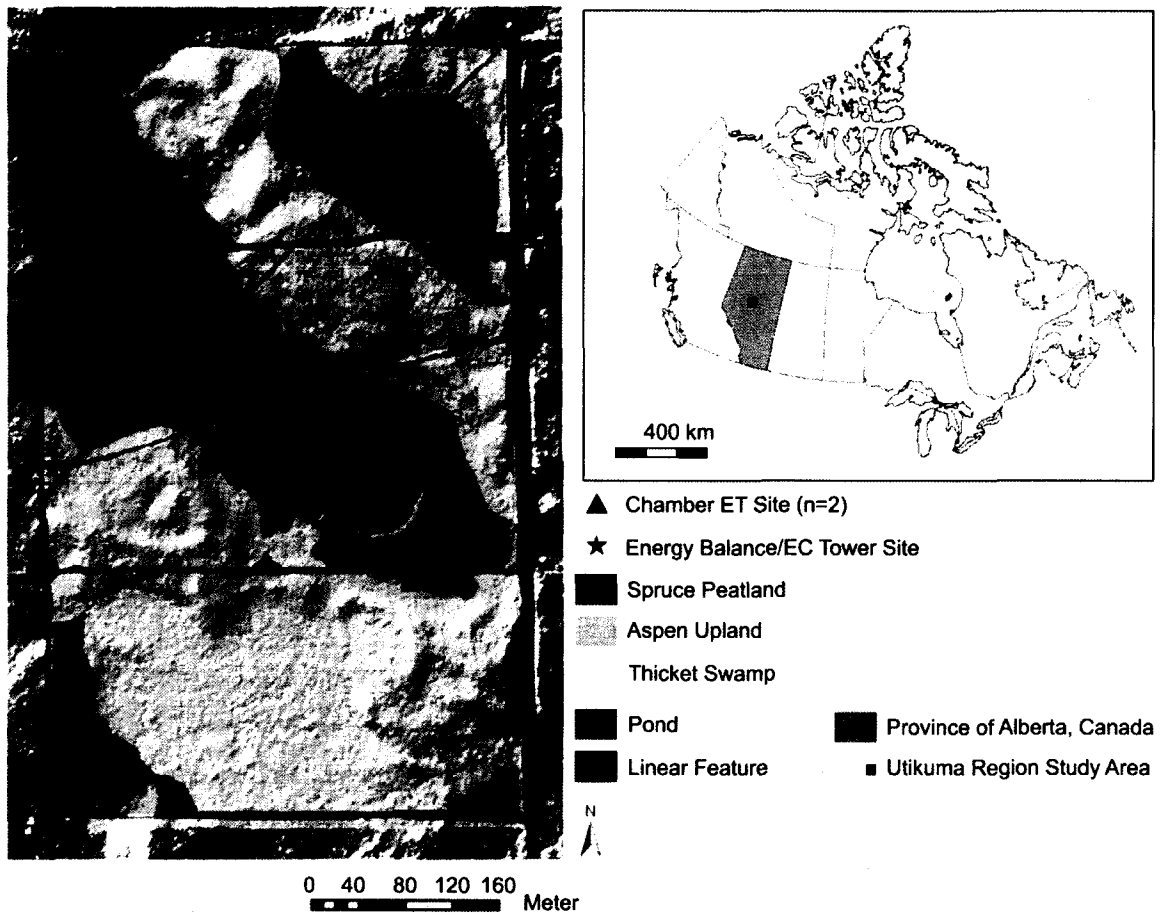


Figure 2.1: Schematic diagram of the Utikuma Region Study Area (URSA) (Pond 40) study site and location within the Western Boreal Plain region of North Central Alberta, Canada. The distribution of the landcover units comprising the study catchment and the location of measurement sites are illustrated.

Site Description	Vegetation (%)				Vascular	Microtopography Max Relief (cm)	Canopy Closure (%)
	Lichen	Sphagnum	Feathermoss				
North Site (NS)							
Lawn (n=3)	15 (± 2)	0	97 (± 2)	13 (± 4)	35 cm (± 6)	Closed ($\sim 80\%$)	
Depression (n=3)	10 (± 1)	0	95 (± 4)	4 (± 1)	45% 55%		
Northwestern Site (NWS)							
Lawn (n=2)	0	60 (± 5)	0	11 (± 5)	76 cm (± 10)	Open ($\sim 35\%$)	
Depression (n=2)	0	75 (± 4)	5 (± 1)	6 (± 2)	63% 37%		
South Site (SS)							
Lawn (n=2)	90 (± 2)	0	0	15 (± 3)	65 cm (± 5)	Open ($\sim 30\%$)	
Depression (n=2)	20 (± 1)	90 (± 8)	0	6 (± 1)	71% 29%		

Table 2.1: Dominant vegetation present at examined sites (% cover), microtopography description (% per 10 m² area) with a description of maximum relief (cm) and estimated canopy closure (%) for all examined peatland sites, Utkuma Region Study Area (URSA), Alberta, Canada. Values within parentheses are standard errors (SE). Vascular vegetation comprising the % cover at each site were *Ledum groenlandicum*, *Vaccinium oxycoccos* and *Rubus chamemorus*.

2.3 Methods

2.3.1 Wetland Energy Balance

In order to better account for the potential spatial variability of ET within the wetland, three energy balance systems were installed on Day of Year (DOY) 160 in 2005 and ran continuously through to DOY 270 of 2006 (Figure 2.1). The three towers consisted of measurements of air temperature (T_a) and relative humidity (RH) (HOBO Onset Pro Temp/RH, Hoskin Scientific, Vancouver, Canada) at 1.5 m above the wetland surface and a net radiometer installed at the same height (NRLite, Kipp and Zonen, The Netherlands). Profiles of soil temperatures were recorded at all 3 wetland sites using thermocouples (Omega copper-constantin, Campbell Scientific Inc, Logan, Utah, USA) at 0.10 m, 0.25 m, 0.50 m and 1.0 m depths in the peat. Soil moisture (θ) was recorded in both a lawn and depression at each site using water content reflectrometry probes (CS616, Campbell Scientific Inc, Utah, USA) placed vertically in order to collect average θ ($\text{m}^3 \text{m}^{-3}$) of the upper 0.3 m of the peat. Water content reflectrometers were calibrated from depth integrated peat cores at each site within the wetland (Solondz, 2007). Published values for heat capacities of peat soils under a range of moisture conditions were used to determine the heat capacity values to be used in the ground heat flux and storage calculations (Oke, 1987). The ground heat flux was measured using the calorimetric method (Halliwell and Rouse, 1987; Petrone et al., 2000; Petrone et al., 2006) using the ground temperature profile and heat capacity calculations for each soil layer accounting for changes in moisture amount and state.

The energy balance of the wetland surface at each location is given by,

$$Q^* = Q_E + Q_H + Q_G \quad (2.1)$$

where Q^* is the net radiative flux at the surface, Q_E is the latent heat flux, Q_H is the sensible heat flux and Q_G is the ground heat flux (W m^{-2}). Vegetated surfaces generally have a mean daily soil heat flux (Q_G) one or two orders of magnitude smaller than the major terms in the surface energy balance (Brutsaert, 1982). However, on shorter temporal scales, Q_G can be quite important. The subsurface soil temperatures, and Q_G , are a function of solar radiation, soil texture, soil moisture content and state, in addition to surface vegetation cover and weather conditions (wind, air temperature, humidity) (Williams and Smith, 1989). This is especially true in systems such as this wetland with persistent seasonal ice (Petrone et al., 2008).

2.3.2 Potential Evapotranspiration

The Priestley–Taylor equation is classified as a radiation-based approach to estimating PET, using Q^* and T_a to evaluate equilibrium evapotranspiration (PET_{EQ}), which assumes that an air mass moving over a homogeneous, well-watered surface would become saturated (Priestley and Taylor, 1972). Under these ideal conditions ET would reach a state of equilibrium (Priestley and Taylor, 1972). Radiation is a very effective parameter to use in measuring equilibrium evaporation or PET. In a review of 30 studies it was commonly found that approximately 95% of the annual evaporative demand was supplied by radiation in vegetated areas with very small, or no, water deficits (Stagnitti et al., 1989). The Priestley–Taylor model obtains PET_{EQ} via,

$$PET_{EQ} = \frac{\Delta}{\Delta + \gamma} (Q^* - Q_G) \quad (2.2)$$

where Δ (kPa °C⁻¹) is the slope of the saturated vapour pressure curve, γ (kPa °C⁻¹) is the psychrometric constant, Q^* (W m⁻²) is net radiation, and Q_G (W m⁻²) is the soil heat transfer. The equilibrium ET is related to the potential ET, defined as the rate of ET if energy or moisture is not limiting, or actual ET via the Priestley–Taylor coefficient. In their original manuscript Priestley and Taylor define α as,

$$\alpha = 1.26 = \frac{PET}{PET_{EQ}} \quad (2.3)$$

where PET is the potential evapotranspiration and PET_{EQ} is the total equilibrium evapotranspiration (Wilson and Baldocchi, 2000). However, equilibrium rarely occurs, as there is almost always horizontal advection and deviations from a ‘wet’ surface (Wilson and Baldocchi, 2000). Therefore, an α less than, or greater than, this value gives “actual ET”. The large range in alpha inherent in this original definition is reflective of the range in natural surface cover and above the large water body on which their work was done. In this manuscript, the technical definitions are insignificant as PET calculated here is converted to actual ET using α values obtained using the mobile EC system.

2.3.3 Eddy Covariance Theory

The eddy covariance (EC) technique is based on the theory of vertical flux gradients which examines an area-integrated surface flux from a known distance upwind of the measuring point on uniform terrain (Brutsaert, 1982). EC measurements provide ecosystem-scale measurements on a time series continuum that permits the investigation of the interactions between energy and mass balance fluxes. A flux can be characterized

as the covariance of an upward wind vector and a scalar flux of the measurement parameter (F),

$$F = -\rho_a \overline{\omega' x'} \quad (2.4)$$

where ρ_a is the average density of air, and $\overline{\omega'}$ is the average instantaneous covariance of the vertical wind velocity and $\overline{x'}$ is the average instantaneous covariance of the scalar flux (Baldocchi et al., 1988).

The EC technique for measuring the surface energy fluxes is based on determining the turbulent fluxes of water vapour, momentum and sensible heat from the covariance of their respective eddies (Petrone et al., 2001). This measures the turbulent exchange directly without restrictive assumptions as to the nature of the surface and the transfer mechanisms involved (Peixoto and Oort, 1992; Petrone et al., 2001). The mean vertical flux of the sensible and latent heat fluxes was calculated via,

$$Q_H = \rho C_p \overline{w' T'} \quad (2.5)$$

$$Q_E = L \rho \overline{w' q'} \quad (2.6)$$

where ρ (kg m^{-3}) is the density of air, C_p ($\text{MJ kg}^{-1} \text{K}^{-1}$) is the heat capacity of the air, L ($\text{MJ kg}^{-1} \text{kPa}^{-1}$) is the latent heat of vaporization, w' (ms^{-1}), T' (K) and q' (kPa) are the instantaneous variances in the vertical windspeed, air temperature and specific humidity measured at the same height. The covariances between w' , q' and T' were conducted by electronic analog computation consisting of a multiplication and averaging process on the CR23X datalogger. The CR23X processor calculated a simple statistical covariance for a

give given time period, and if there were more than one time period in the output interval it averaged the covariance results (denoted by the overbar). ET (mm d⁻¹) was then calculated from the product of $\overline{Q_E}$ via,

$$ET = \frac{\overline{Q_E}}{L_v \rho_w} \quad (2.7)$$

where L_v is the latent heat of vaporization (J kg⁻¹) and ρ_w is the density of water (kg m⁻³) (Oke, 1987).

2.3.4 Eddy Covariance Measurements of ET

A mobile eddy covariance (EC) tower was used to allow for rapid, but rigorous, comparison of surface fluxes within this wetland ecosystem (Eugster et al., 1997). Continuous half-hourly ET fluxes were measured at 2.0 m above the peat surface at the three wetland sites using the EC technique for both the 2005 and 2006 snow free seasons. The EC tower was moved between sites every two weeks from May 5 to October 5 in order to characterize the fluxes over both seasons at the scale of synoptic variability (Eugster et al., 1997). The EC instrumentation consisted of a 3-D sonic anemometer (Campbell Scientific CSAT 3) and an open path infrared gas (CO₂/H₂O) analyzer (IRGA) (LI7500, LI-COR Inc., Lincoln, NE) sampled at 20 Hz and averaged every half hour on a Campbell Scientific 23X datalogger. The IRGA was calibrated as outlined in the LI-COR Instruction Manual (LI-COR Inc, 2000) once after the season along multiple points and adjustments were made to raw fluxes based on the post-field season calibrations if there was any drift in the calibration coefficients (this was typically less than 4%) over the length of the field campaign.

The 2 week rotation among the 3 sites ensured that each wetland site had simultaneous measurements of ET and PET three times per season, coinciding with the main growth periods into which the data were delimited based on observed phenology. Although the actual transition dates varied slightly between the 2 years, period measurements were standardized into Early Green (EG) (DOY 121 – 158), Green (G) (DOY 158 – 218), Late Green (LG) (DOY 219 – 260) and Senescence (S) (DOY 261-290) (Solondz, 2007). During these 2 week periods time series of the Priestley-Taylor Coefficient (α) were obtained. During each of these periods the average α was calculated along with soil moisture for each site in each period, which when used in addition to the continuous radiation data collected at each of the sites permitted the calculation of an actual latent heat flux over the entire season using equations 2.2 and 2.3.

Due to the small fetch of the three wetland sites, the EC sensors were located at 2 m above the peat surface in order to obtain a flux representative of the wetlands being examined. In order to ensure that the low position of the sensors captured a representative flux, a power spectral density function was computed using high frequency EC data to determine if the sensor location and sampling intervals were sufficient to capture the large lower frequency and small higher frequency eddies after Petrone et al., 2001. Prior to analysis, the EC data was first filtered for periods of low turbulence ($u^* < 0.23$ m/s) (Figure 6.3), then corrected for density effects (Webb et al., 1980; Leuning and Judd, 1996) and sensor separation (Leuning and Judd, 1996; Blanford and Gay, 1992) (see Section 6.2). As a final correction to the flux data the energy balance closure was calculated and forced to close for the study period (Petrone et al., 2001). Closure is most reasonably forced by assuming that the measured available energy is representative of the

plot that the EC sensors are measuring (Petrone et al., 2001), leaving the sensible and latent heat fluxes to be adjusted (Twine et al., 2000). It was assumed that the Bowen ratio was correctly measured by the EC system and individual values of the sensible and latent heat fluxes were adjusted to balance the energy budget (Barr et al., 1994; Blanken et al., 1997; Twine et al., 2000; Petrone et al., 2001). A footprint analysis (Scheupp et al., 1990) was performed at all three wetland sites during measurement intervals to determine the source locations of fluxes measured by the EC system. Periods when fluxes originated from outside the wetland area were observed from the EC tower were removed from analysis leaving only those fluxes that originated from within the desired wetland to be included in the final analysis of wetland ET.

2.3.5 Community-Scale Measurements of Evapotranspiration

Vegetation community distributions within the footprints of the 3 towers were determined and community-scale ET measurements were conducted using a closed system EGM-4 Infrared Gas Analyzer (PP Systems, Amesbury, MA). To examine the interactions of the vegetation with environmental conditions vapour pressure, temperature and relative humidity (RH) were collected once per min over a 5 minute interval at each of the chamber sites (Figure 2.1). At each of the 3 sites, lawn and depression areas were selected for communities dominated by *Sphagnum*, feather moss and lichen species. Throughout the measurement campaign, the sampling frequency and duration was routinely tested among sites using higher frequency sampling over a 10 minute period to ensure that gradient conditions were maintained. Clear chambers (0.03 m² surface area, 0.06 m³ volume) were made of clear plexiglass with the ability to transmit 87% of PAR

(Waddington and Roulet, 2000). Collars were constructed of 19 cm (inside diameter) polyvinylchloride (PVC) plastic piping cut to a height of 15 cm with perforated grooves etched in the lower 6 cm of the collar to allow for smooth insertion into the soil. The chamber was then placed in a 3 mm wide groove cut into the top of each collar. Collars were placed 4 cm into the soil two weeks prior to the first sampling measurement being taken to ensure that disturbance was minimized. The use of these collars permits repeated measurements at a single location, while minimizing soil disturbances (root growth into the soil and under the collar) in order to better assess temporal influences (Tufekcioglu et al, 2001). Inside chamber volume was recorded at every collar site for each measurement by averaging the height of the ground surface to the top of the collar at four reference locations. In order to collect point measurements of ET the chambers used were placed on the collars and the grooves were filled with water to obtain an air tight seal.

The sampling protocol was aimed at evaluating the change in ET dynamics over the 2005 and 2006 snow-free seasons. Measurements were obtained between the peak growth hours of 08:00 and 16:00 MST to minimize flux variations caused by the diurnal cycle (Laporte et al., 2002) and to obtain fluxes operating at maximum levels to ensure existing spatial variability is captured. All sites were measured twice per week in order to acquire a greater spatial data set over the study period, rather than the more common approach of extensively replicating a few sites less frequently (LeCain et al., 2002). As chamber measurements provide only point measurements the daily sampling order was altered by randomly selecting the sites on a daily basis to ensure a range in environmental conditions are being captured, and fluxes were grouped into climatically distinct seasonal

periods in order for temporal/seasonal comparisons to be made (see Section 2.3.1) (Petrone et al., 2008; Solondz et al., 2008; Petrone et al., 2003; Waddington et al., 1998).

2.3.6 Chamber Flux Calculations

In order to assess the fluxes of water vapour from these chamber sites, measurements of the rate of vapour density increase inside the measurement chambers were conducted as per McLeod et al. (2004). To calculate the instantaneous rate of evapotranspiration (ET_{in}) the slope of vapour pressure (e) from within the chamber was plotted against time using the least squares method. This calculated slope value was then used within a modified equation (Stannard, 1988) to calculate ET inside the chamber over the 5 min measurement interval,

$$ET_{in} = 3.6 \frac{MVC}{A} \quad (2.8)$$

where ET_{in} is the rate of evapotranspiration (mm hr^{-1}), M is the slope of the vapour pressure over time measurement for each interval ($\text{g/m}^3 \text{ s}^{-1}$), V is the volume inside the chamber (m^3), C is the calibration factor to account for vapour absorption within the chamber (dimensionless) and A is the area of ground surface covered by the chamber (m^2). The conversion factor of 3.6 was used in order to convert a volume of water per unit area ($\text{g H}_2\text{O m}^{-2} \text{ s}^{-1}$) into an hourly flux rate (mm hr^{-1}). The calculation of C was obtained through the methods outlined by McLeod et al., (2004) (see Section 6.1).

2.4 Results

2.4.1 Climate

The study site received 234 mm of precipitation during the 2005 snow-free season with the largest storm occurring on 25 July (DOY 206) delivering 45 mm (Figure 2.2). The average event during the 2005 study season was 6.8 mm. During the 2006 study season approximately 226 mm of precipitation occurred with the largest event occurring on 4 May (DOY 124) with 37.5 mm (Figure 2.2) with the average event being 7 mm. Although precipitation at Pond 40 was evenly distributed during the 2005 study season, larger magnitude events occurred more frequently from 19 June to 28 August (DOY 170–240; Figure 2.2). During the 2006 study season precipitation events occurred earlier than normal and a prolonged event free period existed from 6 August (DOY 218) through to 15 September (DOY 258). Historically 70% of the annual precipitation is received between June and August (Devito et al., 2005). This was observed during the 2005 study period but not during the 2006 study period.

Mean daily air temperatures ranged from 2.3 °C (DOY 141) to 19.6 °C (DOY 215) during 2005. An increase in mean daily air temperatures was observed in 2006, ranging from 2.5°C (DOY 258) to 24.9°C (DOY 204). Over the course of the 2005 study season, the mean daily air temperatures at the study site were similar from June to August, decreasing after DOY 210 (Figure 2.2).

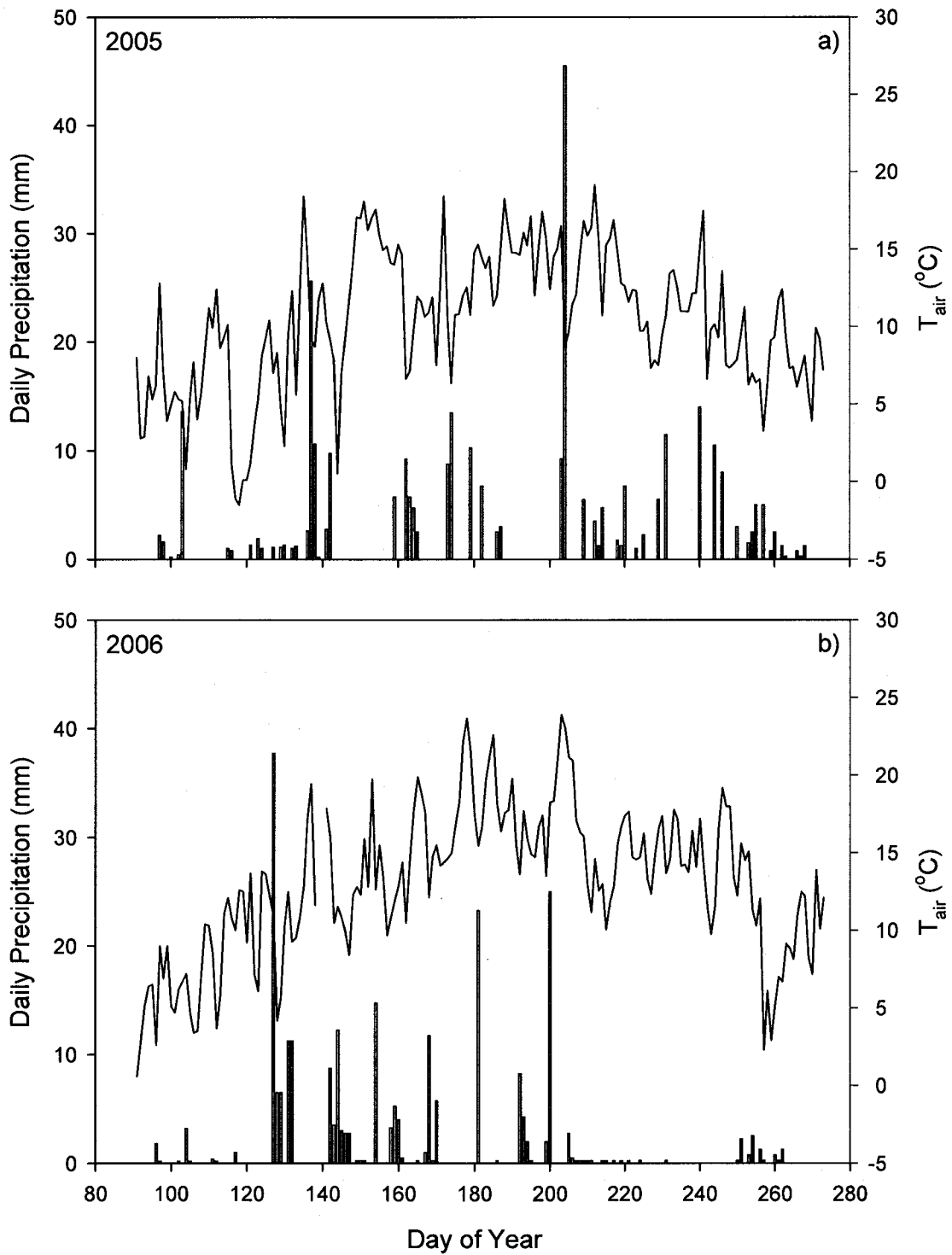


Figure 2.2: Daily precipitation (bars) and daily averaged air temperature (lines) over the (a) 2005 and (b) 2006 snow-free seasons, Pond 40, Utikuma Region Study Area (URSA), Alberta, Canada.

2.4.2 Wetland Energy and Mass Exchange Processes

2.4.2.1 Energy Flux Densities

There was no significant differences in the energy fluxes between the three sites (ANOVA, $P > 0.05$), with all sites showing similar seasonality in energy balance components with the peaks occurring at the same times during both seasons. As a result data from the three sites were averaged in order to characterize the wetland as a single unit (Figure 2.3). Daily net radiation (Q^*) peaked in 2005 on DOY 198 at 187 W m^{-2} and averaged 97 W m^{-2} for the 2005 snow-free season. During the 2006 snow-free season, Q^* peaked on DOY 179 at 156 W m^{-2} with a seasonal average of 86 W m^{-2} .

Latent heat fluxes (Q_E) were calculated using α values attained from the energy balance PET measurements coupled with the roving EC tower. These α values were then applied to the spatially averaged energy balance data to produce Q_E for the wetland over both snow-free seasons (Table 2.2). Q_E for the 2005 season peaked at 87 W m^{-2} on DOY 180 with a seasonal average of 47 W m^{-2} (Figure 2.3). For the 2006 snow-free season Q_E peaked at 82 W m^{-2} (DOY 137) with a seasonal average of 42 W m^{-2} . Statistical analysis between years showed no significant differences (ANOVA, $P > 0.05$). Ground heat fluxes (Q_G) were within 15% of daily Q^* throughout the two snow-free seasons with peaks of 21 W m^{-2} and 28 W m^{-2} for 2005 and 2006 respectively and seasonal averages of 11 W m^{-2} and 13 W m^{-2} (Figure 2.3).

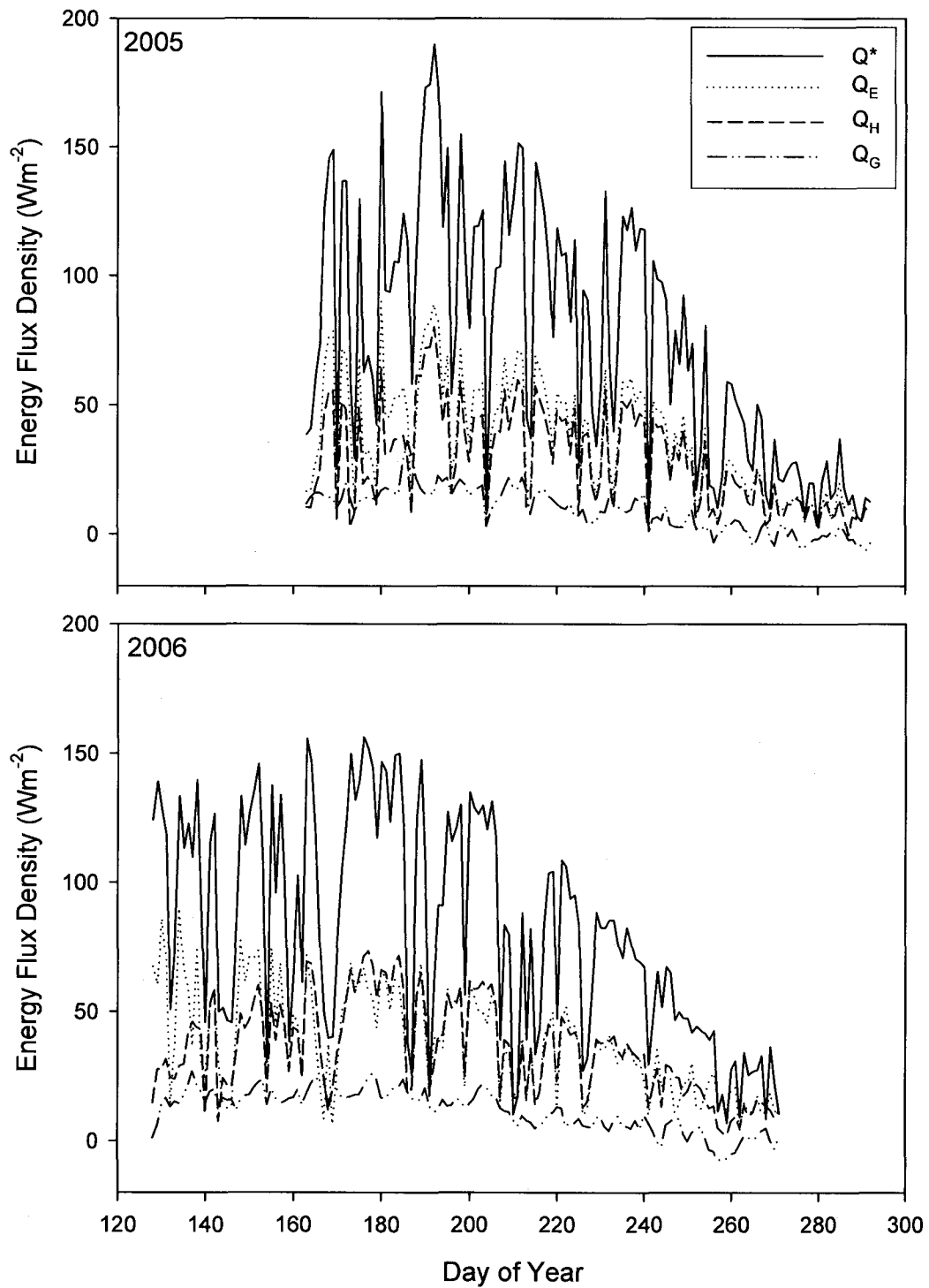


Figure 2.3: Seasonal daily averaged wetland energy flux densities for the 2005 and 2006 snow-free seasons, Pond 40, Utikuma Region Study Area (URSA), Alberta, Canada.

Site Description	2005		2006	
	Period	Alpha (α)	Period	Alpha (α)
North Site (NS)	EG	0.89 (± 0.06)	EG	0.85 (± 0.08)
	G	0.76 (± 0.08)	G	0.81 (± 0.05)
	LG	0.81 (± 0.04)	LG	0.72 (± 0.09)
Northwestern Site (NWS)	EG	n/a	EG	0.87 (± 0.11)
	G	0.84 (± 0.07)	G	0.75 (± 0.09)
	LG	0.75 (± 0.12)	LG	0.79 (± 0.10)
South Site (SS)	EG	n/a	EG	0.94 (± 0.13)
	G	0.89 (± 0.12)	G	0.81 (± 0.12)
	LG	0.81 (± 0.06)	LG	0.75 (± 0.05)

Table 2.2: Alpha (α) values calculated from the comparison of PET values and AET from eddy covariance measurements at all three peatland sites of the 2005 and 2006 snow-free seasons where (n/a) denotes time periods where measurements did not occur. Period measurements were delineated into Early Green (EG) (DOY 121 to DOY 158), Green (G) (DOY 158 to DOY 218) and Late Green (LG) (DOY 219 to DOY 260) periods and reported as arithmetic averages over the periods, Pond 40, Utikuma Region Study Area (URSA), Alberta, Canada. Values in parentheses are standard error (SE) of measurements.

2.4.2.2 Atmosphere-Surface Interactions

Vapour pressure deficits (VPD) (kPa) were measured within the wetland during the 2005 and 2006 snow-free seasons. Measurements were averaged by period for both snow-free seasons (early green (EG), green (G), late green (LG)) (Figure 2.4a). The EG period of 2005 had a VPD average of 0.76 kPa but was reduced in 2006 to 0.68 kPa. Unlike the Q_E data, significant differences were observed between years, during both the G and LG periods (ANOVA, $P < 0.05$). The G period average VPD in 2005 (0.39 kPa) was much lower than the 2006 average of 0.84 kPa, as was the LG period 2005 average VPD of 0.28 kPa (relative to the 2006 average of 0.76 kPa).

Available energy (Q^*-Q_G) provides an indication of the nature of energy use within wetland systems and along with water deficit as it can be used as an indicator for wetland ET efficiency (Stagnitti et al., 1989). Large differences in Q^*-Q_G were observed during the EG periods of 2005 and 2006 (Figure 2.4b). For the 2005 snow-free season, EG Q^*-Q_G averaged 52 W m^{-2} with an increase to 91 W m^{-2} for the 2006 season. Within the G period of 2005 Q^*-Q_G averaged 83 W m^{-2} and decreased to 86 W m^{-2} in 2006. Q^*-Q_G in the LG period averaged 41 W m^{-2} and 77 W m^{-2} in 2005 and 2006, respectively.

ET showed similar patterns within the wetland over both the 2005 and 2006 snow-free seasons (Figure 2.4c). EG period ET in 2005 for the wetland averaged 0.83 mm d^{-1} , while in 2006 it increased to 1.56 mm d^{-1} . The G period for both seasons averaged $\sim 1.46 \text{ mm d}^{-1}$ an increase in 2005 but a slight decrease from the EG period in 2006. Finally during the LG period ET was reduced to 0.74 mm d^{-1} and 1.21 mm d^{-1} in 2005 and 2006, respectively. The 2005 snow-free season showed the “typical” seasonal

variability expected of sub-humid boreal wetlands whereas 2006 saw the largest ET during the EG period.

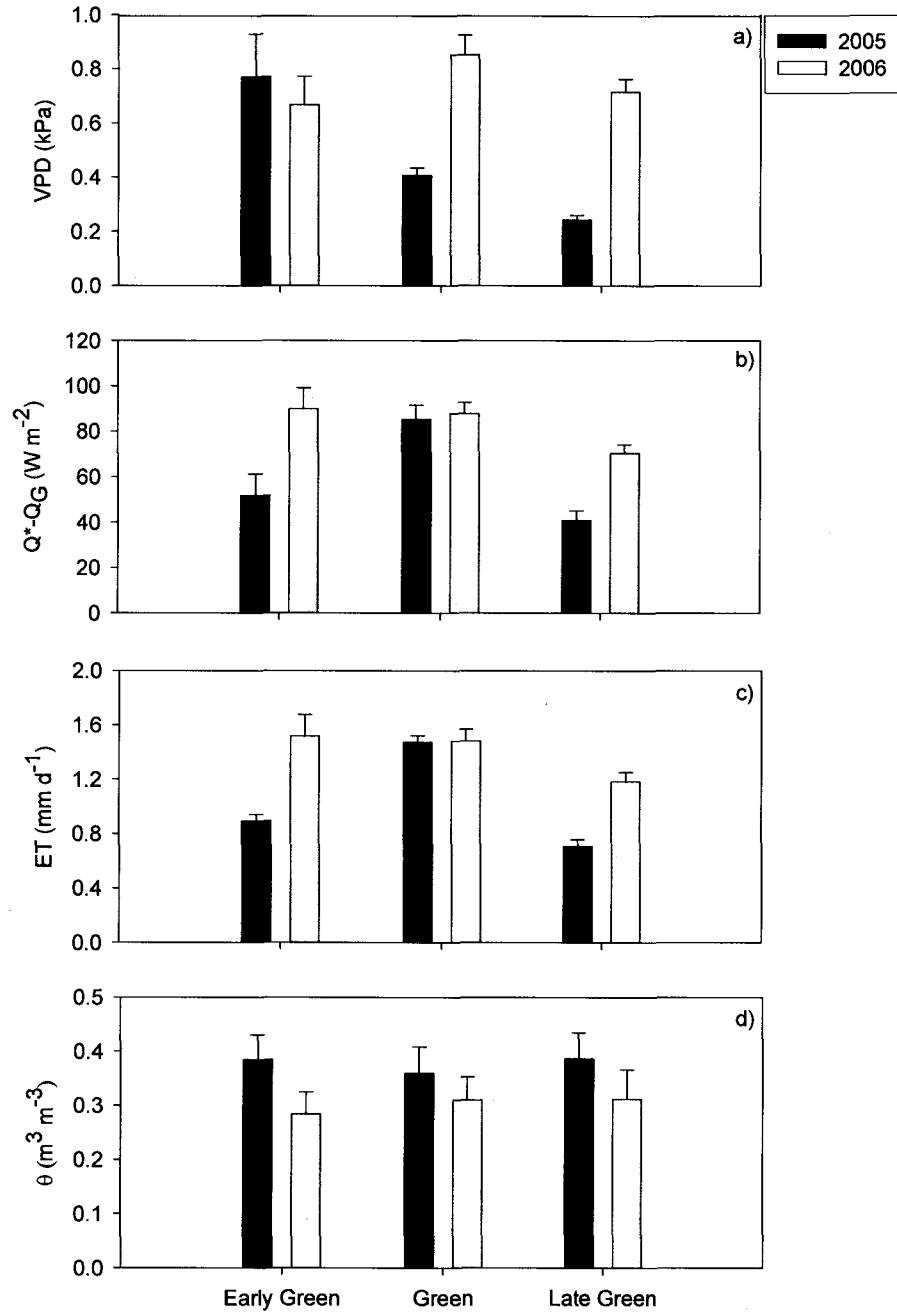


Figure 2.4: Period averages composed of Early Green, Green and Late Green for a) Vapour Pressure Deficit (VPD), b) Available Energy ($Q^* - Q_G$), c) Peatland Evapotranspiration (ET) calculated using the combined methods of eddy covariance and Priestley-Taylor model, and d) Soil Moisture (θ) ($m^3 m^{-3}$) over the 2005 and 2006 snow-free seasons, Pond 40, Utikuma Region Study Area (URSA), Alberta, Canada. Bars denote standard error (SE) of variables.

Volumetric soil moisture (θ) ($\text{m}^3 \text{m}^{-3}$) varied little throughout both snow-free seasons but differed slightly between seasons as 2005 was slightly wetter than 2006 (Figure 2.4d). θ in 2005 averaged $0.37 \text{ m}^3 \text{ m}^{-3}$ during the EG period and $0.29 \text{ m}^3 \text{ m}^{-3}$ in 2006. A decrease was observed in 2005 to $0.35 \text{ m}^3 \text{ m}^{-3}$ while a slight increase to $0.32 \text{ m}^3 \text{ m}^{-3}$ was observed during the 2006 G period. The LG period θ in 2005 increased slightly to $0.37 \text{ m}^3 \text{ m}^{-3}$ but remained steady for the 2006 period at $0.32 \text{ m}^3 \text{ m}^{-3}$.

2.4.3 Vegetation Controls on ET

Vegetation contributions can be considered a significant aspect of wetland ET, where processes at the vegetation community scale will influence total ecosystem scale fluxes. To investigate the role of vegetation, and remove the influence of time, chamber data from 2005 and 2006 were grouped and sorted by dominant surface vegetation communities. Figure 2.5 shows that no significant relationship exists between ET and VPD, or θ , in either year. However, a weak relationship between ET and VPD is observed at lower deficits and ET becomes limited as VPD exceeds 1 kPa (Figure 2.5a). While no significant relationship is present between ET and θ , the clustering of the data among the vegetation communities does suggest some vegetation controls (Figure 2.5b). While all vegetation types experience similar ranges in ET and θ over both years, the lichen tend to be wetter and the *Sphagnum* seem to be able to sustain larger rates of ET over a larger range in θ .

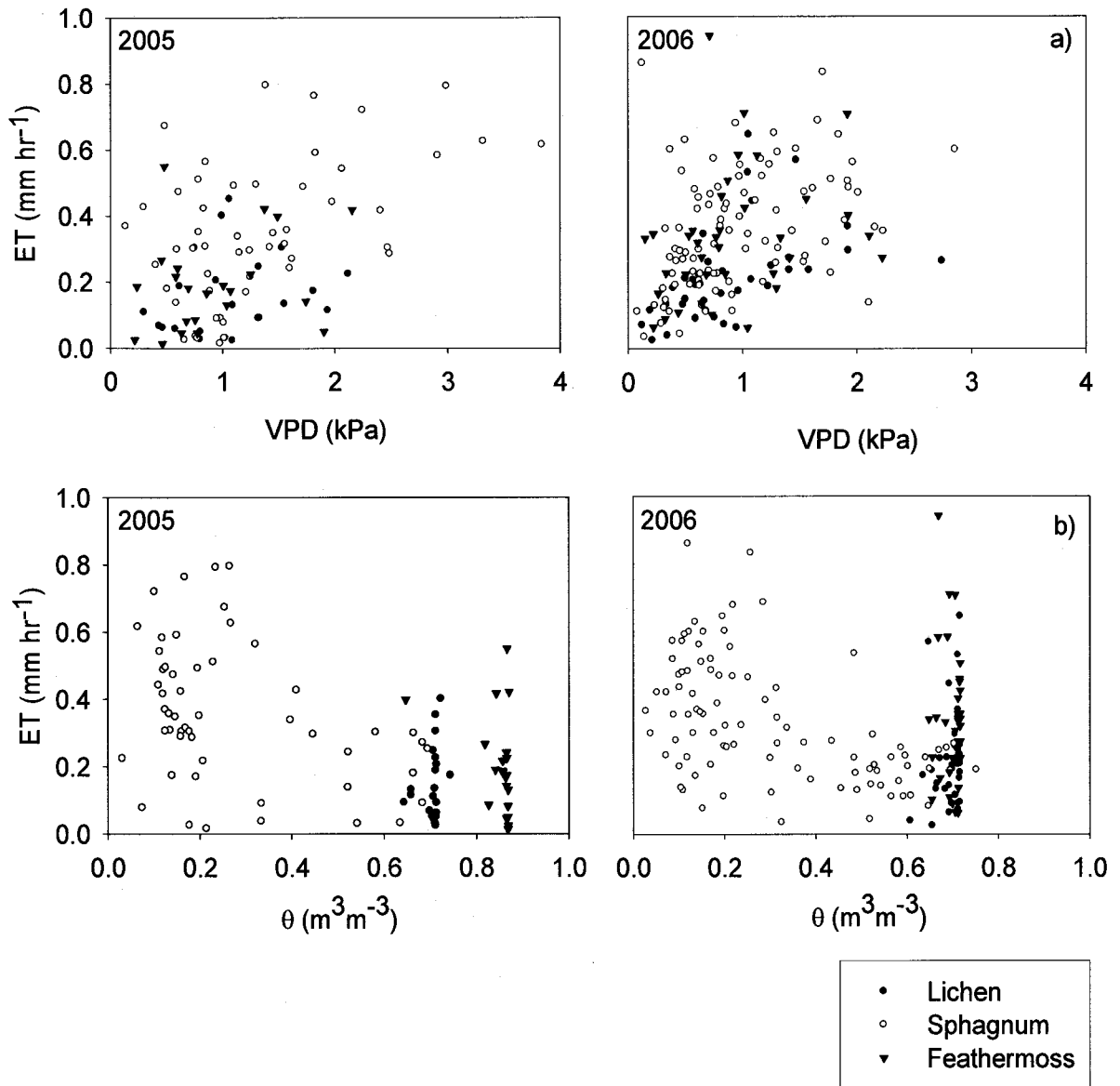


Figure 2.5: Daily chamber evapotranspiration (ET) as a function of a) Vapour Pressure Deficit (VPD) and b) Soil Moisture (θ) (m³ m⁻³) for each dominant wetland vegetation community for the 2005 and 2006 snow-free seasons, Pond 40, Utikuma Region Study Area (URSA), Alberta, Canada.

Sphagnum mosses for both snow-free seasons show the greatest ET rates peaking during the G period at ~ 0.47 mm hr⁻¹ (± 0.06) with the EG at 0.25 mm hr⁻¹ (± 0.09) and

the LG at 0.39 mm hr^{-1} (± 0.04) (Figure 2.6a). Lichen dominated sites exhibited the second largest ET rates, but peaked in the LG period at 0.33 mm hr^{-1} (± 0.10). EG period lichen contributions averaged 0.19 mm hr^{-1} (± 0.08), while G period contributions averaged 0.29 mm hr^{-1} (± 0.04). Feathermoss dominated sites showed the smallest ET rates over both snow-free seasons (Figure 2.6a), reaching a maximum during the G period of 0.27 mm hr^{-1} (± 0.06), and with similar fluxes in the EG and LG periods. Statistical analysis on the differences between vegetation community contributions showed that the *Sphagnum* contributions are significantly different from the lichen and feathermoss species contributions (ANOVA, $P < 0.05$).

θ was organized by vegetation communities in order to characterize the relationships between vegetation ET and the associated moisture regimes. Lichen and feathermoss sites were the wettest sites across both seasons and showed limited variability at ~ 0.67 (± 0.01) and ~ 0.71 (± 0.02), respectively (Figure 2.6b). The *Sphagnum* sites were significantly different from the lichen and feathermoss sites (ANOVA, $P < 0.05$). However, the moisture regimes within each of the three vegetation communities showed little variability among the three periods. The *Sphagnum* sites were relatively dry at 0.28 ± 0.03 during G period and 0.34 ± 0.03 during LG period and were not significantly different between periods. The range in θ from *Sphagnum* (~ 0.3) to lichen and feathermoss (~ 0.7) shows the variability in θ that exist within the sub-humid WBP wetlands among vegetation communities.

Seasonal variations in T_g at 5cm depths in the wetland show that *Sphagnum* sites were the warmest during the EG and G periods (4.7 and 10.1 °C, respectively) and

dropped slightly to 8.4 °C during the LG period (Figure 2.6c). Lichen sites were the coldest across the snow-free season at 2.1°C, 7.8 °C and 8.1 °C during EG, G and LG periods, respectively. Feathermoss sites peaked during the LG and G periods at approximately 9.9 °C, with the coldest temperatures for feathermoss dominated sites occurring during the EG period (3.1 °C) (Figure 2.6c). Lichen sites were significantly different from the other two vegetation communities across the season (ANOVA; $P < 0.05$).

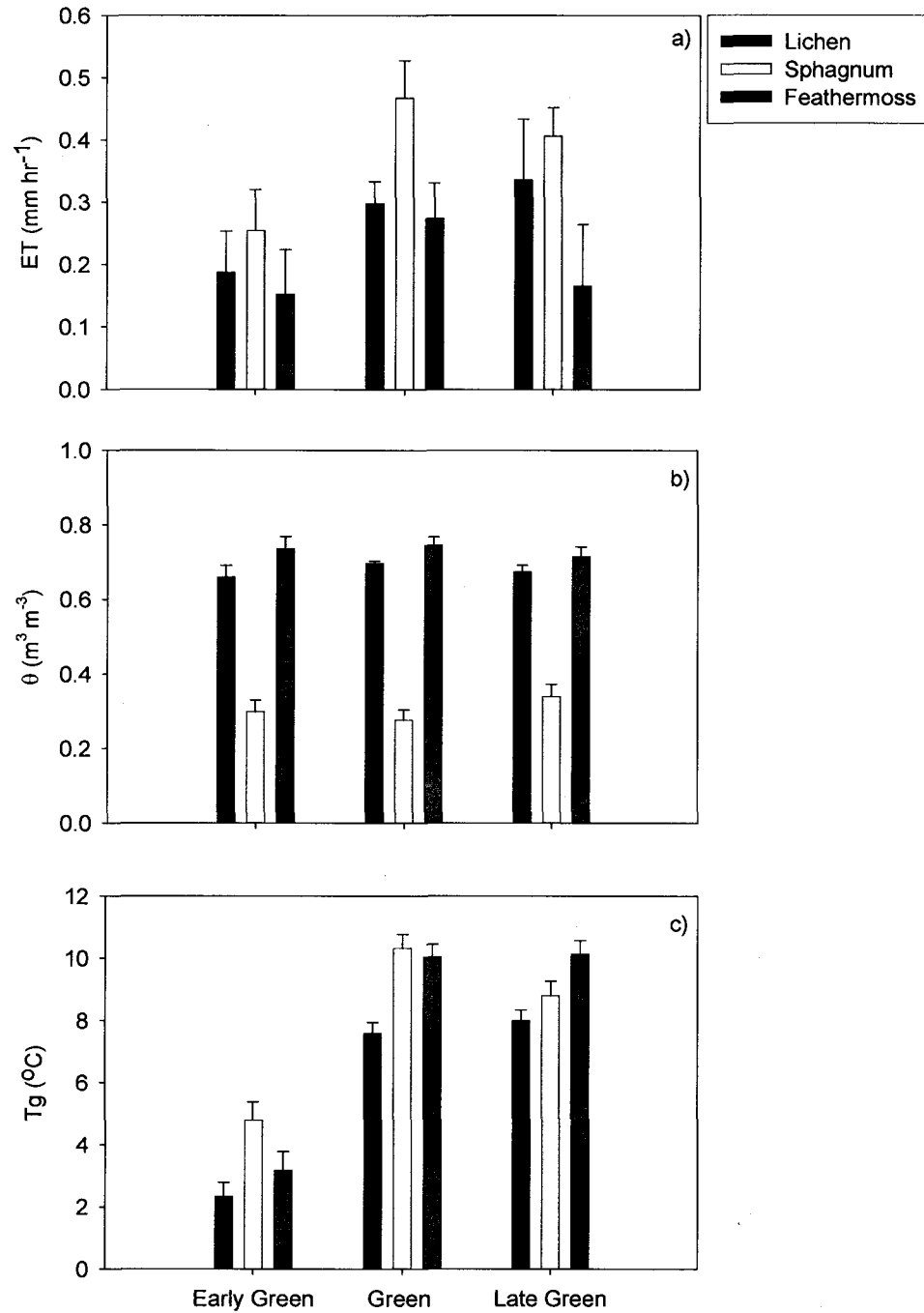


Figure 2.6: Period averaged data of a) Chamber Evapotranspiration (ET), b) Soil Moisture (θ) (m³ m⁻³) and c) Ground Temperatures (at 5 cm below ground) grouped by vegetation composition for both the 2005 and 2006 snow-free seasons, Pond 40, Utikuma Region Study Area (URSA), Alberta, Canada. Bars denote standard error (SE) of measurement variables.

2.4.4 Microtopographical Controls on Wetland ET

The distribution of surface vegetation in wetlands is largely controlled by θ , which is a function of microtopography. The chamber ET data were also grouped by vegetation and microtopography in order to address this question (Figure 2.7a). Lichen located in lawn environments showed seasonal variations in ET of 0.27 mm hr^{-1} (EG), 0.34 mm hr^{-1} (G) and 0.32 mm hr^{-1} (LG). However, lichen situated in depressions had ET rates of 0.12 mm hr^{-1} (EG), 0.22 mm hr^{-1} (G) and 0.23 mm hr^{-1} (LG). *Sphagnum* had the largest ET rates in either microtopographical unit, with no statistically significant difference (ANOVA, $P > 0.05$) between units. *Sphagnum* lawn sites had ET rates of 0.23 mm hr^{-1} , 0.41 mm hr^{-1} and 0.39 mm hr^{-1} during the EG, G and LG periods, respectively. While depression sites with *Sphagnum* had ET rates of 0.21 mm hr^{-1} , 0.40 mm hr^{-1} and 0.38 mm hr^{-1} in the EG, G and LG periods, respectively. Feathermosses were significantly different between microtopographical units (ANOVA, $P < 0.05$). Contributions from feathermoss dominated lawn sites were 0.27 mm hr^{-1} , 0.35 mm hr^{-1} and 0.33 mm hr^{-1} during the EG, G and LG periods, respectively. However, depression sites with feathermoss species had water losses of 0.10 mm hr^{-1} , 0.22 mm hr^{-1} and 0.24 mm hr^{-1} in the EG, G and LG periods, respectively.

Thermal regimes in wetland environments can also be influenced by the microtopographical changes. Lichen sites had T_g ranges that were significantly different between lawns and depressions (ANOVA; $P < 0.05$) (Figure 2.7b). Within lawn sites, T_g at lichen sites during the EG period were $6.0 \text{ }^\circ\text{C}$ (± 0.02) and climbed to $11.3 \text{ }^\circ\text{C}$ (± 0.03) during the G period and dropped slightly to $9.6 \text{ }^\circ\text{C}$ (± 0.03) during the LG period. However, the lichen depressions had temperatures of $2.2 \text{ }^\circ\text{C}$ (± 0.02), $7.5 \text{ }^\circ\text{C}$ (± 0.03) and

7.9 °C (± 0.02) for the EG, G and LG periods, respectively. T_g among *Sphagnum* sites were not significantly different between microtopographical units (ANOVA, $P > 0.05$) averaging approximately 6.1 °C for the EG period, 10.1 °C for the G period and 9.5 °C for the LG period. Feathermoss dominated sites displayed similar trends to that of the *Sphagnum* dominated sites with regards to their thermal regimes. For lawn sites, the T_g was 4.1 °C (± 0.02), 9.8 °C (± 0.03) and 9.5 °C (± 0.02) during the EG, G and LG periods, respectively. Depression sites dominated by feathermoss communities had EG T_g values of 2.5 °C (± 0.03), G period T_g of 9.4 °C (± 0.02) and LG period T_g of 9.6 °C (± 0.02).

Moisture regimes grouped by vegetation and delineated by microtopography also showed distinct trends correlated to ET rates. Lawn sites were dry with θ values ranging from 0.19 to 0.39 (± 0.04) and showed limited variability throughout the snow-free seasons (Figure 2.7c). Depression sites were significantly different when comparing lichen and feathermoss to *Sphagnum* (ANOVA; $P < 0.05$). Lichen and feathermoss showed limited seasonal variations in θ , ranging from 0.65 to 0.71 (± 0.02), while *Sphagnum* were significantly drier at approximately 0.25 (± 0.03) across the snow-free seasons. The most significant feature of Figure 2.7c is the fact that there is no significant difference in *Sphagnum* θ between lawns or depressions (ANOVA, $P < 0.05$).

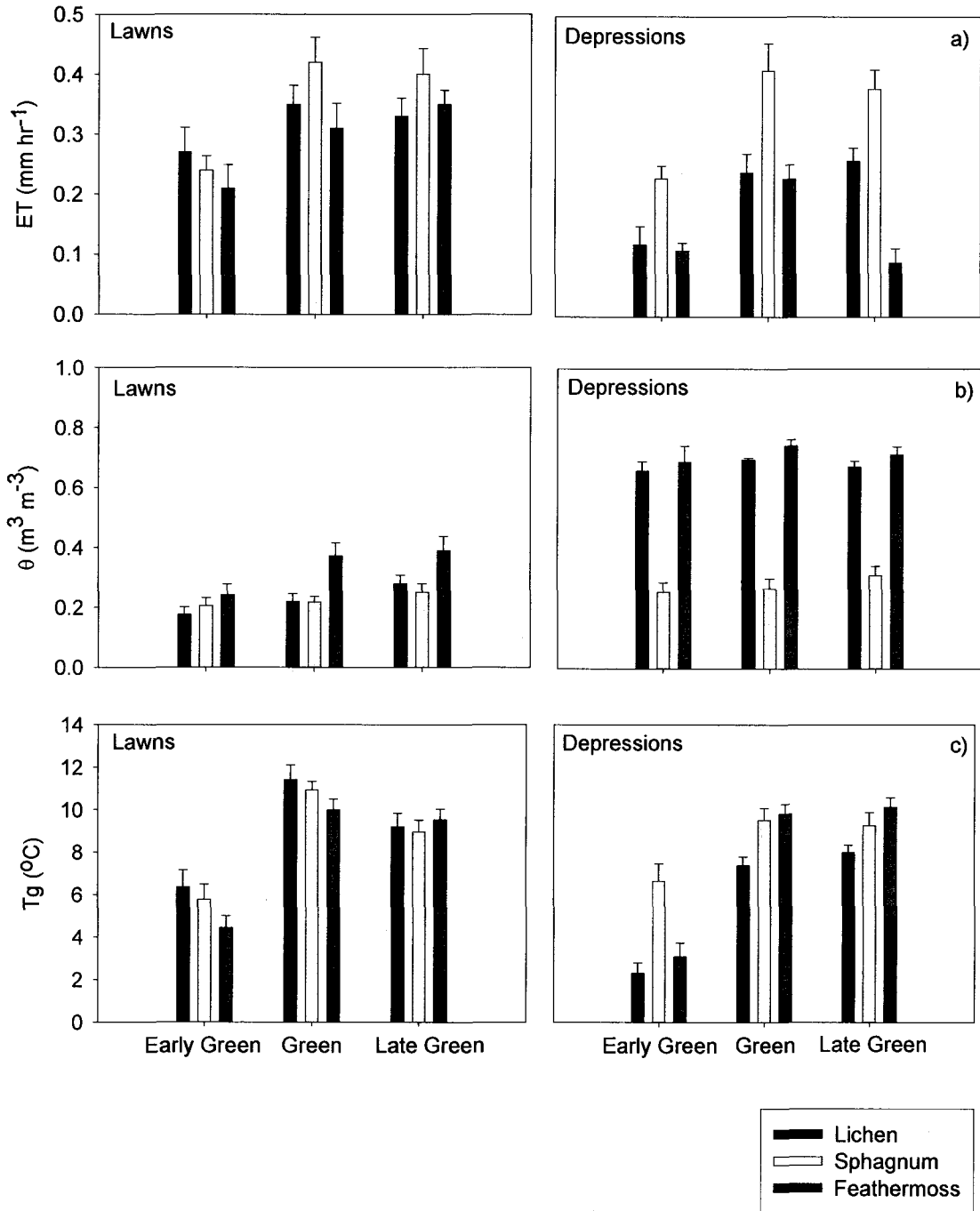


Figure 2.7: Period averaged a) Chamber Evapotranspiration (ET), b) Soil Moisture (θ) ($\text{m}^3 \text{m}^{-3}$), and c) Ground Temperatures (at 5 cm below ground) (T_g) for microtopography (lawns and depressions) over 2005 and 2006 snow-free seasons, Pond 40, Utikuma Region Study Area (URSA), Alberta, Canada. Bars denote standard error (SE) of measurement variables.

2.4.5 Regulation of Wetland ET by Persistent Seasonal Ground Ice

Examining the cumulative ET for the three main wetland sites over the snow-free season indicate the differences in controls on ET that occur within a wetland environment in the WBP over the course of a season (Figure 2.8a). Seasonal totals in ET for the wetland were 226 mm and 247 mm in 2005 and 2006, respectively. An interesting feature of Figure 2.8a is the response of the slope of the cumulative ET curve early in the season, where despite lower available energy the slope of the ET curve is still quite steep. This is especially true in 2005, for example, where the ice layer is at a significant depth below the surface.

A persistent ice lens was measured and observed throughout the wetland over both the 2005 and 2006 snow-free seasons (Figure 2.8b). When comparing the ice lens data to the change in water table (WT), it can be noted that the position of the WT during the early season is trapped above the ice lens resulting in early season peaks in WT position until the wetland responds to mid season precipitation events when ice out has occurred. It was determined that ice out has effectively occurred once the depth to ice had reached 70 cm and the influence of the ice lens on the near-surface hydrology of the wetlands would be limited. Melt rates for both seasons were not significantly different from each other (ANOVA, $P > 0.05$). Early season WT fluctuations were observed at all sites over both years but were limited by the position of the ice lens within the wetland. As the water is trapped by the slowly melting ice layer WT position fluctuates close to the retreating ice lens and is sustained only by lateral flow within the wetland or by precipitation events. This occurs until ~DOY 204 in 2005, and DOY 198 in 2006, where the retreat of the ice lens is sufficient enough to allow the WT to rise close to the wetland

surface and steadily decline for the remainder of the season, albeit at a greater rate in 2006 (Figure 2.8c).

Figure 2.8d shows the seasonal daily averaged θ of the upper 20cm for the examined wetland over both the 2005 and 2006 snow-free seasons. During the 2005 season sharp increases in θ were observed on DOY 204 of $0.15 \text{ m}^3 \text{ m}^{-3}$ as a result of a large precipitation event (45 mm). A similar trend is not observed during the 2006 snow-free season. Wetland θ remained relatively steady throughout the 2006 season ranging between $0.39 \text{ m}^3 \text{ m}^{-3}$ and $0.45 \text{ m}^3 \text{ m}^{-3}$.

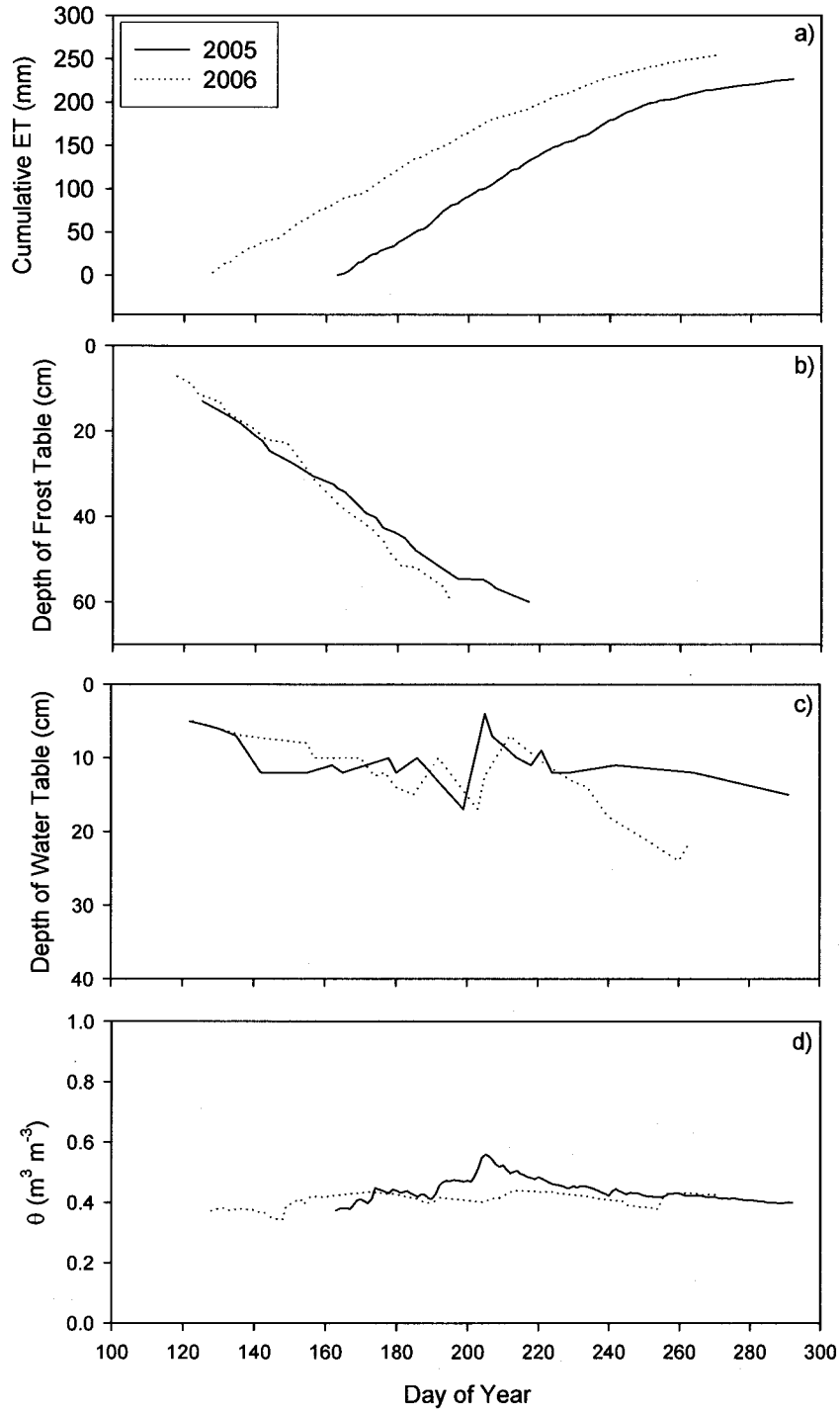


Figure 2.8: Daily averaged a) Cumulative Wetland Evapotranspiration (ET), b) Depth of Frost Table (cm below ground surface), c) Depth of Water Table (WT) (cm below ground surface) and d) Soil Moisture (θ) ($\text{m}^3 \text{m}^{-3}$) of the upper 20 cm of peat soil for both the 2005 and 2006 snow-free seasons, Pond 40, Utikuma Region Study Area (URSA), Alberta, Canada.

2.5 Discussion

ET and ground temperature patterns here do not follow the “typical” seasonal variability as depicted by other ET studies in the boreal forest (Baldocchi et al., 1997; Cuenca et al., 1997; Grelle et al., 1997; Cienciala et al., 1998; Rouse, 2000; Amiro et al., 2006), where seasonal trends are depicted on the variability of evaporative fluxes and the predicted peaks in ET coupled with the warmest temperatures (July). However, the temperature regimes during the early green period, when the presence of a melting ice layer consumes a significant portion of the available energy are associated with peak ET rates. That is, vegetation communities such as *Sphagnum* mosses show unique and consistent ET characteristics that are not a function of soil moisture and the typical catchment characteristics that control the patterns in soil moisture.

2.5.1 Vegetation Controls on Wetland Evapotranspiration

The vegetation composition within wetland environments of the WBP is highly dependent on the spatial variability of the wetlands moisture regime. *Sphagnum* mosses exist within less wet moisture regimes, whereas feathermosses have the ability to thrive in moisture rich environments. ET rates from differing vegetation communities within a wetland environment show the extent to which these relationships occur within a natural system. *Sphagnum* mosses lose water at the highest rates throughout the growing seasons of the WBP despite their drier conditions, a result of their ability to retain moisture within the cushion and their self-regulating of water table position (Price, 1997). Lichen species ET rates are second to those contributed by *Sphagnum* mosses, a result primarily of their location within the wetlands. For all sites, lichen species were located as additional

growth above *Sphagnum* moss mats. Thus, the ability to completely delineate the contributions of lichen species was inhibited by the presence of an underlying *Sphagnum* mat, where the greatest rates of ET were observed during both seasons. Lab experiments conducted on isolated lichen species show a reduced rate of evaporative losses compared to this study (Bisbee et al., 2001). However, within the natural system, a lichen patch underlain by *Sphagnum* mat is common (Bisbee et al., 2001), indicating that the contributions of both wetland species in a combined setting is a more appropriate approach to analysis within the WBP.

The physiological controls of *Sphagnum*, feathermoss and lichen species vary considerably between species. As *Sphagnum* lack specialized water absorption and internal water conduction systems (Nichols and Brown, 1980), water is transported and conducted by an external wicking system and adsorption along the stem and leaf surfaces (Bold, 1957; Nichols and Brown, 1980). Whereas, the growth of feathermoss species (*Hylocomium splendens*) is controlled by rainfall frequency and degree of protection from evaporation stress. Therefore, feathermosses are primarily restricted to areas sheltered by trees and shrubs and require shade, moderate water levels, and high nutrient levels (National Wetlands Working Group, 1988). Feathermoss species have a tendency to dry up quickly when canopy cover is not adequate to prevent high evaporation. This is evident in the distribution of feathermosses seen here.

Soil moisture and vegetation interactions are a significant control on wetland ET because while the presence of vegetation is dependent on the localized soil moisture regime, it is more strongly controlled by microclimatic factors, especially canopy closure

(Solondz et al., 2008). Further, as shown here the moisture regime of a wetland is utilized differently by the dominant vegetation units. Williams and Flanagan (1996) found that ET decreases with wetland moisture even though the VPD increased, a result of a decrease in the surface conductance as moss systems lack the vascular tissues and stomata to transmit water through the leaf structure. Further, limited lateral gradients of flow exist within the WBP (Devito et al., 2005) and the vertical components of moisture exchange are enhanced (Smerdon, 2005). Thus, any increased localized moisture patterns only act to promote the vertical movement of water within the WBP as the gradients are induced by the differences between moisture rich peat surface and the drier air above (Williams and Flanagan, 1996).

The atmospheric controls on ET from the wetland environment studied show that little correlation can be made between the VPD and ET. With the presence of smooth canopies the strongest relationships are found between ET and available energy with limited, if any controls by the VPD and stomata of the resident communities (McNaughton and Jarvis, 1991). The importance of the sheltering between and among sites shows distinct trends in ET rates across the examined wetland. Direct canopy cover is a control in terms of limiting incoming radiation receipt at the surface along with limiting the boundary layer and subsequent leaf surface interaction with convection. Thus, gradients that are created from the leaf surface to the atmosphere (VPD) are dependent on the nature of the temperature regime, along with the available moisture conditions in which the gradient is formed.

2.5.2 Vegetation and Ground Thermal Influences on Wetland Evapotranspiration

Thermal controls of vegetation on ET have also been determined to be significant when examining wetland ET rates across Boreal landscapes (Nijssen et al., 2002; Rouse, 2000). However, this study observed limited, if any, direct relationships between soil thermal regime and wetland ET from this WBP wetland. Nichols and Brown (1980) found that within wet *Sphagnum* moss mats an increase in temperature (air temperature), which can be transferred to the thermal ground regime (as *Sphagnum* and feathermoss leaf and associated ground temperatures appear to follow the diurnal fluctuations of localized air temperatures closely), resulted in an increased rate of ET from the moss surface. That is, in environments where ET can be expected to occur at near potential rates, temperature is strongly correlated with ET. This was not the case for this study in a much drier environment. The thermal regime here showed a distinct seasonal pattern, while ET rates showed spikes during the early season, when moisture is high (a result of the underlying ice lenses) and moss growth was limited, and generally lower rates during the drier growing period (despite peak moss growth rates), with periodic spikes following rain events. In this system the net effect of the thermal regime is the magnitude of soil heat flux, which peaks during the early season, but is drastically reduced after the ice retreats below 0.30 m. This 0.30 m threshold for which a change in soil heat flux is observed also approaches the position to which capillary action is limited by *Sphagnum* mosses (Price, 1997), indicating a relationship between thermal and moisture characteristics of the wetlands.

The surface vegetation and canopy cover also controls ET by influencing rates of ground thaw, especially early in the season (Petrone et al., 2006). Examining the seasonal energy balance of the wetland, a clear peak in early green ET rates can be observed. A persistent early season ice lens throughout the wetland acts as an impermeable layer to moisture close to the surface. This impermeable layer acts to prevent infiltration of incoming precipitation events, and early season snow and ice melt thus creating a moisture rich wetland beyond the initial snowmelt period. As the ice begins to melt out and T_g is increased, ET will begin to be reduced within the systems. The water that is present at the surface will then gain the ability to infiltrate downwards and merge with the existent groundwater that is trapped from vertical movement. As the majority of flow within WBP catchments is vertical in nature, the system becomes infused with the additional water that is received below the surface of the peat with the melt out of the ice lenses. Acting to raise the water table above the decreasing ice lens via fissures and cracks that have been created with the melt process allows for the ET rates to remain relatively constant and proceed under the aforementioned controls through the remainder of the growing season.

2.6 Conclusions

The role that vegetation plays in controlling wetland ET within the WBP is significant. However, the significance of that role is governed by the moisture regimes in which the vegetation are present. The dynamics of wetlands, especially within the WBP, and their respective ET contributions can be directly connected to their respective constituent vegetation communities. *Sphagnum* dominated sites have shown to lose water at the

greatest rates to ET, yet *Sphagnum* sites show the lowest moisture regimes and no control of microtopography. This is a result of the existence of weak hydrological gradients between lawn and depression units of wetlands, consistent with the climatic and moisture regimes of such sub-humid environments, where precipitation is typically less than PET.

Finally, the presence of seasonal ice lenses plays a significant role in controlling ET within all units of wetlands of the WBP. It can be concluded that, the net effects of the presence of ice will not affect the ET rates on an annual scale, but will rather affect the early season rates of ET, and therefore the seasonal distribution of ET. Ice lenses have the potential to shift peak ET rates from wetlands to earlier on in the snow-free season when peak vegetation growth has not yet occurred creating a situation where peak ET rates occur before the maximum soil moisture demands of seasonal maximum vegetation growth. Given the role of ice lenses in wetlands of the WBP, the role that climatic variability will play could potentially have an impact on the severity of early season ET fluctuations.

Therefore, when designing an approach to quantify or model wetland ET from sub-humid regions such as the WBP, it is essential to characterize vegetation community patterns. That is, differences in surface cover vegetation, regardless of the overlying canopy cover and general nature (classification) of the wetland can contribute to significant spatiotemporal variability in ET.

Chapter Three

Evapotranspiration from above and within a Western Boreal Plain aspen forest

3.0 Introduction

At the southern edge of the boreal forest, deciduous aspen are found with a northern limit roughly corresponding to the 13°C July isotherm (Peterson and Peterson, 1992). Of the geographical areas where *Populus* are the predominant genus, over 71% (ground area basis) occurs in the boreal forest region with 20-40% of Canada's aspen/poplar stands located in the prairie provinces (Peterson and Peterson, 1992). In fact, 13.5% of the southern boreal forest is dominated by aspen stands while another 15.4% is covered by mixed deciduous forests (Hall and Allen, 1997; Blanken et al., 2001). However, only recently has aspen been recognized as an economically important species with a variety of uses such as pulp, stand board, lumber, plywood and fuel experiencing an increase in harvesting practices. Further, the impact of global climate change on precipitation and temperature regimes on the Western Boreal Forest (WBF) threatens to significantly alter forest water budgets (Wullschleger and Hanson, 2006). Although aspen are intolerant to shade, they are able to colonize disturbed areas quickly since they are a clonal species (Blanken et al., 2001). This is especially significant in the Western Boreal Plain (WBP) portion of the WBF, which supports a significant portion of Canada's merchantable aspen stands within a sub-humid climate. The role of aspen within this climatic setting is significant as aspen are a high water use species and as such require an ample regional water supply (Blanken et al, 2001). Thus, the atmospheric interactions of aspen stands with the hydrologic cycle need to be understood within this climatic setting.

Over many landscapes, plants exert a strong control on evaporation processes, because of their ability to access, transport, and evaporate water that would otherwise be detached from terrestrial water cycles (Calder 1998; Nosoetto et al. 2005). The deciduous nature of aspen in addition to their clonal root systems has an especially important effect on the water and energy exchanges from these southern boreal portions of the boreal forest (Blanken et al., 2001). In addition, the sparse and trembling nature of aspen crowns often allows a sufficient amount of light penetration and the proliferation of understory species such as *Rosa acicularis* and *Viburnum edule*, which also contributes to the canopy energy and mass exchanges. Whether the shrub understory found in aspen stands is a result of the ample light penetration or due to the relatively higher nutrient status of *Populus* ecosystems is not clear (Blanken, 1998). Regardless though, well developed deciduous shrub understories (*Rosa acicularis* and *Viburnum edule*) are typical within aspen stands (Peterson and Peterson, 1992) and the extensive areal cover and relatively large leaf area of this understory species necessitates the importance of the understory relative to the overstory in terms of water and energy exchange be quantified.

Total evapotranspiration (ET) from a boreal forest stand can be partitioned into three main source components: canopy evapotranspiration (ET_C), understorey evapotranspiration (ET_B) and evaporation from the soil surface (E_s) (including bare soil, grasses, mosses and herbaceous species), with ET given as:

$$ET = ET_C + ET_B + E_s \quad (3.1)$$

Despite a large body of literature, there is still considerable uncertainty about this partitioning of ET into its various components and their key controls in boreal forest ecosystems, especially in the climatically tenuous WBP. Previous studies in other regions

of the boreal forest have recognized canopy wetness as the main driver of the above canopy water flux (Barbour et al. 2005). The degree, to which these two main (ET_C and ET_B) components dominate the partitioning of forest water fluxes on daily or annual timescales is largely determined by the openness of the canopy and character of the rainfall. Closed-canopy forests often see limited contributions from the other sources of forest water flux (i.e. understorey evapotranspiration and evaporation from the forest floor) because of the small amounts of advected and radiant energy available below the canopy (Wullschleger et al. 1998a). In contrast, open-canopy forests may see much larger contributions from these components (Barbour et al. 2005; Unsworth et al. 2004), but few studies have examined this relative to the different layers within the forest stand (Blanken et al., 1998).

ET_C is generally the largest component of both the total water vapour flux to the atmosphere and the water budget in forested ecosystems (Schafer et al. 2002). Extensive work has been conducted investigating the environmental controls on ET_C by comparing measurements of sap flow velocity with soil and environmental variables (Bovard et al., 2005; Kurpius et al, 2003; Wullschleger et al. 1998a; Hogg and Hurdle, 1997). Studies have shown that much of the variation in ET_C can be explained by variation in vapour pressure deficit (VPD) (Kurpius et al, 2003; Hogg et al., 2000; Hogg et al., 1997; Hogg and Hurdle, 1997) suggesting a strong linear relationship until a transitional VPD threshold is reached, after which ET_C tends to remain relatively constant. Linear dependencies of ET_C to VPD were found to exist until a threshold VPD of 1.0 kPa in a boreal trembling aspen (*Populus tremuloides*) stand in Saskatchewan, Canada, above

which, a lack of a transpiration response to VPD to be a stomatal response to high VPD (Hogg and Hurdle, 1997).

The ET and VPD relationship can also be sensitive to soil water supply (Cinnirella et al., 2002; Wullschleger et al. 1998a), but even fewer have examined this relative to the different layers within the stand (Blanken, 1998). Relatively little is known about how soil moisture (θ) and VPD interact with each other to influence ET_C (Bovard et al., 2005). Previous studies have suggested a strong negative feedback between VPD and canopy conductance, which when coupled with insensitivity to typical θ variations, may result in similar growing season ET_C rates between forests growing in comparable climates (Humphreys et al., 2003; Oren and Pataki, 2001; Roberts, 1983). Some studies have shown that stomatal conductance is generally unaffected by θ until a deficit occurs, at which point transpiration is limited, as trees close stomata in an effort to conserve water (Cinnirella et al., 2002; Irvine et al., 2002; Phillips and Oren, 2001; Wullschleger et al., 1998a). Further, the deficit required to induce change in canopy transpiration differs from site to site, and within a stand, most likely due to differences in vegetation type and soil texture, as different plants respond differently to given soil water states (Roberts, 2000).

3.1 Study Objectives

The objective of this study is to characterize the dynamics of the energy balance and ET above and within an aspen dominated upland in the sub-humid WBP with a focus on the roles of vegetation and atmospheric conditions. It is hypothesized that above canopy aspen dominated ET will be controlled primarily by the vegetation present, thus outlining the roles of aspen overstory (*Populus tremuloides*) with an herbaceous

understory (*Rosa acicularis* and *Viburnum edule*) structure within a small boreal forest catchment. Consequently, these controls are characterized spatially and temporally throughout the 2005 and 2006 snow free seasons. Secondly, it is hypothesized that *VPD* and θ will act as both a control and limitation on whole stand ET, primarily through their influence on the above canopy flux.

3.2 Study Site

3.2.1. Utikuma Region Study Area

The catchment studied here is located within the Utikuma Region Study Area (URSA), 370 km north of Edmonton, Alberta, Canada (56°4' N, 115°28' W; Figure 3.1). URSA is situated approximately 150km south of the discontinuous permafrost zone (Woo and Winter, 1993) within the Plains region of the Western Boreal Forest. Climate within URSA can be characterized by cold winters and warm summers with average temperatures of -14.6 to 15.6 °C (Environment Canada, 2005). Annual potential evapotranspiration (PET) averages 517 mm (Bothe and Abraham, 1993), which is slightly higher than the average annual precipitation of URSA (481 mm) (Environment Canada, 2005). However, Devito et al. (2005) report that on an average cycle of 10-15 years, annual precipitation surpasses evapotranspiration, although within the sub-humid WBP, a water deficit exists during most years. Further, approximately 70% of annual precipitation occurs between June and August and is followed by a relatively dry period during the fall (Ferone et al, 2004); this period of peak precipitation also coincides with the period of maximum evaporation demand (Devito et al, 2005a; Petrone et al, 2006).

Snowfall in this area averages less than 100 mm yr⁻¹ and represents less than 25% of the total annual precipitation for the region (Marshall et al., 1999; Devito et al, 2005a).

URSA is characterized by the presence of low relief rolling moraines, low lying clay plains and coarse textured outwash plains (Ferone et al, 2004). This study was conducted on the moraine portion of the region where glacial tills range from 20 to 240 m in thickness and overlie the Upper Cretaceous Smoky Shale Group (Vogwill, 1978) (Figure 3.1). The natural drainage patterns of the region are northward towards the Peace River Basin but are not well developed due to the presence of many depression lakes, ponds and wetland systems that are not connected with the integrated drainage network of the region (Vogwill, 1978). The moraine landscape was chosen as these systems are dominated by the presence of vertical exchanges of water (Devito et al., 2005a; Redding et al., 2006; Redding and Devito, 2008) making this the most susceptible area to any fluctuations in climate (Devito et al, 2005b).

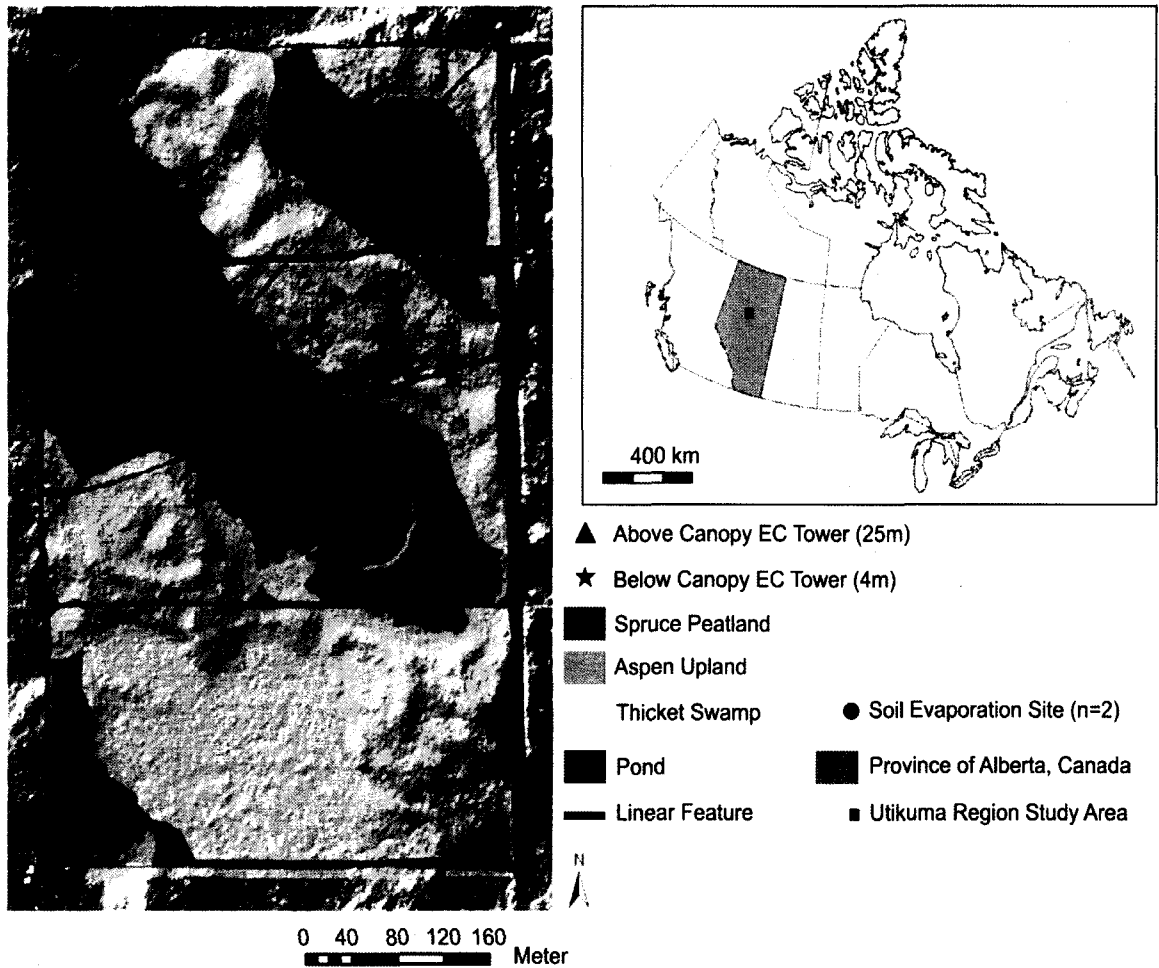


Figure 3.1: Schematic diagram of the research catchment, location of the instrumentation and dominant vegetation landcover units comprising the catchment, Pond 40, Utikuma Region Study Area (URSA), Alberta, Canada.

3.2.2 Study Catchment

The overstory canopy of the study catchment is predominantly trembling aspen (*Populus tremuloides*), with sporadic clusters of black poplar (*Populus balsamifera*) in depressions and ephemeral draws (Figure 1). The understory vegetation at the site is dominated by Alberta rose (*Rosa acicularis*) and low bush-cranberry (*Viburnum edule*) in the shrub

layer, and twinflower (*Linnea borealis*) in the herb layer. The forest floor surface is dominated by aspen litter with small amounts of mosses (*spp*) and lichens (*spp*). Above canopy (ACEC) and below canopy (BCEC) eddy covariance measurements were established at two towers in an upland area consisting of Gray Luvisolic soils (Soil Classification Working Group, 1998) developed from disintegration moraine deposits, which are typically silt-rich but spatially heterogeneous, with zones of high clay or sand contents (Redding and Devito, 2008; Fenton et al., 2003).

3.3 Methods

3.3.1 Above and Below Canopy Eddy Covariance Measurements

The EC technique was used to measure vertical fluxes of momentum, sensible heat (Q_H) and latent heat (Q_E) on a continuous basis above an aspen dominated stand during the 2005 and 2006 snow-free seasons. The ACEC tower was located on the upland south facing slope (SFS) of the study catchment at 7.0 m above the canopy at peak growth. The measurement system consisted of a three dimensional sonic anemometer (CSAT3; Campbell Scientific, USA), an open-path infrared gas analyser (LI-7500; Li-Cor, USA) and a fine-wire thermocouple located in the approximate centre of the sonic head, which was located 25.0 m above the ground. The IRGA was calibrated as outlined in section 2.3.4. Both wind speed and water vapour concentration measurements and their fluctuations were obtained at a frequency of 20 Hz. Mean horizontal (v') and vertical (w') wind velocities were mathematically rotated to zero following the procedure of Kaimal and Finnigan (1994). Q_E and Q_H were calculated as the product of the mean covariance of the vertical wind speed fluctuations (w') and the scalar fluctuations in water vapour

density (ρ_v') and temperature (T') as described by Webb *et al.* (1980). The running mean was based on a 300 s time constant; the resultant mean fluxes and various wind components were computed every 30 min on a CR23X data-logger (Campbell Scientific, USA). The ACEC also consisted of a net all-wave radiation sensor (NR-lite; Kipp and Zonen, Netherlands) mounted 24.5 m above the ground on a boom that projected 1.5 m horizontally from the tower. Air temperature and relative humidity were measured at 24.5 m above the ground surface (HMP45C; Vaisala Oyj, Finland). Power to the tower was supplied via six solar-powered 12 volt deep-cycle marine batteries with regulators, maintained by two 60 watt solar panels.

Supplemental soil thermal and moisture data was collected at a second tower approximately 20 m up slope from the ACEC tower. Soil heat fluxes (Q_G) were measured using two heat flux transducers (HFT-03; Campbell Scientific, USA), buried 0.05 m below the litterfall horizon (LFH) - soil interface, and soil temperature and heat storage in the upper 0.05 m with a thermopile (TCAV-L; Campbell Scientific, USA). Supplemental data was sampled at 60 s intervals and recorded every 30 min on a CR10X data-logger (Campbell Scientific, USA). Soil moisture (CS616 TDR; Campbell Scientific, USA) and soil temperature using thermistors (107B; Campbell Scientific, USA) were recorded at depths of 0.01, 0.10, 0.30, 0.50, and 1.0 m below the LFH-mineral soil interface. Soil suction (ψ) was measured in profile at 0.1, 0.3 and 0.5 m using soil tensionmeters (SW-033; Soil Measurement Systems, USA). Precipitation was measured 30 m south of the ACEC tower using a RM Young Tipping Bucket (52202;

R.M. Young, USA) with a Tru-Chek metric rain gauge as backup for any missing data points.

A mobile eddy covariance (EC) tower was used to permit the rapid, but rigorous, comparison of surface fluxes among the understory components of the catchment (Eugster et al., 1997). Continuous half-hourly ET fluxes were measured at 3.5 m above the surface within the aspen understory for both the 2005 and 2006 snow free seasons. The BCEC tower was situated 20 m upslope of the ACEC tower for a 35 day period during green up in 2005 and 33 days in 2006 before being rotated every two weeks from June 3 to October 5 in order to characterize the fluxes from varying sites within the catchment over both seasons at the temporal scale of synoptic variability (Eugster et al., 1997). The BCEC was comprised of identical instrumentation and sampling protocols as outlined above for the ACEC. Due to the relatively small fetch area of the BCEC site, the EC sensors were located at 3.5 m above the surface in order to obtain a flux representative of the understory species examined.

3.3.2 EC Data Filtering and Gap Filling

Footprint analysis to determine the contributing areas to the measured fluxes at the two tower heights was done according to Schuepp et al. (1990). Results from the footprint model were used to filter-out data that originated outside the area of interest. In order to ensure that both the ACEC and BCEC sensors captured a representative flux power spectral density functions were computed using high frequency EC data (20 Hz) to determine if the sensor location and sampling intervals were sufficient to capture the large lower frequency and small higher frequency eddies (Petrone et al., 2001). Prior to

analysis, the EC data was corrected for density effects (Webb et al., 1980; Leuning and Judd, 1996) and sensor separation (Leuning and Judd, 1996; Blanford and Gay, 1992) (see Section 6.2). As a final correction to the flux data the energy balance closure was calculated and forced for the study period (Petrone et al., 2001). The energy budget for ACEC and BCEC can be described as;

$$Q^* = Q_E + Q_H + Q_G + J_t \quad (3.2)$$

where Q^* is net radiation (Wm^{-2}), Q_E is the latent heat flux (Wm^{-2}), Q_H is the sensible heat flux (Wm^{-2}), Q_G is the soil heat flux (Wm^{-2}) and J_t is the canopy storage (Wm^{-2}). It was calculated based on slope regressions of Q^* as outlined in Blanken et al. (1998). Typically, eddy covariance underestimates turbulent fluxes (Q_H and Q_E) resulting in a residual flux density. Causes for this underestimation have been examined in great detail within the literature and are commonly ascribed to high- and low frequency eddies that are not measured at the sampling frequency (20 Hz) (i.e. Mahrt, 1998; Massman, 2000; Finnigan et al., 2003) and different effective measurement areas of radiation components and flux components and their respective measurement errors (Aubinet et al., 2000; Twine et al., 2000). In this study, Q_H and Q_E were corrected for underestimation by EC by adjusting for energy balance closure (i.e. Barr et al., 2002; Wilson et al., 2000). The slope of the relationship between net radiation minus ground heat flux (Q^*-Q_G) and the total turbulent flux ($Q_H + Q_E$) indicated that EC underestimates turbulent fluxes by 21% for all measurement periods. There were no significant inter-annual differences in the closure estimates, nor were there significant differences associated with wind direction. Closure is most reasonably forced by assuming that the measured available energy is

representative of the plot that the EC sensors are measuring (Petrone et al., 2001), leaving the sensible and latent heat fluxes to be adjusted (Twine et al., 2000). It was assumed that the Bowen ratio was correctly measured by the EC system and individual values of the sensible and latent heat fluxes were adjusted to balance the energy budget (Barr et al., 1994; Blanken et al., 1997; Twine et al., 2000; Petrone et al., 2001).

Above canopy fluxes were removed when $u^* < 0.1 \text{ m s}^{-1}$, where u^* is the friction velocity as measured by EC (Figure 6.4), while within canopy fluxes were filtered when $u^* < 0.29 \text{ m s}^{-1}$ (Figure 6.5). These thresholds were defined from poor energy balance closure at low wind speeds (see Section 6.2). Flux measurements were also removed during periods of rainfall and when rapid and unexpected changes in state variables occurred over halfhour intervals using a criteria of 1.5 standard deviations from the mean value for that time period (Restrepo and Arain, 2005). Quality controlled EC measurements of ET had an error of approximately 23% prior to correction.

Several strategies were used to compensate for missing data due to the above conditions and occasional power failure. Short half-hour breaks were filled by linear interpolation. For longer breaks (i.e. >12 half-hour periods), turbulent fluxes were estimated using the mean diurnal variation method (Falge et al., 2001) replacing missing observations by the mean for that time period based on previous and subsequent 14-day periods. Missing or rejected data occurred for a total of 19% of all possible time periods during the study, mostly during major precipitation events and nocturnal periods. Finally, the flux footprint, or integrated area from which the tower is measuring scalar fluxes was calculated as described by Scheupp et al., (1990). The peak flux ranged from 70 to 110 m

upwind, with approximately 95% of the cumulative flux footprint within 300 m upwind of the tower, indicating that fluxes represent aspen dominated upland.

3.3.3 Chamber Measurements of Surface Evaporation

Surface evaporation measurements were conducted using a closed system EGM-4 Infrared Gas Analyzer (PP Systems, Amesbury, MA.) where CO₂, vapour pressure, temperature, PAR and relative humidity (RH) were collected once per minute over a 5min interval. Calculations were adapted from (McLeod et al., 2004) by integrating micrometeorological factors into the calculations. The sampling protocol was aimed at evaluating the change in surface E dynamics over the 2005 and 2006 snow-free seasons (May – September). The majority of samples were obtained between the peak growth hours of 08:00 and 16:00 MST to minimize flux variations caused by the diurnal cycle (Laporte et al., 2002) and to obtain fluxes operating at maximum levels to ensure existing spatial variability is captured. All collars were measured twice per week in order to acquire a greater spatial data set over the study period, rather than the more common approach of extensively replicating a few sites, less frequently (LeCain et al., 2002). As chamber measurements provide only point measurements the daily sampling scheme was altered by randomly selecting the sampling sites on a daily basis and fluxes were grouped into climatically distinct seasonal periods in order for temporal/seasonal comparisons to be made (Petrone et al., 2008; Petrone et al., 2003; Waddington et al., 1998).

Collars were constructed of 19 cm (inside diameter) polyvinylchloride (PVC) plastic piping cut to a height of 15 cm with perforated grooves etched in the lower 6 cm of the collar to allow for smooth insertion into the soil. The chamber was then placed in

a 3 mm wide groove cut into the top of each collar. Collars were placed 4 cm into the soil, 2 weeks prior to the first sampling measurement being taken to ensure that disturbance was minimized. The use of these collars permits repeated measurements at a single location, while minimizing soil disturbances (root growth into the soil and under the collar) in order to better assess temporal influences (Tufekcioglu et al, 2001).

In order to collect point measurements of soil E the chambers used were placed on the collars and the grooves were filled with water to obtain an air tight seal. Chambers (0.03 m² surface area, 0.06 m³ volume) were made of clear plexiglass with the ability to transmit 87% of PAR (Waddington and Roulet, 2000). Inside chamber volume and adjustment height was recorded at every collar site for each measurement by averaging the height of the ground surface to the top of the collar at 4 reference locations.

3.3.4 Chamber Flux Calculations

In order to assess the fluxes of water vapour from forest environments, measurements of the rate of vapour density increase inside the measurement chambers were conducted as per McLeod et al., (2004). To calculate the instantaneous rate of evaporation (E_{in}) the slope of vapour pressure from within the chamber was plotted against time using the least squares method. This calculated slope value was then used within a modified equation (Stannard, 1988) to calculate E_m over the 5 min measurement interval,

$$E_{in} = 3.6 \frac{MVC}{A} \quad (3.3)$$

where E_m is the rate of surface evaporation (mm hr⁻¹), M is the slope of the vapour pressure over time measurement for each interval (g/m³ s⁻¹), V is the volume inside the

chamber (m^3), C is the calibration factor to account for vapour absorption within the chamber (dimensionless) and A is the area of ground surface covered by the chamber (m^2) (Brown et al., in press). The conversion factor of 3.6 was used in order to convert a volume of water per unit area ($\text{g H}_2\text{O m}^{-2} \text{s}^{-1}$) into an hourly flux rate (mm hr^{-1}). The calculation of C was obtained through the methods outlined by McLeod et al., (2004) whereby an absorption factor was determined (see Section 6.1).

3.3.5 LAI Measurements

Forest mensuration plots were established at Pond 40 in order to assess the variations in LAI and other forest stand characteristics within the catchment. Three 15 m x 15 m plots were sampled. Tree height and live crown length were measured using a vertex sonic hypsometer (for crown apices that were not distinct, the average of three measurements was recorded), diameter at breast height (DBH) was measured with a standard DBH caliper, and crown diameter was measured along a north-south and east-west crown axes using a survey tape measure. All trees with a DBH greater than 9 cm were included within the survey as trees with a DBH of less than 9 cm were determined to not constitute a significant element in the overall canopy (Table 3.1).

Max. Leaf Area Index, <i>LAI</i>	1.4 (± 0.13)
Max. Plant Area Index, <i>PAI</i>	0.9 (± 0.06)
Diameter at breast height, <i>DBH</i> (cm)	12.9 (± 1.5)
Base Diameter (cm)	15.5 (± 2.6)
Tree Height (m)	16.6 (± 0.73)

Table 3.1: Summary table of catchment forest characteristics for the upland aspen dominated forest situated at “Pond 40”, Utikuma Region, Alberta Canada. Measurements consisted of three 15 m x 15 m plots situated on the south facing slope (SFS) of the catchment within the calculated footprint of the EC tower. Values in parentheses are standard errors (SE) of measurement variables.

3.4 Results and Discussion

3.4.1 Climate and Environmental Conditions

Mean daily air temperatures (T_a) ranged between 2.3 °C (DOY 141) and 19.6 °C (DOY 215) during the 2005 study period (Figure 3.2a) and 2.5°C (DOY 258) to 24.9°C (DOY 204) during the 2005 and 2006 study periods respectively. Overall seasonal patterns in daily averaged T_a were similar from June to August in 2005 and 2006, decreasing after DOY 210 (Figure 3.2a). Seasonal patterns in PAR were similar to those observed for T_a while PAR showed seasonal variation across both the 2005 and 2006 snow-free seasons with peaks in average daily PAR occurring mid season, between DOY 175 and DOY 215 of approximately 170 Wm^{-2} (Figure 3.2b).

The study site received approximately 235 mm of precipitation during the 2005 snow-free season with the largest event occurring on 25 July (DOY 206) delivering 45 mm (Figure 3.2c). The average event during the 2005 study season was approximately 6.8 mm. During the 2006 study season approximately 226 mm of precipitation occurred with the largest event occurring on May 4 (DOY 124) with 28 mm (Figure 3.2d) and an average event being 7.4mm. Although precipitation events in the area of Pond 40 were

generally evenly distributed during the 2005 study season, larger magnitude events occurred more frequently from 19 June to 28 August (DOY 170–240; Figure 3.2c). During the 2006 study season precipitation events occurred earlier than normal and a prolonged “event free” period existed from 6 August through to 15 September. Historically June–August represents 70% of the annual precipitation (Devito et al., 2005). This was observed during the 2005 study period but was not observed during the 2006 study period.

Daily averaged rooting zone (0-50cm) volumetric moisture content (θ) (m^3m^{-3}) in 2005 peaked on DOY 206 at 0.27 in response to a 45 mm precipitation event (Figure 3.2c). This event acted to replenish soil moisture storage for the upland soils. However, limited responses to subsequent precipitation events occurred during the 2005 season and the θ steadily declined throughout the remainder of the snow-free season. During the 2006 period, θ peaked much earlier on DOY 127 in response to a 47 mm precipitation event over a three day period and was adequately replenished by several smaller events until DOY 201 where an event free period of 40 days occurred and θ decreased along with evaporative demand (Figure 3.2d).

Daily averaged early season VPD fluctuations were greatest during the 2006 season ranging between 1.5 kPa (DOY 123) and 0.2 kPa (DOY 169) (Figure 3.2e). Early season measurements were unavailable in the 2005 season as the instruments were not functional until DOY 187. Mid-season (peak growth) VPD for both seasons stabilized around 0.8 kPa but ranged from 1.0 kPa to 0.4 kPa. Increases in daily averaged VPD

occurred once senescence began for both seasons with an average of 0.9 kPa during this time period.

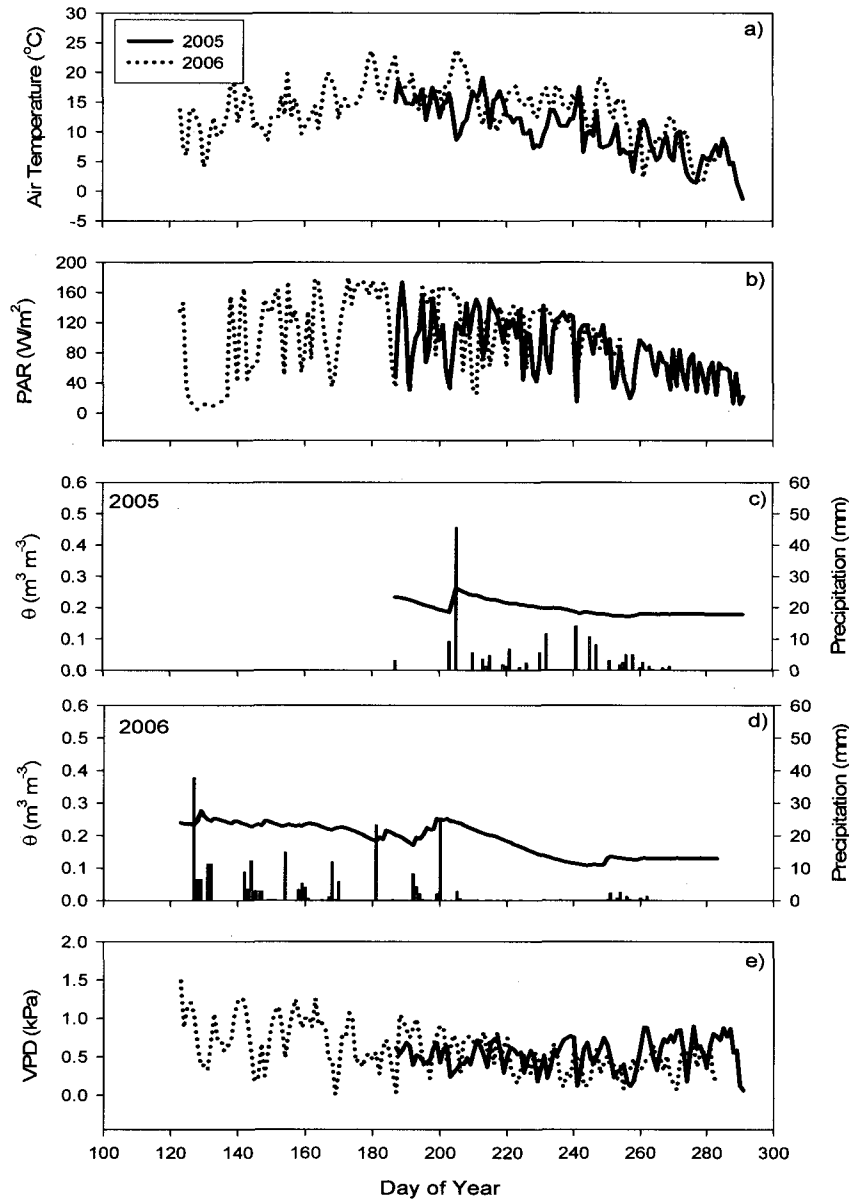


Figure 3.2: Daily Averaged a) Air Temperature ($^{\circ}\text{C}$), b) Photosynthetic Active Radiation (PAR) (W m^{-2}), c) 2005 Soil Moisture (θ) ($\text{m}^3 \text{m}^{-3}$) of the rooting zone (0-50cm depth) and daily precipitation, d) 2006 Soil Moisture (θ) ($\text{m}^3 \text{m}^{-3}$) of the rooting zone (0-50cm depth) and daily precipitation and e) Vapour Pressure Deficits (VPD) (kPa) for the 2005 and 2006 snow-free seasons, Pond 40, Utikuma Region Study Area (URSA), Alberta, Canada.

3.4.2 Flux Footprint Analysis

Analysis of the above canopy flux source indicates that the majority of the fluxes originated from the westerly upwind area, encompassing a predominantly aspen dominated hillslope (Table 3.2a). The 2005 season saw the maximum flux (max) originate from 95 m during the green/late green periods and 99 m during the senescence period for a seasonal average of 96 m. During the 2006 season, the maximum flux originated from 68 m during the early green period and grew to 71 m and 92 m during the green/late green and senescence periods, respectively producing a seasonal average of 74 m, a 12% decrease in maximum flux source area. Flux source areas are dependent on windspeed (u) (m s^{-1}) and wind direction (degrees) along with the upwind source vegetation and canopy structure components. Period averaged u was 2.1 m s^{-1} during the green/late green period and 2.5 m s^{-1} during senescence in 2005. In 2006, period averaged u during the early green period was 1.6 m s^{-1} , 1.9 m s^{-1} and 2.4 m s^{-1} during the green/late green and senescence periods, which ultimately contributed to a reduction in flux source area between both years. Friction velocity (u^*) (m s^{-1}) averaged 0.40 in 2005 and 0.38 in 2006, with daily maximums occurring during the green period for both years. Given these factors the area contributing to 80% of the flux averaged 347 m during green/late green and 376 m during senescence periods giving a seasonal average of 356 m. During the 2006 season the 80% flux contribution originated from 289 m during the early green period and grew to 290 m during the green/late green period with a peak during the senescence period of 366 m for a seasonal average of 304 m.

For ET_B fluxes the 2005 season saw the maximum flux (max) originate from 19 m during the early green period, 15 m during the green/late green periods and 22 m during

the senescence period for a seasonal average of 19 m (Table 3.2b). During the 2006 season, the maximum flux originated from 21 m during the early green period and was reduced to 19 m and 20 m during the green/late green and senescence periods, respectively producing a seasonal average of 20 m. Friction velocity (u^*) (m s^{-1}) averaged 0.3 in 2005 and in 2006, with daily maximums occurring during the early green period for both years. Given these factors, the area contributing to 80% of the flux in 2005 averaged 89 m during the early green, 76 m during green/late green and 96 m during senescence periods giving a seasonal average of 87 m. During the 2006 season the 80% flux contribution originated from 93 m during the early green period and was reduced to 82 m during the green/late green period with a peak during the senescence period of 97 m for a seasonal average of 91 m.

Period	2005				2006			
	x max	x frac	\bar{u}	wind dir	x max	x frac	\bar{u}	wind dir
	(m)	(m)	(ms^{-1})	(deg)	(m)	(m)	(ms^{-1})	(deg)
Early Green	n/a	n/a	n/a	n/a	67.8	289.1	1.63	291.7
Green/Late Green	94.6	347.0	2.05	272.5	71.2	290.1	1.88	273.6
Senescence	98.6	376.0	2.51	264.2	92.4	366.1	2.44	261.5
Season	95.9	356.0	2.2	268.3	74.3	304.0	1.9	275.6

Period	2005				2006			
	x max	x frac	\bar{u}	wind dir	x max	x frac	\bar{u}	wind dir
	(m)	(m)	(ms^{-1})	(deg)	(m)	(m)	(ms^{-1})	(deg)
Early Green	19.2	89.5	1.48	217.9	21.4	93.3	1.35	226.3
Green/Late Green	15.4	76.4	1.31	245.4	18.6	82.4	1.24	209.5
Senescence	21.5	95.8	1.53	213.3	19.7	97.4	1.61	218.8
Season	18.7	87.2	1.4	225.5	19.9	91.0	1.4	218.2

Table 3.2: Snow-free season period averaged flux footprint characteristics of maximum flux contribution (x max) (m), fractional flux source at 80% of flux contribution (x frac) (m), mean wind speed (\bar{u}) (m s^{-1}), wind direction (degrees) and friction velocity (u^*) (m s^{-1}) for a) Above canopy EC tower (ACEC) and b) Below Canopy EC Tower (BCEC), Pond 40, Utikuma Region Study Area (URSA), Alberta, Canada.

With knowledge of the flux source distance and magnitudes, an understanding of the directions of the upwind source is crucial in interpreting the nature of EC fluxes and associating the fluxes with a spatial component within the catchment. Figure 3.3 outlines a daily averaged histogram of the upwind source areas in degrees from the tower. In 2005, there were 36 days during the examined period where the flux originated from the west, while 29 days saw a flux originating from the southwest. The 2006 study period had 43 days in which the flux originated from the west and 41 days where the flux originated from the southwest. There were 30 days in 2006 where the flux source was from the NW, a significant increase from 2005, which saw only 11 days. Combining the knowledge of the orientation of the sensors with both the flux source distance and direction it can be determined that the majority of the fluxes seen over both seasons were from the aspen dominated upland where *Populus tremuloides* was the dominant species present.

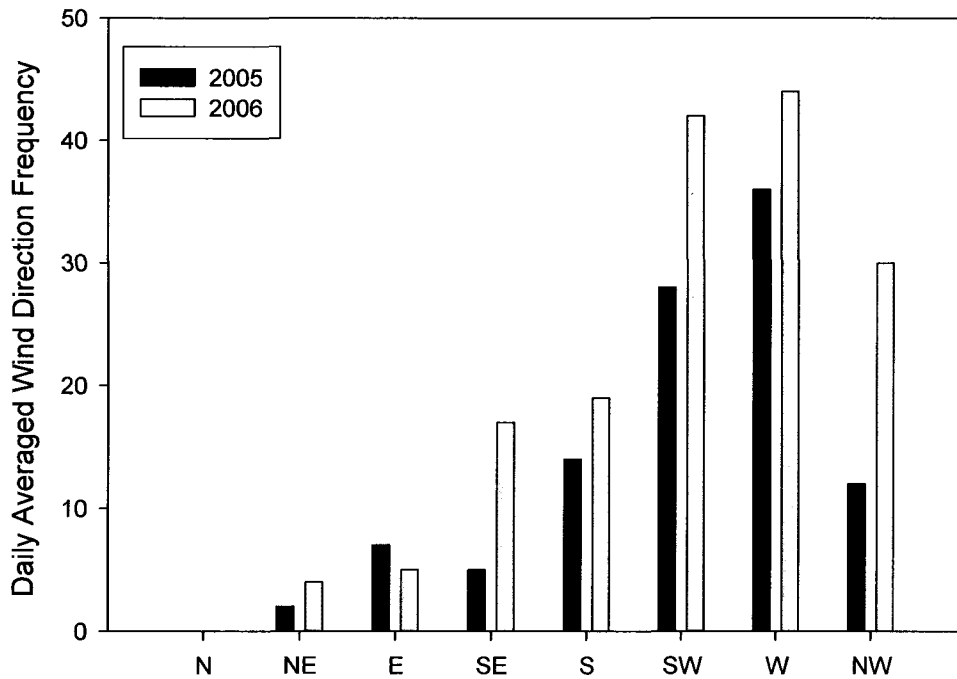


Figure 3.3: Histogram of daily averaged above canopy wind direction frequency as classified in 45° intervals for the 2005 and 2006 snow-free seasons, Pond 40, Utikuma Region Study Area (URSA), Alberta, Canada.

3.4.3 Temporal Dynamics of the Energy Balance

The ACEC tower was installed on DOY 187 of 2005 and was removed on DOY 291. Seasonal patterns in surface energy balance components were similar within 2005 and 2006 study seasons (Figure 3.4). Q^* averaged 106 W m^{-2} and 165 W m^{-2} during the growth periods in 2005 and 2006 respectively. Q_E followed patterns in Q^* quite closely in both years and represented 61% and 68% of Q^* during the green period in 2005 and 2006, respectively (Figure 3.4). Q_H was the dominant flux in the early green and late green periods and remained relatively constant throughout the green period in both seasons. Q_G fluxes had the greatest contribution during the early green period with an average of 25 W m^{-2} but dropped to approximately 10 W m^{-2} once peak growth had

occurred in the canopy (Figure 3.4b). Q_G was similar between both study seasons. Daily averaged J_t again remained relatively constant through the study period at approximately 10 Wm^{-2} , with also little seasonal variation.

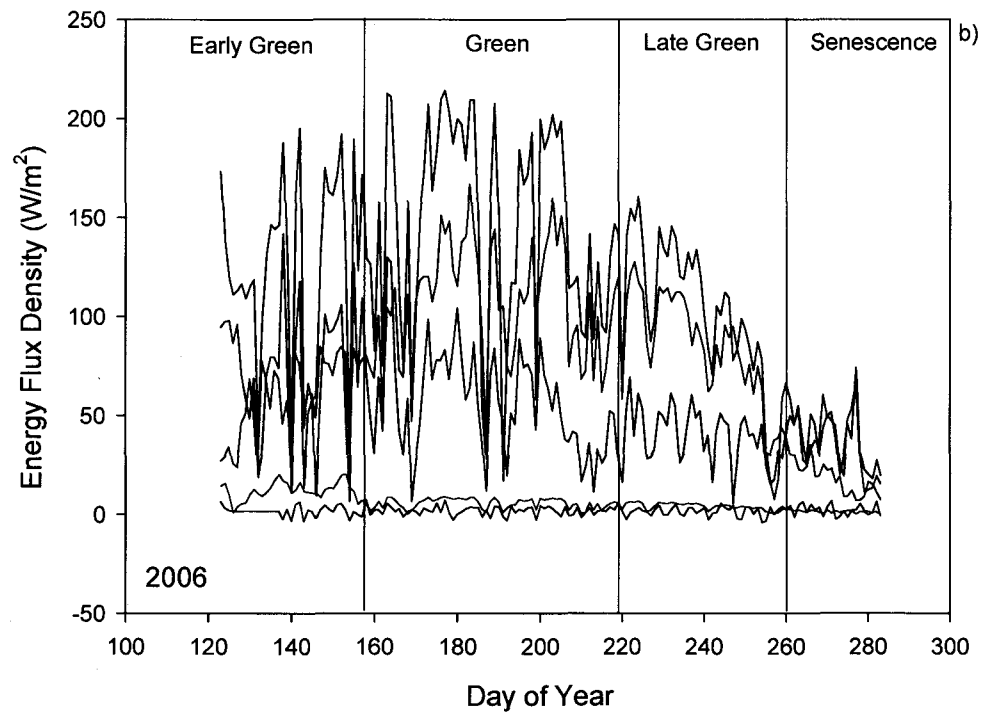
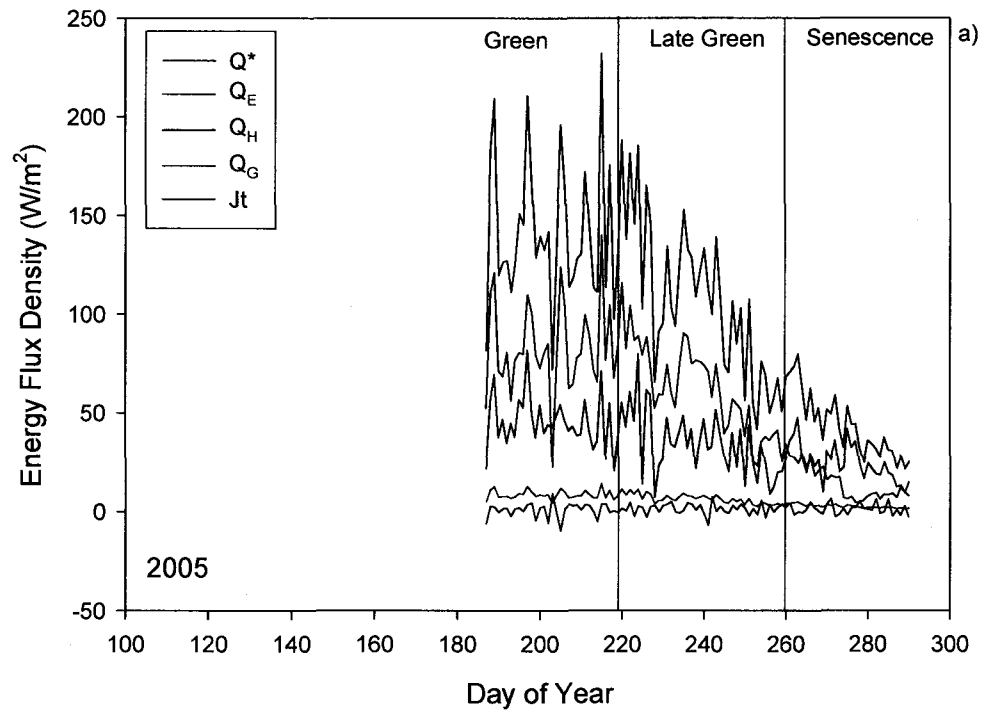


Figure 3.4: Daily averaged above canopy energy flux densities for the a) 2005 and b) 2006 snow-free seasons, Pond 40, Utikuma Region Study Area (URSA), Alberta, Canada. Transitions between defined growth periods are denoted by vertical lines.

The diurnal partitioning of energy fluxes from above the canopy throughout the 3 seasonal periods is shown in Figure 3.5. The early green period of 2006 (Figure 3.5a) experienced peak Q^* mid-afternoon (MST) (401 Wm^{-2}) with a Q_H being the dominant flux at 296 Wm^{-2} and Q_E at 120 Wm^{-2} . J_t fluxes were greatest in the early morning but decreased during the afternoon hours. Green period for 2005 (Figure 3.5b) and 2006 (Figure 3.5c) indicate the overtaking of Q_E fluxes as the dominant flux source, with 2006 fluxes being only slightly larger. Figures 3.5d and 3.5e show the senescence period diurnal flux partitioning in both seasons during which Q^* is reduced to peak of $\sim 200 \text{ Wm}^{-2}$ in both years, and Q_H again becomes the dominant flux.

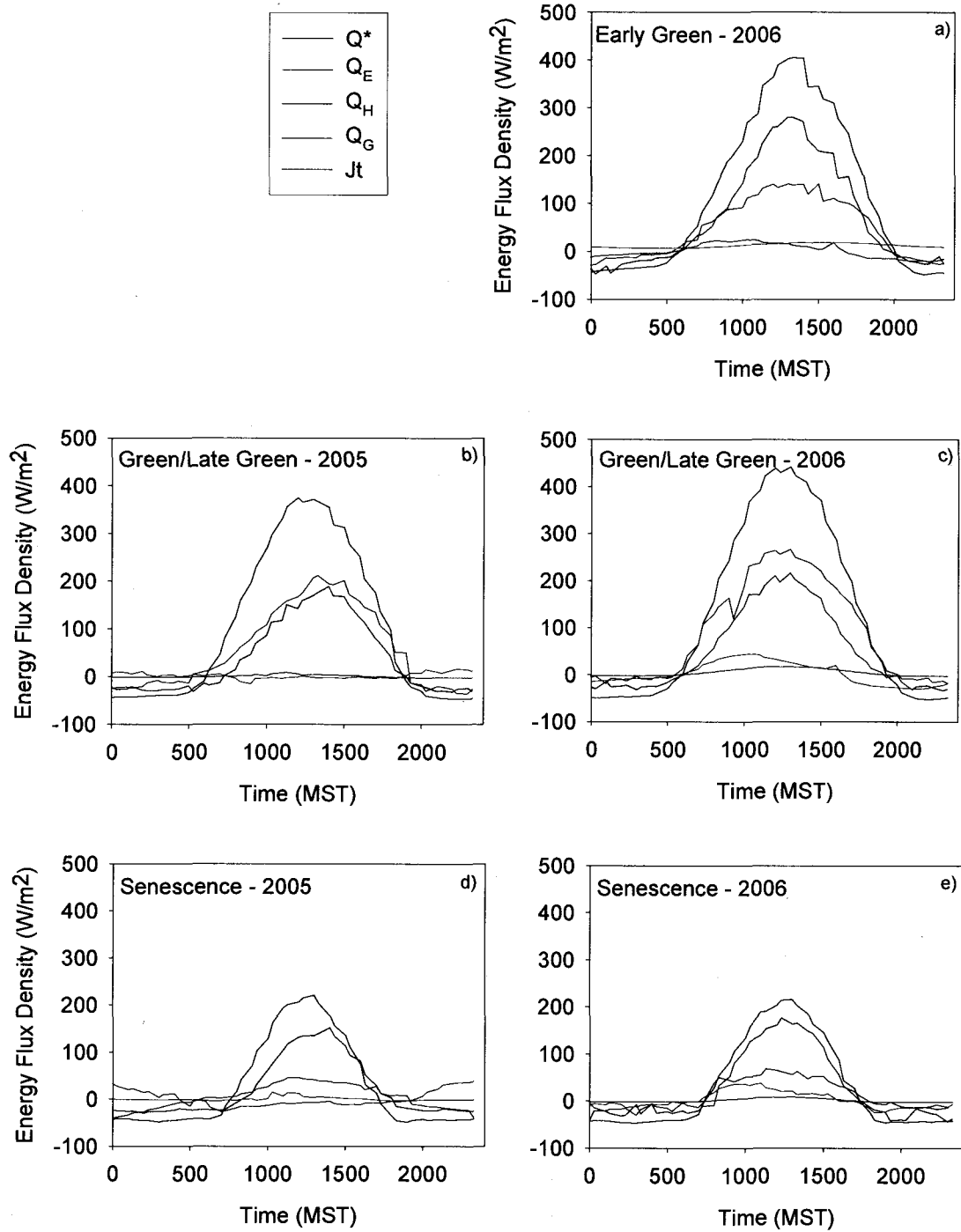


Figure 3.5: Period averaged diurnal above canopy energy flux densities for a) Early Green period 2006, b) 2005 Green/Late Green Period, c) 2006 Green/Late Green Period, d) Senescence 2005 and e) Senescence 2006, Pond 40, Utikuma Region Study Area (URSA), Alberta, Canada.

3.4.4 Overstory and Understory Flux Partitioning

Examining the relationships between the above and below canopy fluxes shows the nature of the understory contributions in determining whole stand-scale energy fluxes. With limited development of the aspen canopy during the early green period maximum incoming solar radiation is available for understory development. Q^* within the canopy during the early green period is at or equal to the above canopy measurements, which acts to promote the initial growth and development of the understory herbaceous species (*Rosa acicularis* and *Viburnum edule*) (Figure 3.6a). The partitioning of that increased Q^* during the early green period that reaches the understory contributes more to Q_E as compared to the above canopy measurements. Q_E fluxes increases steadily over the early green period as an increase in herbaceous development occurs eventually surpassing the above canopy contributions where green up has yet to begin. Q_H shows an inverse relationship to Q_E with greater contributions from the understory during leaf development up until approximately DOY 135, where it is surpassed by the above canopy contributions and Q_E becomes the dominant flux from the understory (Figure 3.6b and 3.6c).

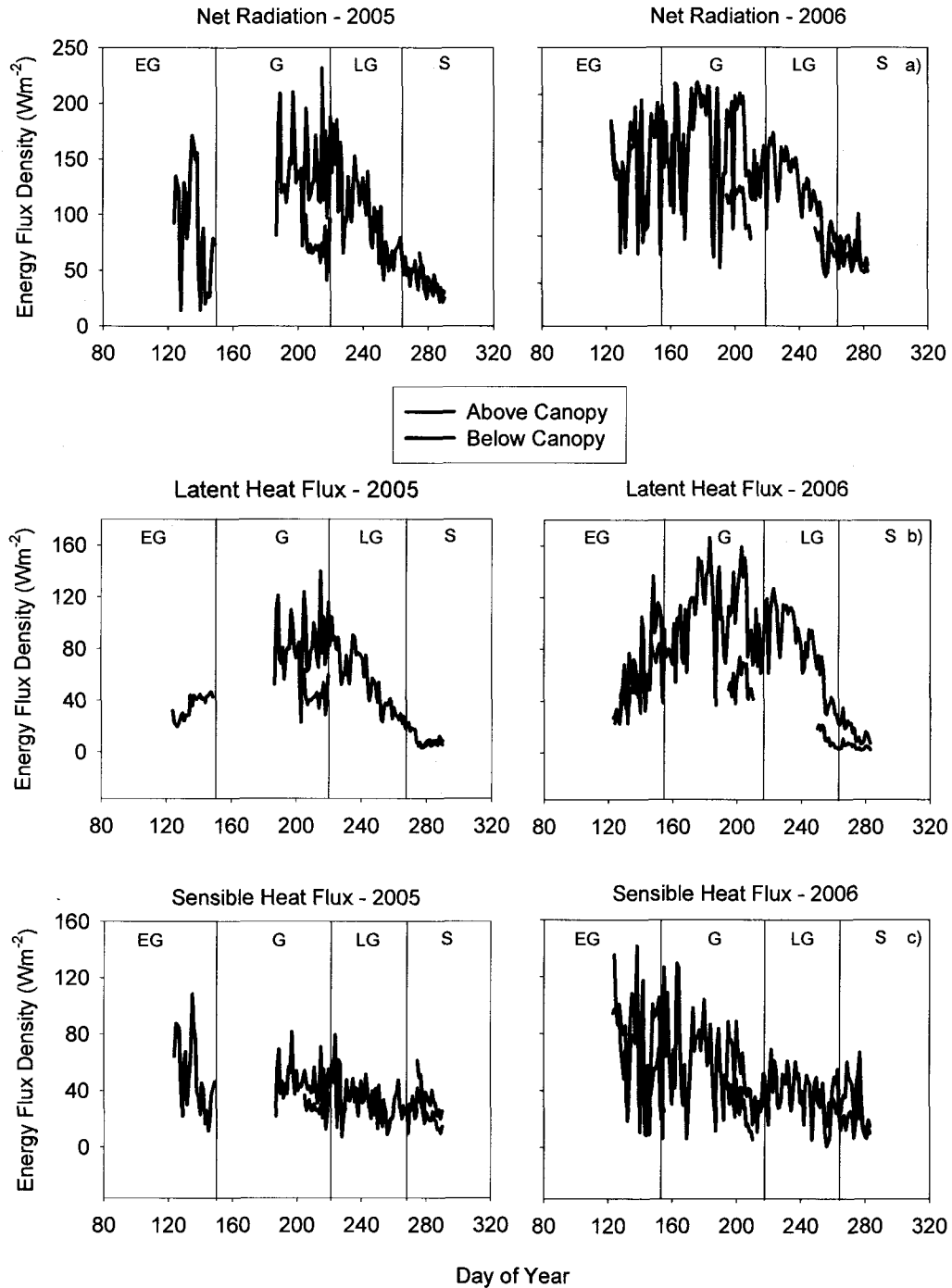


Figure 3.6: Daily averaged energy flux densities of a) Net Radiation (Q^*) ($W m^{-2}$), b) Latent Heat Flux (Q_E) ($W m^{-2}$) and c) Sensible Heat Flux (Q_H) ($W m^{-2}$) for both above and within canopy measurements during the 2005 and 2006 snow-free seasons, Pond 40, Utikuma Region Study Area (URSA), Alberta, Canada. Transitions between defined growth periods are denoted by vertical lines. EG represents early green period, G represents green period, LG represents the late green period and S represents senescence.

During the green period when full canopy leaf out has occurred at both levels Q^* within the understory is approximately half of the above canopy values. Similarly, the partitioning of Q_H and Q_E are reduced in magnitude during the green period averaging $\sim 65 \text{ Wm}^{-2}$ and 45 Wm^{-2} , respectively (Figure 3.6b and 3.6c). During the green period the below canopy is contributing $\sim 20\%$ on average of the canopy Q_E (Figure 3.6b). During the late green period Q^* is $\sim 76\%$ of the above canopy Q^* , which translates to a reduction in both Q_E and Q_H of similar magnitudes.

3.4.5 Seasonal and Diurnal Partitioning of Evapotranspiration

Above canopy evapotranspiration (ET_C) shows a direct response to net precipitation inputs across both the 2005 and 2006 snow-free seasons (Figure 3.7b). Peaks in daily ET_C can be seen following precipitation events, while the magnitude of the precipitation events also affects the maximum rate of daily ET_C across both seasons. As precipitation is intercepted by the canopy during green periods, ET_C increases, suggesting the dominance of diurnal evaporation of intercepted water from leaf catch atop the canopy. Following times of no precipitation, ET_C is reduced and is presumed to follow the controls of transpiration across the upper canopy. In 2006, early green period ET_C averaged 1.9 mm d^{-1} with a maximum occurring on DOY 144 of 2.9 mm d^{-1} (Figure 3.7b). Green/late green period ET_C in 2005 averaged 3.1 mm d^{-1} with maximum ET_C occurring on DOY 216 of 4.9 mm d^{-1} , while in 2006 ET_C averaged 3.5 mm d^{-1} with a period maximum of 5.9 mm d^{-1} following a 23 mm precipitation event (Figure 3.7b). Peaks in ET_C across both seasons occurred following days where precipitation events occurred that were greater than 10 mm. In 2006 late green period ET_C averaged 1.1 mm

d^{-1} and peaked on DOY 249 at 1.6 mm d^{-1} , again following a five day period of precipitation totaling 10 mm. Senescence period ET_C in 2005 averaged 0.6 mm d^{-1} and were relatively stable during that time period, while in 2006 ET_C averaged 0.7 mm d^{-1} .

Below canopy evapotranspiration (ET_B) averages 1.1 mm d^{-1} during the early green period and increases by 12% on DOY 139 in 2005, corresponding with understory vegetation emergence (Figure 3.7c). Larger shorter period increases in ET_B were observed in 2006 relative to 2005. For example, an increase in ET_B occurred on DOY 141 from an average of 1.1 mm d^{-1} before understory leaf out to an average of 3.5 mm d^{-1} once the understory canopy had developed. Green/late green period ET_B was approximately 45% of ET_C over both study seasons with averages in 2005 of 1.6 mm d^{-1} and 1.9 mm d^{-1} in 2006. ET_B during the green period showed maximum rates of 2.1 mm d^{-1} on DOY 205, which followed the 45 mm precipitation event in 2005 and 2.8 mm d^{-1} on DOY 203 in 2006, again following a 25 mm precipitation event. Senescence period ET_B in 2005 was approximately 60% of ET_C rates with an average of 0.4 mm d^{-1} and was stable across the late season measurement period, in which no precipitation events occurred. In 2006, ET_B during late green averaged 0.9 mm d^{-1} peaking during the early portion of late green when canopy development had just begun to cease. A sharp decrease in ET_B was observed on DOY 256, following the leaf off and saw a peak following the 10 mm event in which there was limited canopy interception, allowing for the majority of precipitation to reach the understory.

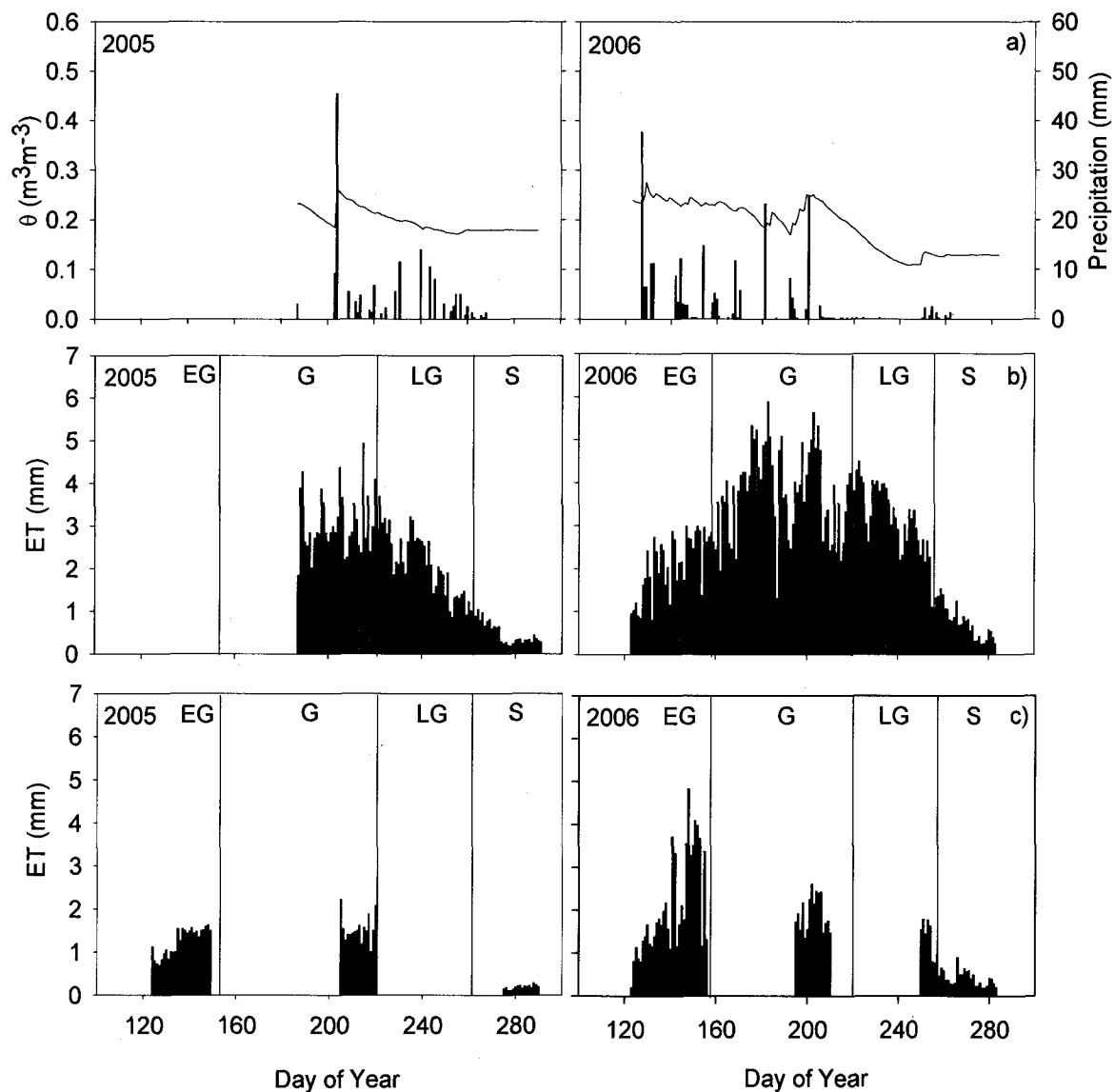


Figure 3.7: Daily averaged a) rooting zone Soil Moisture (θ) ($\text{m}^3 \text{m}^{-3}$) (0-50cm) and daily precipitation (mm), b) above canopy ET (mm) and c) within canopy ET (mm) for the 2005 and 2006 snow-free seasons, Pond 40, Utikuma Region Study Area (URSA), Alberta, Canada. Transitions between defined growth periods are denoted by vertical lines. EG represents early green period, G represents green period, LG represents the late green period and S represents senescence.

During the 2005 study season E_S remained constant with averages of $0.13 (\pm 0.04)$, $0.18 (\pm 0.09)$ and $0.11 (\pm 0.08)$ mm hr^{-1} during the early green, green/late green and senescence periods, respectively (Table 3.3). In an effort to partition scalar fluxes of ET between differing layers within the structure of the aspen forest measurements of ET_C and ET_B were time matched to the closest half-hour interval when E_S was measured. Subtracting E_S values from BCEC data shows that ET_B averaged $0.17 \text{ mm hr}^{-1} (\pm 0.06)$ with $0.13 \text{ mm hr}^{-1} (\pm 0.04)$ and $0.10 \text{ mm hr}^{-1} (\pm 0.04)$ occurring during the early green, green/late green and senescence periods respectively. ET_C averaged $0.25 \text{ mm hr}^{-1} (\pm 0.12)$ and $0.15 \text{ mm hr}^{-1} (\pm 0.08)$ during the green/late green and senescence periods, respectively. There were no ET_C measurements made during the early green period of 2005. In 2006 E_S again remained relatively constant across the season with averages of $0.14 \text{ mm hr}^{-1} (\pm 0.05)$ during early green, $0.19 \text{ mm hr}^{-1} (\pm 0.08)$ during the green/late green and $0.13 \text{ mm hr}^{-1} (\pm 0.04)$ during the senescence period (Table 3.3). ET_B contributions averaged $0.21 \text{ mm hr}^{-1} (\pm 0.09)$ during the early green period, and decreased during the green/late green period to an average of $0.15 \text{ mm hr}^{-1} (\pm 0.06)$ and $0.14 \text{ mm hr}^{-1} (\pm 0.06)$ during the senescence period. Finally, ET_C contributions averaged $0.19 \text{ mm hr}^{-1} (\pm 0.11)$, $0.28 \text{ mm hr}^{-1} (\pm 0.13)$ and $0.17 \text{ mm hr}^{-1} (\pm 0.08)$ during the early green, green/late green and senescence periods.

Period	2005				2006			
	Daily ET _C mm d ⁻¹	ET _C mm hr ⁻¹	ET _B mm hr ⁻¹	E _S mm hr ⁻¹	Daily ET _C mm d ⁻¹	ET _C mm hr ⁻¹	ET _B mm hr ⁻¹	E _S mm hr ⁻¹
Early Green			0.17 (±0.06)	0.13 (±0.04)	2.09	0.19 (±0.11)	0.21 (±0.09)	0.14 (±0.05)
Green/Late Green	3.08	0.25 (±0.12)	0.13 (±0.04)	0.18 (±0.09)	3.45	0.28 (±0.13)	0.15 (±0.06)	0.19 (±0.08)
Senescence	0.59	0.15 (±0.08)	0.10 (±0.04)	0.11 (±0.08)	0.65	0.17 (±0.08)	0.14 (±0.06)	0.13 (±0.04)
Season	1.84	0.20	0.13	0.14	2.06	0.21	0.17	0.15

Table 3.3: Period averaged daily maximum (defined as between 1100MST and 1500MST) scalar catchment flux partitioning of above canopy ET (ET_C) (mm hr⁻¹), within canopy ET (ET_B) (mm hr⁻¹) and surface evaporation (E_S) (mm hr⁻¹) for the 2005 and 2006 snow-free seasons, Pond 40, Utkuma Region Study Area (URSA), Alberta, Canada. As E_S was examined as spot measurements, fluxes from both ET_C and ET_B were matched to the closest half hour interval when E_S was sampled. The data was then grouped and averaged by defined growth periods. Values in parentheses are standard errors (SE) of measurements.

3.4.6 Soil Moisture (θ), Soil Suction (ψ) and Evapotranspiration

The relationships between rooting zone soil moisture (θ) (average θ over the top 50cm) and soil suction (ψ) with ET_C over three selected periods in 2005 and four selected periods of growth through the 2006 season shows the interconnected dependence of the variables (Figure 3.8 and 3.9). During the 2005 study season the green period θ depletion is greatest and shows direct correlation with peak daily ET_C and maximum daily ψ . Maximum rooting zone ψ peaks midday at 158 kPa corresponding with peak ET_C of 0.28 mm hr^{-1} (Figure 3.8a). The peak ψ and maximum seasonal ET_C rates result in a reduction in θ from 0.232 $\text{m}^3 \text{m}^{-3}$ to 0.218 $\text{m}^3 \text{m}^{-3}$. During the late green period ψ is reduced in magnitude (94 kPa) compared with the green period but the amplitude of the variation remains approximately the same and is correlated with a θ depletion of 0.203 $\text{m}^3 \text{m}^{-3}$ to 0.193 $\text{m}^3 \text{m}^{-3}$ while peak daily ET_C rates reach $\sim 0.2 \text{ mm}$ with peak midday ψ reaching 94 kPa (Figure 3.8b). The senescence period in 2005 shows limited response to θ depletion as a drastic reduction in ET_C ($\sim 0.07 \text{ mm hr}^{-1}$) coupled with limited ψ in the rooting zone ($\sim 35 \text{ kPa}$). These senescence period patterns are a result of the rooting zone demand being reduced and the plants beginning to shut down or become dormant for the winter season.

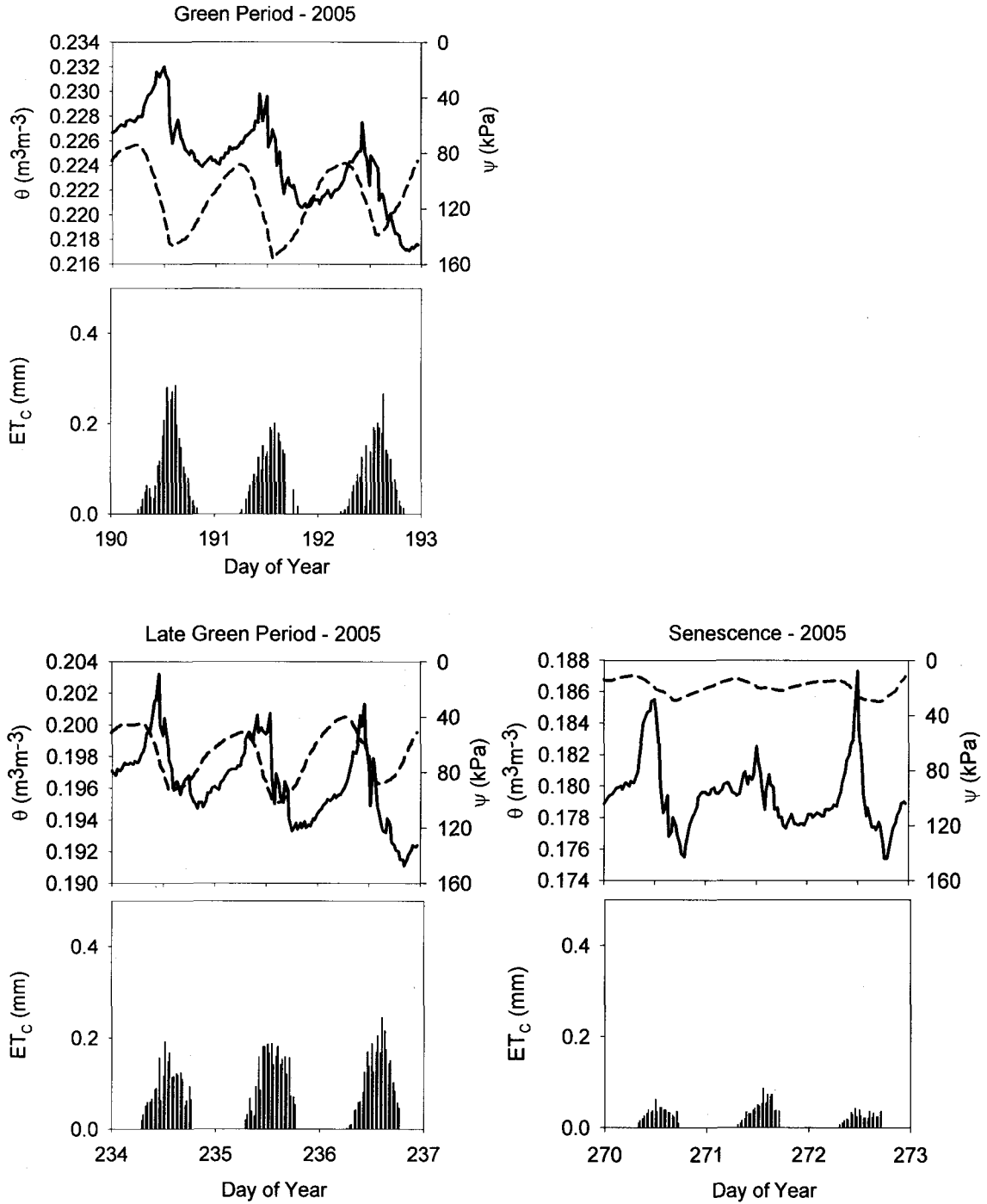


Figure 3.8: Precipitation free 4 day periods for the green (G), late green (LG) and senescence (S) periods of rooting zone Soil Moisture (θ) ($m^3 m^{-3}$) (solid blue line), rooting zone soil tension (ψ) (kPa) (dashed red line) and above canopy ET (ET_c) (mm) for the 2005 snow-free season, Pond 40, Utikuma Region Study Area (URSA), Alberta, Canada.

During the 2006 study season early green period (DOY 135-138) θ depletion from 0.255 to 0.235 $\text{m}^3 \text{m}^{-3}$ occurs when ψ and ET_C reach daily maximums of 82 kPa and 0.18 mm hr^{-1} , respectively (Figure 3.9a). Similar trends are observed for the green period with θ depletion of 0.208 to 0.187 $\text{m}^3 \text{m}^{-3}$ coupled with a peak ψ of 120 kPa and maximum daily ET_C rate of 0.31 mm hr^{-1} (Figure 3.9b). Late green period shows a θ depletion of 0.203 to 0.182 $\text{m}^3 \text{m}^{-3}$ and a maximum daily ψ of 96 kPa and ET_C of 0.29 mm hr^{-1} (Figure 3.9c). Senescence in 2006 again shows limited θ depletion with reduced daily maximum ψ (~37 kPa) and limited ET_C (0.12 mm hr^{-1}) (Figure 3.9d). This results in limited θ depletion within the rooting zone.

Other studies (c.f. McLaren et al., 2008) have suggested that the diurnal increases in θ are evidence of hydraulic lift. However, even after calibration and temperature corrections the range in TDR data reported here are generally not greater than the range in potential instrumental error. While the downward trend in θ over the 3 day period does provide evidence of general decline in rooting zone θ , the diurnal patterns in ψ provide a clearer indication of the occurrence of hydraulic lift occurring in response to ET demand. This is especially evident when comparing green and senescence period data where ET and θ diurnal variation and maximums are decreased but the amplitude of the daily changes in θ remains basically the same.

Figure 3.8 and 3.9 show that a delay exists in the response of θ to morning increases in ψ throughout the snow-free season of both 2005 and 2006. As evaporative demand begins during early morning hours an increase in ψ is observed along with ET.

However, over all periods the θ response is delayed until ET_C reaches peak daily values at which time ψ decreases until daily ET_C is limited and a “bleeding effect” of soil water demand permits the capillary rise to occur, causing θ to increase gradually (McLaren et al., 2008). These subtle changes in θ occur throughout the snow-free seasons of 2005 and 2006, however are most pronounced during peak growth when water demand from the aspen roots is at its greatest (Caldwell et al., 1998). While during senescence periods when root water uptake is all but removed a limited response is observed in θ within the rooting zone.

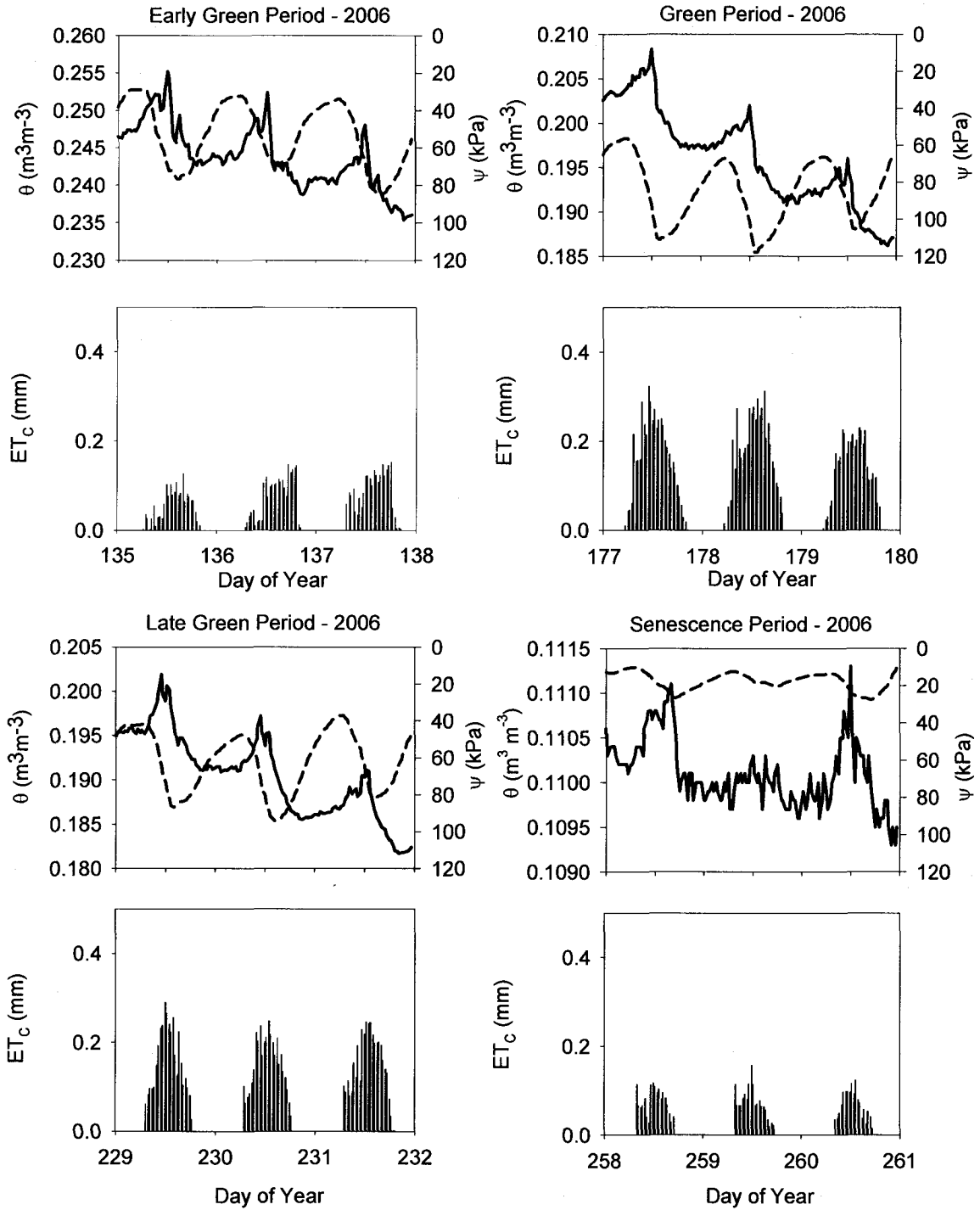


Figure 3.9: Precipitation free 4 day periods for the early green (EG), green (G), late green (LG) and senescence (S) periods of rooting zone Soil Moisture (θ) ($m^3 m^{-3}$) (solid blue line), rooting zone soil tension (ψ) (kPa) (dashed red line) and above canopy ET (ET_c) (mm) for the 2006 snow-free season, Pond 40, Utikuma Region Study Area (URSA), Alberta, Canada.

3.4.7 Atmospheric Controls and Evapotranspiration

Vapour pressure deficit (VPD) is expected to be the most important environmental factor governing the transpiration of boreal deciduous forests when θ and radiation is not limiting (Hogg et al., 1997; Blanken et al., 1997). Atmospheric controls on ET including VPD and photosynthetic active radiation (PAR) over the three periods of the snow-free season and the differences between canopies are depicted in Figure 3.10. Peak above canopy ET rates during the early green period are observed closer to mid afternoon (~16:00 MST) at 0.1 mm hr^{-1} . Peak ET rates from above the canopy occur just prior to midday (12:00 MST) at 0.18 mm hr^{-1} during green periods while senescence peak rates occur again closer to midday (12:00 MST), similar to early green period timing at 0.04 mm hr^{-1} . Early green from below the canopy shows similar diurnal ET patterns and is slightly less than the above canopy measurements when averaged over the entire growing period with peak ET occurring late afternoon at 0.08 mm hr^{-1} . Below canopy ET shows similar timing to that of the peak daily ET measured from above the canopy however is reduced to 0.11 mm hr^{-1} . Senescence period from below the canopy peaks in a similar fashion to the above canopy measurements in timing at $\sim 0.02 \text{ mm hr}^{-1}$ close to 12:00 MST.

Maximum and minimum atmospheric demand as indicated by the maximum of VPD from above and below the canopy can provide insight into the nature of diurnal ET patterns at both scales. Figure 3.10b shows the diurnal patterns of VPD over the three snow-free seasons from above and below the canopy layers. Above canopy peak VPD occurs during the green period and is delayed compared to peak ET for the same growth period which occurs at 13:00 MST of 1.2 kPa . For the early green period, peak VPD

occurs close to 12:00 MST at 1.1 kPa, approximately 4 hours earlier than peak ET rates during the same growth period, while senescence occurs during the same time period of the day however at a much less magnitude (0.65 kPa) (Figure 3.10b). Below the canopy, peak VPD is observed during the early green period with daily maximums of 0.9 kPa occurring around solar noon. Peaks in VPD during both the green and senescence periods of the canopy occur during a similar time window but are reduced to 0.62 kPa and 0.39 kPa, respectively (Figure 3.10b).

PAR measurements show similar patterns to those of ET from above the canopy with peaks occurring at 12:00 MST of 350 W m^{-2} for the green period (Figure 3.10c). Comparing the early green and senescence phases of the snow-free seasons shows that similar PAR values and peaks are recorded. Peaks of $\sim 210 \text{ W m}^{-2}$ are observed for both early green and senescence, the only differences between the two growth periods is the duration of positive PAR values, as early green experiences longer positive PAR hours as compared to senescence. However the magnitudes of the peaks are similar. Below canopy PAR, as with VPD had the highest values during the early green period at just less than 200 W m^{-2} with peaks at approximately 14:00 MST (Figure 3.10c). Similar PAR values are observed for both the green and senescence periods with peaks occurring at 12:00 MST of approximately 125 W m^{-2} , with the senescence period being slightly greater. This indicates the role of the fully developed canopy layer on PAR levels available to below canopy vegetation. Further, during the green periods solar radiation is not limited in this aspen dominated system. Figure 3.10 also indicates that the observed midday peaks in ET occur just before peak VPD and at approximately the same time as PAR, as

demonstrated in other studies (Hogg et al., 1997; Blanken et al., 1997, Grelle et al., 1999).

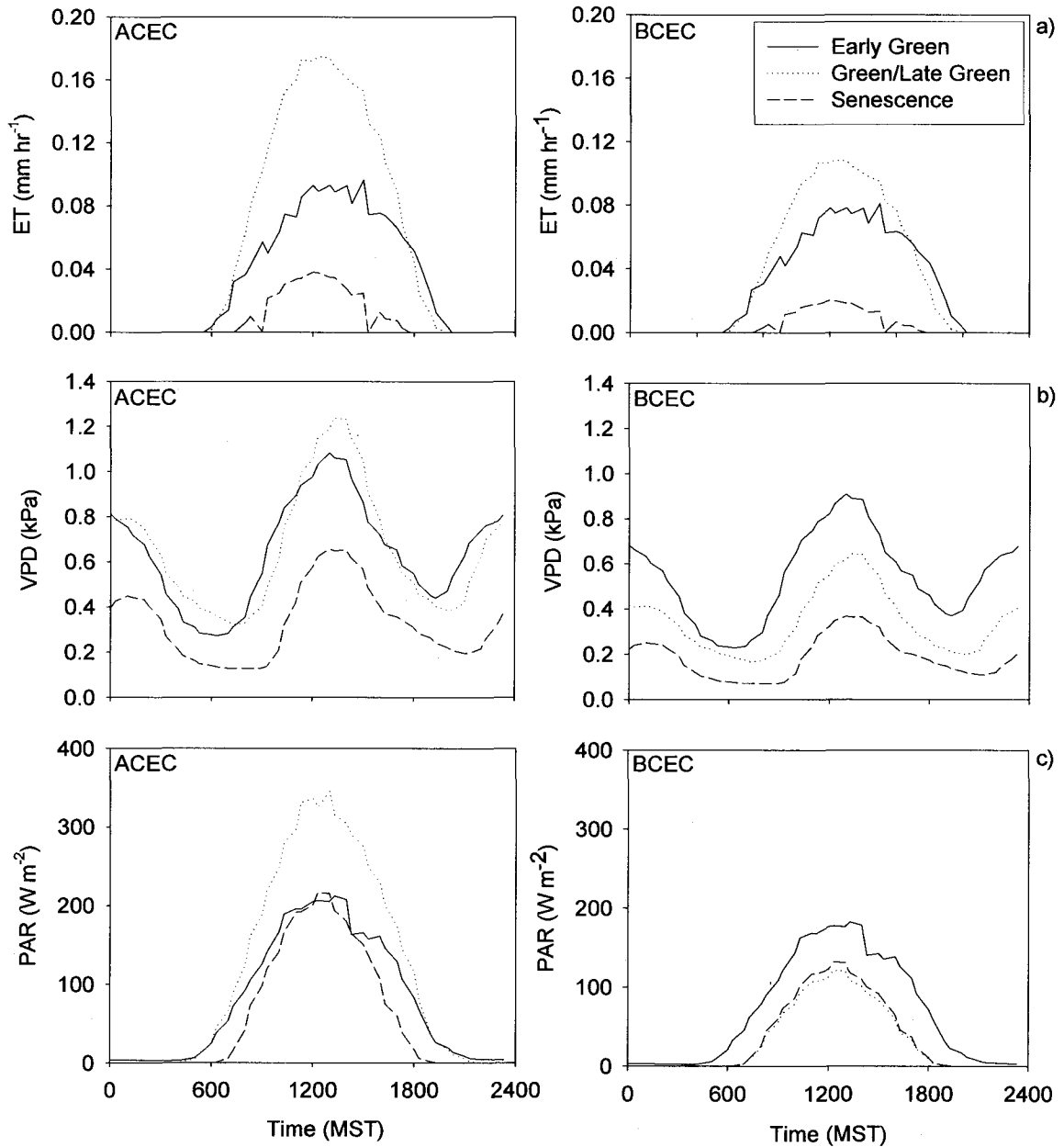


Figure 3.10: Above (ACEC) and within canopy (BCEC) period averaged diurnal comparisons of a) Evapotranspiration (ET) (mm hr^{-1}), b) Vapour Pressure Deficits (VPD) (kPa) and c) Photosynthetic Active Radiation (PAR) (W m^{-2}) Pond 40, Utikuma Region Study Area (URSA), Alberta, Canada.

3.4.8 Interaction Between Atmospheric Demand and θ

The stomatal dynamics responsible for this ET response to VPD variations are a function of the hydraulic response from the soil to leaf (Meinzer and Grantz, 1991; Hogg and Hurdle, 1997). However, VPD and θ are not always independent of each other while a relationship should be observable between VPD and canopy ET under differing θ conditions, VPD and θ may not always be independent of each other (McLaren et al., 2008; Kurpius et al., 2003). If VPD is high at the beginning of the diurnal transition cycle (early in the day) initial rates of water transport from the soil through the tree will be lower regardless of the regulation of VPD later in the cycle, because stomatal closure are met earlier in the day (Kurpius et al., 2003). Examining the relationships between initial Vapour Pressure Deficit (VPD_O) and ET_C shows distinct clustering and breaks in the ET_C data (Figure 3.11). VPD_O is defined as the average VPD between 06:00 and 08:00 MST. Here we group the data into three distinct categories

- a) VPD_O LOW is defined as $VPD_O < 0.05$ kPa
- b) VPD_O MID > 0.05 kPa and < 0.15 kPa
- c) VPD_O HIGH > 0.15 kPa

On days when VPD_O was classified as HIGH (ie: high morning atmospheric demand) maximum ET_C rates are observed. ET_C rates reached peak daily maximums (> 0.3 mm hr⁻¹) during periods when high atmospheric demand was observed during the time period when daily atmospheric demand was at the onset. ET_C rates were thus controlled by the VPD origins for that specific day (ie: high morning atmospheric demand translates to high ET_C rates for the given days). Days in which VPD_O was classified as MID reach maximum ET_C rates of < 0.2 mm hr⁻¹. Consequently, days classified as VPD_O LOW

showed the most limited ET_C rates ($< 0.15 \text{ mm hr}^{-1}$). These distinct clustering patterns observed between the three categories, show that for URSA the use of VPD_0 as a proxy for ET_C is an appropriate method for characterizing the daily catchment ET rates. Thus, to investigate whether changes in θ can produce diurnal shifts in maximum ET relative to maximum VPD data were first grouped by daily initial VPD (6:00 and 8:00 MST) (VPD_0).

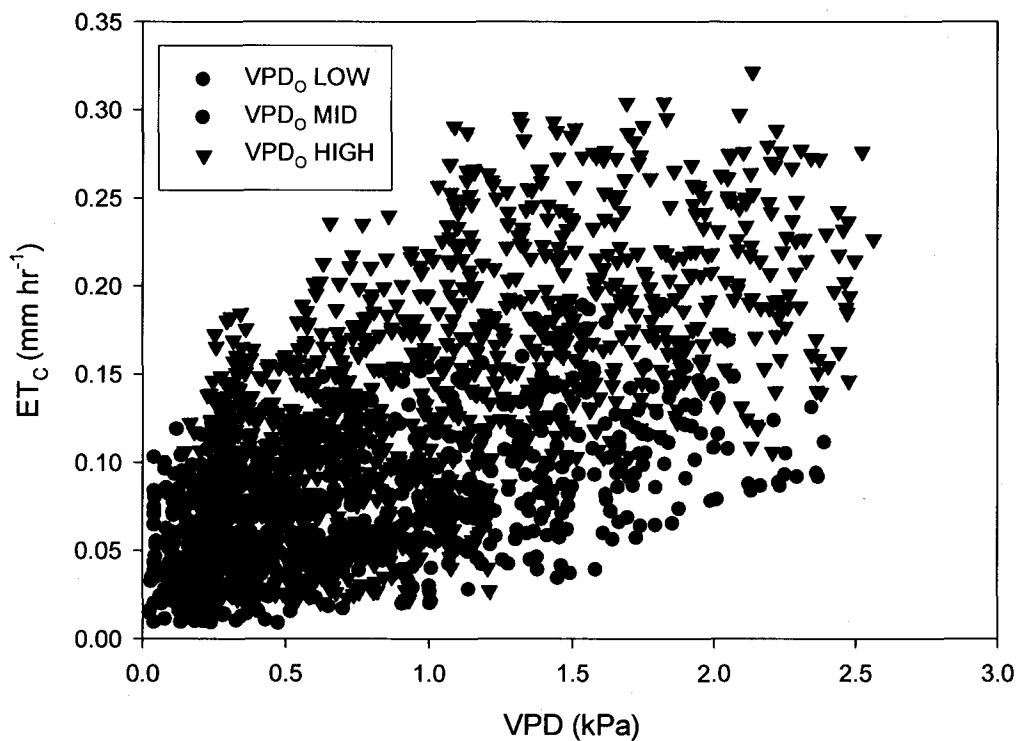


Figure 3.11: Relationship between above canopy ET (ET_C) (mm hr^{-1}) and VPD (kPa) based on VPD_0 thresholds of a) VPD_0 LOW $< 0.05 \text{ kPa}$, b) VPD_0 MID $> 0.05 \text{ kPa}$ and $< 0.15 \text{ kPa}$ and c) VPD_0 HIGH $> 0.15 \text{ kPa}$, Pond 40, Utikuma Region Study Area (URSA), Alberta, Canada.

Given that the vegetation comprising the understory will differ in the amount of solar radiation received and root structure, it can be expected that this relationship will

differ for ET_C and ET_B . The relationship between daily maximum ET and VPD_O for both above and within the canopy layer during the green periods of 2005 and 2006 are shown in Figure 3.12. A distinct separation of the data is clear between canopy layers. Significant clustering occurs for both the above and within canopy measurements at low VPD_O levels (< 0.10 kPa). Maximum ET_B rates reach 0.16 mm hr^{-1} at VPD_O levels less than 0.1 kPa. An increase in VPD_O from below the canopy does not result in an increased maximum daily ET above approximately 0.1 kPa. The same is observed for the relationship between daily maximum ET_C and VPD_O with a leveling of ET_C across a range of VPD_O values above ~ 0.10 kPa. Significant clustering of daily maximum ET_C is observed at VPD_O levels less than 0.10 kPa. However, the range in ET_C at VPD_O 's between 0.1 and 0.4 kPa is greater than observations in ET_B (Figure 3.12). The lower limit of ET_C is approximately 0.15 mm hr^{-1} with the exception of minimal outliers, which corresponds to the upper threshold of the daily maximum ET_B . This shows that VPD tends to constrain ET within a much narrower range in the understory (Schwartz et al, 2006). Despite the controls of atmospheric demand on stomatal capture, the root systems of the aspen are still able to maintain critical hydraulic gradients from the soil to the leaf (Schwartz et al., 2006).

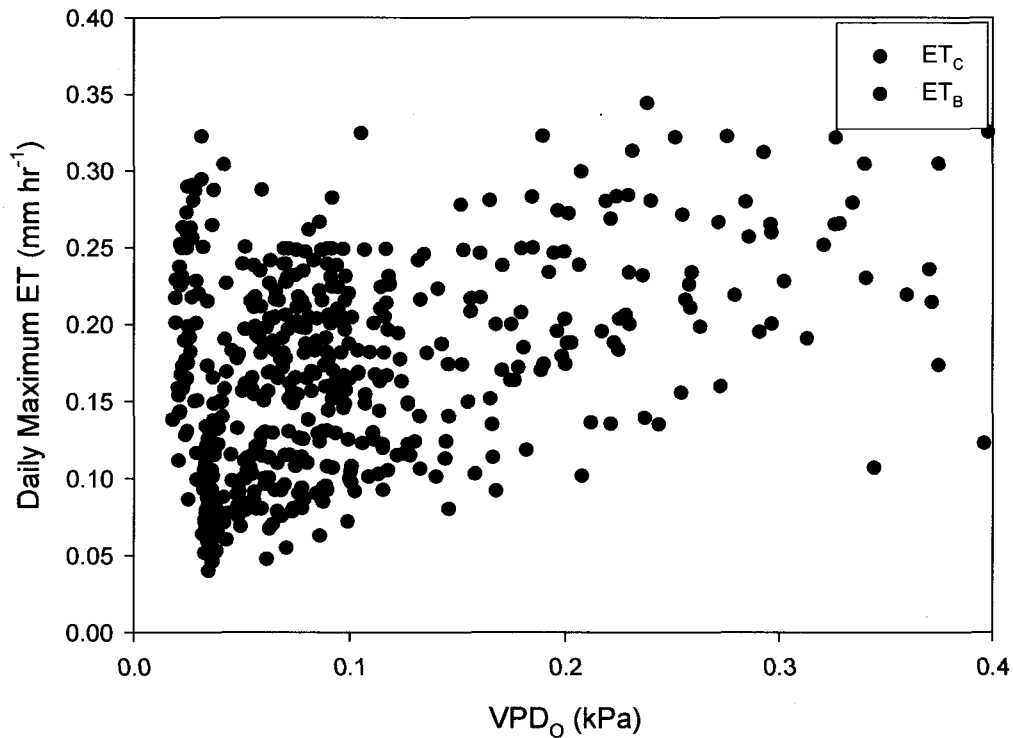


Figure 3.12: Relationship between daily maximum ET (mm hr^{-1}) and VPD_0 (kPa) for above and within canopy layers of the forest canopy during defined green periods of the 2005 and 2006 snow-free seasons, Pond 40, Utikuma Region Study Area (URSA), Alberta, Canada.

Thus, it is expected that θ will influence this relationship between VPD and ET and will likely be the limiting factor on ET regardless of atmospheric demand. A 50 day precipitation free period in 2006 (DOY 205 to 255) is examined (Figure 3.13). During this period of no precipitation inputs the data was binned into 2 θ categories; $\theta > 0.20 \text{ m}^3 \text{ m}^{-3}$ and $\theta < 0.20 \text{ m}^3 \text{ m}^{-3}$. Maximum ET_C rates of 0.33 mm hr^{-1} are observed when $\theta > 0.20 \text{ m}^3 \text{ m}^{-3}$ (Figure 3.13). Whereas when θ is limiting ($\theta < 0.20 \text{ m}^3 \text{ m}^{-3}$) ET_C only reaches a maximum of 0.17 mm hr^{-1} , with the majority of the ET_C clustering below 0.10 mm hr^{-1} . Thus, it can be observed that ET_C rates are limited when θ approaches the

wilting point of the soil ($0.15 \text{ m}^3 \text{ m}^{-3}$) regardless of VPD (Saxton et al, 1986) (Table 3.4). During periods when θ is not limited in the rooting zone ET_C rates can be maintained at higher levels, even at higher VPD's, as long as there is sufficient θ and hydraulic response from soil to leaf is minimized (Meinzer and Grantz, 1991).

Soil Texture Properties	Sand (%)	7.0
	Clay (%)	28.0
	Silt (%)	65.0
Soil Moisture Properties	Wilting Point ($\text{m}^3 \text{m}^{-3}$)	0.15
	Field Capacity ($\text{m}^3 \text{m}^{-3}$)	0.34
	Bulk Density (g cm^{-3})	1.29
	Saturation ($\text{m}^3 \text{m}^{-3}$)	0.51
	Soil hydraulic conductivity (cm hr^{-1})	0.72
	Available Water ($\text{m}^3 \text{m}^{-3}$)	0.18

Table 3.4: Soil texture properties for the rooting zone (0-50 cm) of this silty clay loam soil below the litter fall horizon based on soil cores and taken during installation (May 2005), soil texture classifications and soil moisture properties based on Saxton et al, 1986.

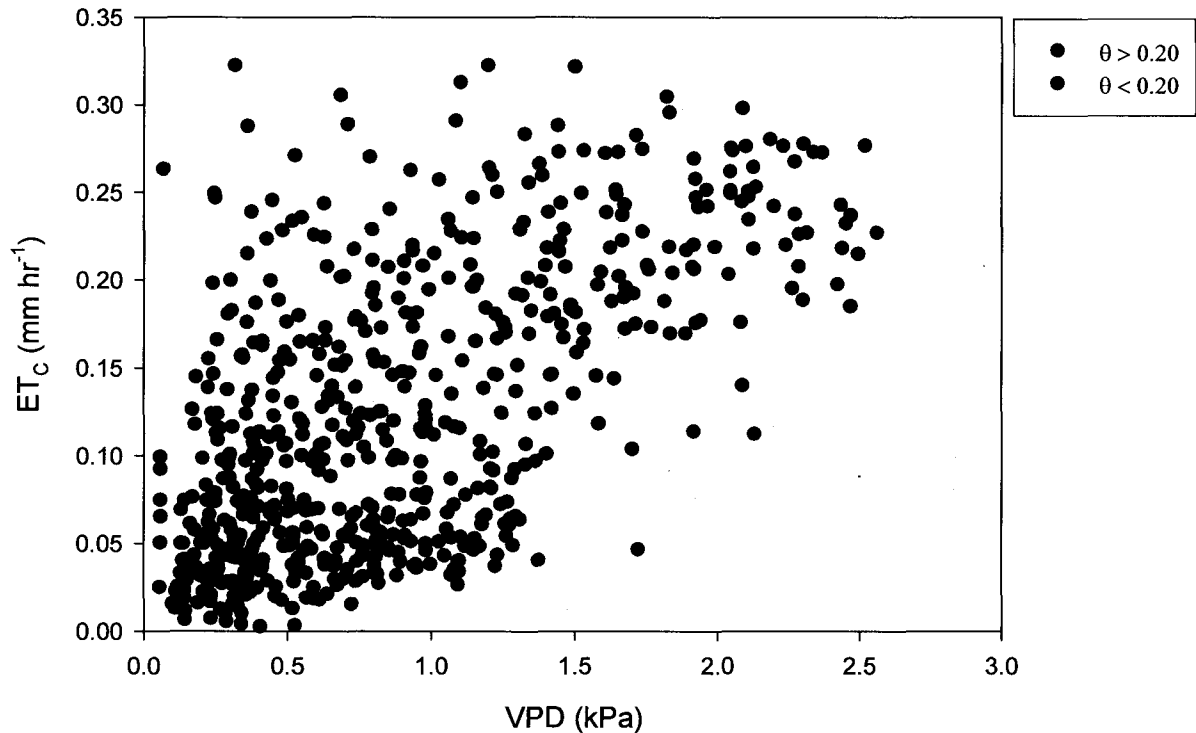


Figure 3.13: Relationship between above canopy ET (ET_C) (mm hr^{-1}) and VPD (kPa) for periods during the 2005 and 2006 peak growth periods when Soil Moisture (θ) become limited and approaches the wilting point ($0.15 \text{ m}^3 \text{ m}^{-3}$) (Saxton et al, 1986), Pond 40, Utikuma Region Study Area (URSA), Alberta, Canada.

3.5 Conclusions

Strong seasonality is observed in ET_C across both snow-free seasons, with maximum daily averages in ET_C of 3.08 and 3.45 mm d^{-1} occurring during the green periods of 2005 and 2006 respectively. ET_B can be an important contribution of overall canopy ET and varies seasonally. This seasonal variation in ET_B is largely a function of the aspen canopies ability to alternate radiation and the aspen root systems influence on the availability of root zone θ . For the 2005 and 2006 snow-free seasons understory ET was

the dominant flux during the early green period, which was a direct result of the timing of understory canopy shrub layer development. As the understory developed before the overstory canopy, increased energy was able to penetrate the canopy layer allowing for increased productivity during this time period. For the remainder of the growth period seasons ET_B averaged 32% of ET_C .

Ψ displayed evidence of hydraulic lift and correlated well with changes in ET_C rates. Further, relationships between Ψ , θ and ET_C showed strong seasonal variation corresponding with aspen phenology.

VPD shows differing controls on ET_C and ET_B rates. However, similar ranges in VPD produce smaller ET fluxes from the understory, which is a function of access to available rooting zone θ . Further, in all levels of the canopy θ exerts the ultimate control on ET. That is, regardless of the degree of atmospheric demand ET can be maintained at higher levels if there is sufficient θ in the rooting zone.

Chapter Four

Summary and Management Implications

4.1 Spatial and temporal variability in evapotranspiration within a forested wetland complex

Examination of the controls on ET from different landcover units in a wetland-forested upland complex of the WBP allows for the enhancement of: (1) our understanding of the dynamics of ET in a wetland-forested upland complex and the role of vegetation communities within differing canopy structures; and (2) evaluate whether these land cover units can be assessed as homogeneous units during the growing season, or that they exhibit large spatial and temporal variability. The latter has direct implications on hydrologic modeling and forest management practices (FMP's) within the WBP, an ultimate goal for this research program.

4.1.1 Wetland Evapotranspiration

The role that vegetation plays in controlling wetland ET within the WBP is significant. However, the significance of that role is governed by the moisture regimes in which the vegetation are present. The dynamics of wetlands, especially within this site of the WBP, and their respective ET contributions can be directly connected to their respective constituent vegetation communities. *Sphagnum* dominated sites have shown to lose water at the greatest rates to ET, yet *Sphagnum* sites show the lowest moisture regimes and no control of microtopography. This is a result of the existence of weak hydrological gradients between lawn and depression units of wetlands, consistent with the climatic and

moisture regimes of such sub-humid environments, where precipitation is typically less than PET.

The presence of seasonal ice lenses plays a significant role in controlling ET throughout wetlands of the WBP. The net effects of the presence of ice does not affect the ET rates on an annual scale, but rather affects the early season rates of ET, and therefore the seasonal distribution of ET. Ice lenses have the potential to shift peak ET rates from wetlands to earlier on in the snow-free season when peak vegetation growth has not yet occurred creating an situation where peak ET rates occur before the maximum soil moisture demands of seasonal maximum vegetation growth. Given the role of ice lenses in wetlands of the WBP, the role that climatic variability will play could potentially have an impact on the severity of early season ET fluctuations.

4.1.2 Aspen Upland Evapotranspiration

Within aspen uplands strong seasonality is observed in above canopy ET (ET_C) across two snow-free seasons, with maximum daily averages in ET_C of 3.08 and 3.45 mm d⁻¹ occurring during the green periods of 2005 and 2006 respectively. The shrub layer and soil ET (ET_B) can be an important contribution of overall forest ET and varies seasonally. The seasonal variation in ET_B was largely a function of the aspen canopies ability to alternate radiation and the aspen root systems influence on the availability of root zone soil moisture (θ). For the 2005 and 2006 snow-free seasons understory ET was the dominant flux during the early green period, which was a direct result of the timing of understory canopy shrub layer development. As the understory leafed out before the overstory forest canopy, increased energy was able to penetrate the canopy layer allowing

for increased productivity during this time period. For the remainder of the snow-free seasons ET_B averaged 32% of ET_C .

Soil tensions (Ψ) showed upward water movement in strong correlation with increased ET, suggesting evidence of hydraulic lift. Further, relationships between Ψ , θ and ET_C showed strong seasonal variation corresponding with aspen phenology. VPD shows differing controls on ET_C and ET_B rates. However, similar ranges in VPD produce smaller ET fluxes from the understory, which is a function of access to available rooting zone θ . Further, in all levels of the canopy θ exerts the ultimate control on ET. That is, regardless of the degree of atmospheric demand ET can be maintained at higher levels if there is sufficient θ in the rooting zone.

4.2 Implications for Watershed Management

The ultimate goal of this research was to accurately assess the natural pre-disturbance controls on ET, which is the dominant hydrologic flux in this region, from forest and wetland landcover units in the WBP. Watershed management practices have become an integral aspect for the sustainable development of Boreal forest systems in North Central Alberta (Ducks Unlimited Canada, 2006). Several industries are currently developing vast areas of the WBP, with major disturbances from the forestry and conventional oil/gas industries, as well as development of oil sands resources (Ducks Unlimited Canada, 2006). Pressure from government and non-governmental organizations on sustainable development of forestry and oil and gas industries requires an accurate assessment of the controls and seasonal contributions of ET from the WBP.

4.2.1 Forest Harvesting Impacts on Evapotranspiration

Within the Boreal Forest region of Canada and elsewhere, forestry operations are conducted within terrestrial and adjacent to aquatic wildlife habitat areas, and in close proximity to agricultural activities, rural communities, and parks (Putz et al., 2003). Harr (1982) found that forest soils are wetter after tree removal, which results in a net reduction in forest ET after harvest (Putz et al., 2003), although ET rates at the edges of remaining boreal forest fragments may be higher than in the forest interior (Cienciala et al., 2002). Further, compaction by harvest machinery traffic can increase soil moisture and bulk density (Whitson et al., 2003; McNabb et al., 2001; Johnson et al., 1991) leading to enhanced overland flow, and a rise in water tables (Lamontagne et al., 2000), which enhances baseflow. After a lodgepole pine clear-cutting in a large watershed (>2000 ha), annual water yield increased by 52% (Burton, 1997). A less intensive harvest (<25% of basin area) on the Shield was not associated with a clear water yield response in medium to large sized watersheds (100–1000 km²; Buttle and Metcalfe, 2000). It has been shown with this research that the role of vegetation in controlling ET rates is significant for the WBP. The removal of vegetation through forest harvesting practices would significantly alter the dynamics of the hydrologic cycle for the region, potentially impacting the already tenuous relationship between P and ET.

Increased pressure on proper FMP's with regards to forest harvesting practices in the WBP region of North Central Alberta will ensure that the natural cycles of ET will be impacted on a less intensive scale. As this region is sub-humid in nature (Devito et al, 2005a) the balance between P and ET is what ultimately drives the hydrologic cycle of the region. Improper FMP's and misguided forest harvesting practices will only serve to

augment the water deficits that dominate the region. Implementing alternative harvesting practices (shelter and selective cutting) could serve as viable alternatives to large scale clearcut practices for the region. The impacts of alternative harvesting methods would need to be explored in greater detail within this region, but could serve as a benchmark for sustainable forest management, a goal of both industry and conservationist alike.

4.2.2 Impacts of Oil and Gas Development on Evapotranspiration

Forest fragmentation is one of the most significant impacts associated with oil and gas exploration and development in the forested region of Alberta, Canada. Not only is Alberta fortunate to have substantial oil and gas reserves, it also has a substantial forest resource that supports a sizable forest industry (MacFarlane, 2003). The exploration and development of energy deposits requires access to the surface immediately above these reserves. Subsequently, considerable areas of forest are cleared to make way for equipment and infrastructure. This has significant social and environmental implications such as the clearing and fragmentation of the boreal forest. The forested area of Alberta, covering over 50% of the provincial area, has been converted from nearly completely intact in the early 1900s, to over 90% fragmented forested landscape in 2002 (MacFarlane, 2003). In fact, land clearing for oil and gas activities accounts for more than double the land cleared for forestry each year (Alberta Environment Protection, 1998). As a result, forest fragmentation has become one of the most significant land management challenges within forested regions of Alberta.

A major hydrologic consequence of oil and gas exploration is reduced ET caused by removal of vegetation. Forest canopy and understorey removal decreases ET rates by

reducing the transpiration and interception surface area and by reducing the water uptake by vegetation. Oil and gas exploration and development causes decreases in ET because above-ground biomass and leaf area are reduced or eliminated (Putz et al., 2003). A slight compensatory increase in E_s may occur because the lower albedo of the darkened soil surface relative to vegetated surfaces results in higher net solar radiation input (Putz et al., 2003). In addition, wind movement over soil surfaces increases after vegetation removal and this further enhances evaporative losses. The impacts of oil and gas development on the fragmentation of Boreal Forest landscapes require significant attention with regards to the magnitudes of fluxes and the nature of ET dynamics. Proper FMP's with greater attention to the dynamics of ET within this sub-humid climate will not only enhance the sustainability of the region, but also ensure that the hydrologic cycle of this tenuous region will be minimally impacted.

4.3 Conclusion

The boreal forest constitutes one of the largest biomes on Earth, and as we attempt to monitor and model the dynamics of it there is an increasing need to recognize the directions and magnitudes of ET, a significant aspect of the hydrologic cycle in this sub-humid region of the WBP within different landcover units. Treating the catchment as a whole unit, that is combining the landcover units of wetlands and uplands to produce a single value for ET, is insufficient and will provide limited insight into the actual conditions and balance between P and ET for the region. By understanding the dynamics in vegetation composition in wetlands and structure of aspen dominated uplands as separate units that comprise the catchments of typical boreal forest landscapes and

quantifying the contributions of ET and dynamics of the hydrologic cycle separately, a more complete understanding of the region would be produced. This would be to the benefit of forest management practitioners as it would provide a more complete understanding the systems they are looking to manage.

Chapter Five

References

- Alberta Environmental Protection, 1998. The boreal forest natural region of Alberta. Natural Resource Services, Recreation and Protection, Special Report.
- Amiro, B.D., 2001. Paired-tower measurements of carbon and energy fluxes following disturbance in the boreal forest. *Global Change Biology*. **7**: 253–268.
- Amiro, B.D., Barr, A.G., Black, T.A., Iwashita, H., Kljun, N., McCaughey, J.H., Morgenstern, K., Murayama, S., Nesic, Z., Orchansky, A.L. and Saigusa, N., 2006. Carbon, energy and water fluxes at mature and disturbed forest sites, Saskatchewan, Canada. *Agriculture and Forest Meteorology*. **136**: 237–251.
- Aubinet, M., Grelle, A., Ibrom, A., Rannik, U., Moncrieff, J., Foken, T., Kowalski, A.S., Martin, P.H., Berbigier, P., Bernhofer, C., Clement, R., Elbers, J., Granier, A., Grunwald, T., Morgenstern, K., Pilegaard, K., Rebmann, C., Snijders, W., Valentini, R. and Vesala T. 2000. Estimates of the annual net carbon and water exchange of forests: the Euroflux methodology. *Advances in Ecological Research* **30**: 113–175.
- Baldocchi, D.D., Hicks, B.B. and Meyers, T.P. 1988. Measuring biosphere atmosphere exchanges of biologically related gases with micrometeorological methods. *Ecology* **69**: 1331–1340.
- Baldocchi, D.D., Vogel, C.A. and Hall, B. 1997. Seasonal variation of energy and water vapour exchange rates above and below a boreal jack pine forest canopy. *Journal of Geophysical Research*. **102 (D24)**: 28939-28951.
- Baldocchi, D.D., Finnigan, J., Wilson, K., Paw U, K.T., Falge, E., 2000. On measuring net ecosystem carbon exchange over tall vegetation on complex terrain. *Boundary Layer Meteorology*. **96**: 257–291.
- Baldocchi, D.D., Kelliher, F.M., Black, T.A. and Jarvis, P. 2000. Climate and vegetation controls on boreal zone energy exchange. *Global Change Biology*. **6**: 69-83.
- Baldocchi, D.D. 2003. Assessing the eddy covariance technique for evaluating the carbon dioxide exchange rates of ecosystems: past, present and future balance of ecosystems. *Global Change Biology*. **9**: 1-14.
- Barbour, M.M., Hunt, J.E., Walcroft, A.S., Rogers G.N.D., McSeveny, T.M. and Whitehead, D. 2005. Components of ecosystem evaporation in a temperate coniferous rainforest, with canopy transpiration scaled using sapwood density. *New Phytologist*. **165**: 549-558.

- Barr, A.G., King, K.M., Gillespie, T.J., den Hartog, G., Neumann, H.H., 1994. A comparison of Bowen ratio and eddy correlation sensible and latent heat flux measurements above deciduous forest. *Boundary Layer Meteorology*. **71**: 21–41.
- Barr, A.G., Griffis, T.J., Black, T.A., Lee, X., Staebler, R.M., Fuentes, J.D., Chen, Z. and Morgenstern, K. 2002. Comparing the carbon budgets of boreal and temperate deciduous forest stands. *Canadian Journal of Forest Research* **32**: 813–822.
- Bisbee, K.E., Gower, S.T., Norman, J.M. and Nordheim, E.V. 2001. Environmental controls on ground cover species composition and productivity in a boreal black spruce forest. *Oecologia*. **129**: 261–270.
- Blancher, P. and Wells, J., 2005. North America's bird nursery: The Boreal Forest Region and its global responsibility toward sustaining bird populations. Boreal Songbird Initiative and the Canadian Boreal Initiative. Ottawa, Ontario.
- Blanford, J.H., Gay, L.W. 1992. Tests of a robust eddy correlation system for sensible heat flux. *Theoretical and Applied Climatology*. **46**: 53–60.
- Blanken, P.D., Black, T.A., Yang, P.C., Neumann, H.H., Staebler, R., Nesic, Z., den Hartog, G., Novak, M.D., Lee, X. 1997. The energy balance and canopy conductance of a boreal aspen forest: Partitioning overstory and understory components. *Journal of Geophysical Research*. **102**: 915–927.
- Blanken, P.D., Black, T.A., Neumann, H.H., den Hartog, G. Yang, P.C., Nesic, Z., Staebler, R., Chen, W. & Novak, M.D. 1998. Turbulent flux measurements above and below the overstory of a boreal aspen forest. *Boundary-Layer Meteorology*, **89** (1), 109-140
- Blanken, P.D., Black, T.A., Neumann, H.H., den Hartog, G., Yang, P.C., Nesic, Z. and Lee, X. 2001. The seasonal water and energy exchange above and within a boreal aspen forest. *Journal of Hydrology*. **245**: 118-136.
- Bothe, R.A., Abraham, C. 1993. Evaporation and evapotranspiration in Alberta, 1986–1992 Addendum. Water Resources Services, Alberta Environmental Protection: Edmonton, Canada.
- Bovard, B.D., Curtis, P.S., Vogel, C.S., Su, H.B. and Schmid, H.P. 2005. Environmental controls on sap flow in a northern hardwood forest. *Tree physiology*. **25**: 31-38.
- Brown, S.M., Petrone, R.M., Mendoza, C and Devito, K.J. 2009. Surface vegetation controls on evapotranspiration from a sub-humid Western Boreal Plain wetland. *Hydrological Processes*. In Press. Accepted November 4, 2009.
- Brutsaert, W. 1982. Evaporation into the Atmosphere: Theory, History and Applications. Springer: New York; 299.

- Bryant, D., Nelson, D. and Tangle, L. 1997. The last frontier forests: Ecosystems and economics on the edge. Washington D.C., World Resources Institute.
- Burton, T.A. 1997. Effects of basin-scale timber harvest on water yield and peak streamflow. *Journal of American Water Resources Association*. **33**: 1187–1196.
- Busby, J.R., Bliss, L.C. and Hamilton, C.D. 1978. Microclimate control of growth rates and habitat of boreal forest mosses, *Thompentypnum nitens* and *Hylocomium splendens*. *Ecological Monogr.* **48**: 95-110.
- Buttle, J.M., and Metcalfe, R.A. 2000. Boreal forest disturbance and streamflow response, northeastern Ontario. *Canadian Journal of Fisheries and Aquatic Sciences*. **57**: 5–18.
- Calder, I.R. 1998. Water use by forests, limits and controls. *Tree physiology*. **18**: 625-631.
- Caldwell, M.M., Dawson, T.E. and Richard, J.H. 1998. Hydraulic lift: Consequences of water efflux from the roots of plants. *Oecologia*. **113**: 306-311.
- Canadian Forest Service, 2006. The state of Canada's forests 2004-2005: The boreal forest. Canadian Forest Service, Ottawa, Ontario.
- Cienciala, E., Running, S.W., Lindroth, A., Grelle, A. and Ryan, M.G. 1998. Analysis of carbon and water fluxes from the NOPEX boreal forest: comparison of measurements with FOREST-BGC simulations. *Journal of Hydrology*. **212–213**: 62–78.
- Cinnirella, S., Magnani, F., Saracino, A. and Borghetti, M. 2002. Response of a mature *Pinus laricio* plantation to a three-year restriction of water supply: structural and function acclimation to drought. *Tree physiology*. **22**: 21-30.
- Cuenca, R.H., Strangel, D.E. and Kelly, S.F. 1997. Soil water balance in a boreal forest. *Journal of Geophysical Research*. **102 (D24)**: 29355-29365.
- Devito, K., Creed, I., Gan, T., Mendoza, C., Petrone, R., Silins, U. and Smerdon, B., 2005a. A framework for broad scale classification of hydrologic response units on the Boreal Plains: Is topography the last thing to think of? *Hydrological Processes*. **19(8)**: 1705-1714.
- Devito, K.J., Creed, I.F. and Fraser, C.J.D., 2005b. Controls on runoff from a partially harvested aspen-forested headwater catchment, Boreal Plain, Canada. *Hydrological Processes*, **19(1)**: 3-25.
- Ducks Unlimited Canada. 2006. Waterfowl of the Boreal Forest. Ducks Unlimited Canada, Stonewall, Manitoba. 107p.

Environment Canada (2005) Climate Data Online, Slave Lake Alberta. http://www.climate.weatheroffice.ec.gc.ca/climateData/canada_e.html.

Eugster, W., McFadden, J.P. and Chapin, F.S.III. 1997. A Comparative approach to regional variation in surface fluxes using eddy correlation towers. *Boundary Layer Meteorology*. **85**: 293–307.

Falge, E., Baldocchi, D., Olson, R.J., Anthoni, P., Aubinet, M., Bernhofer, C., Burba, G., Ceulemans, R., Clement, R., Dolman, H., Granier, A., Gross, P., Grünwald, T., Hollinger, D., Jensen, N-O., Katul, G., Keronen, P., Kowalski, A., Ta, Lai C., Law, B.E., Meyers, T., Moncrieff, J., Moors, E., Munger, J.W., Pilegaard, K., Rannik, U., Rebmann, C., Suyker, A., Tenhunen, J., Tu, K., Verma, S., Vesala, T., Wilson, K. and Wofsy, S. 2001. Gap filling strategies for defensible annual sums of net ecosystem exchange. *Agricultural and Forest Meteorology* **107**: 43–69.

Fenton, M.M., Paulen, R.C. and Pawlowicz, J.G., 2003. Surficial geology of the Lubicon Lake area, Alberta (NTS 84B/SW). Alberta Geological Survey.

Ferone, J.M. and Devito, K.J., 2004. Shallow groundwater-surface water interactions in pond-peatland complexes along a Boreal Plains topographic gradient. *Journal of Hydrology*. **292(1-4)**: 75-95.

Finnigan, J.J., Clement, R., Mahli, Y., Leuning, R. and Cleugh, H.A. 2003. A reevaluation of long-term flux measurement techniques part I: averaging and coordinate rotation. *Boundary-Layer Meteorology* **107**: 1–48.

Grelle, A., Lundberg, A., Lindroth, A., Moren, A.S., and Cienciala E. 1997. Evaporation components of a boreal forest: Variations during the growing season. *Journal of Hydrology*. **197**: 70-87.

Grelle, A., Lindroth, A. and Mölder, M., 1999. Seasonal variation of boreal forest surface conductance and evaporation. *Agricultural and Forest Meteorology*. **98–99**, 563–578.

Hall, R.L. and Allen, S.J., 1997. Water use of poplar clones grown as short-rotation coppice at two sites in the United Kingdom. In: Bullard, M.J., Ellis, R.G., Heath, M.C., Knight, J.D., Lainsbury, M.A., Parker, S.R. (Eds.), *Aspects of Applied Biology* 49, Biomass and Bioenergy Crops. Association of Applied Biologists. Wellesbourne, Warwick, UK, pp. 163-172.

Halliwell, D.H., Rouse, W.R. 1987. Soil heat flux in permafrost: characteristics and accuracy of measurement. *Journal of Climatology*. **7**: 571–584.

Harr, R.D. 1982. Fog drip on the Bull Run municipal watershed, Oregon. *Water Resources Bulletin*. **18**: 785–789.

- Heijmans, M.P.D, Arp, W.J. and Berendse, F., 2001. Effects of elevated CO₂ and vascular plants on evapotranspiration in bog vegetation. *Global Change Biology*. **7**: 817-827.
- Heijmans, M., Arp, W.J. and Chapin III, F.S. 2004. Carbon dioxide and water vapour exchange from understory species in boreal forest. *Agricultural and Forest Meteorology*. **123**: 135-147.
- Hogg, E.H. 1994. Climate and the southern limit of the western Canadian boreal forest. *Canadian Journal of Forest Research*. **24**: 1835-1845.
- Hogg, E.H. and Hurdle, P.A. 1997. Sap flow in trembling aspen: implications for stomatal responses to vapour pressure deficits. *Tree physiology*. **17**: 501-509.
- Hogg, E.H., Black, T.A. and den Hartog, G. 1997. A comparison of sap flow and eddy fluxes of water vapour from a boreal deciduous forest. *Journal of Geophysical Research-Atmospheres*. **102**: 28929-28937.
- Hogg, E.H., Saugier, B., Pontauiller, J.-Y., Black, T.A., Chen, W., Hurdle, P.A., and Wu, A. 2000. Responses of trembling aspen and hazelnut to vapor pressure deficit in a boreal deciduous forest. *Tree Physiology*. **20**: 725-734.
- Horst, T.W. and Weil, J.C. 1994. How far is far enough?: The fetch requirements for micrometeorological measurement of surface fluxes. *Journal of Atmosphere and Ocean Technology* **11**: 1018-1025.
- Humphreys, E.R., Black, T.A., Ethier, G.J., Drewitt, G.B., Spittlehouse, D.L., Jork, E.M., Nestic, Z. and Livingston, N.J. 2003. Annual and seasonal variability of sensible and latent heat flux above a coastal Douglas-fir forest, British Columbia, Canada. *Agricultural and Forest Meteorology* **115**: 109-125.
- Irvine, J., Law, B.E., Anthoni, P.M. and Meinzer, F.C. 2002. Water limitations to carbon exchange in old-growth and young ponderosa pine stands. *Tree Physiology*. **22**: 189-196.
- Johnson, C.E., Johnson, A.H., Huntington, T.G., and Siccama, T.G. 1991. Whole-tree clear-cutting effects on soil horizons and organic matter pools. *Soil Science Society of America Journal*. **55**: 497-502.
- Kaimal, J.C. and J. Finnigan, J. 1994. Atmospheric Boundary Layer Flows: Their Structure and Measurement, Oxford University Press, New York. pp. 255-261.
- Kim, J. and Verma, S.B. 1996. Surface exchange of water vapour between and open sphagnum fen and the atmosphere. *Boundary Layer Meteorology*. **79**: 243-264.
- Klassen, R.W., 1989. Quaternary geology of the southern Canadian interior plains. In: R.J. Fulton (Editor), Quaternary Geology of Canada and Greenland. Geology of North America. Geological Survey of Canada, Ottawa, Canada: 138-174.

- Kurpius, M.R., Panek, J.A., Nikolov, N.T., McKay, M. and Goldstein, A.H. 2003. Partitioning of water flux in a Sierra Nevada ponderosa pine plantation. *Agricultural and Forest Meteorology*. **117**: 173-192.
- Lafleur, P.M. 1990. Evaporation from Wetland in N. T. Roulet (ed.). Focus: Aspects of the Physical Geography of Wetland. *Canadian Geographer*. **34**: 79-88.
- Lafleur, P.M. and Schraeder, C.P. 1994. Water loss from the floor of a sub-arctic forest. *Arctic Alpine Research*. **26**: 152-158.
- Lamontagne, S., Carignan, R., D'Arcy, P., Prairie, Y.T., and Paré, D. 2000. Element export in runoff from eastern Canadian Boreal Shield drainage basins following forest harvesting and wildfires. *Canadian Journal of Fisheries and Aquatic Sciences*. **57**: 118–128.
- Laporte, M., Duchesne, L.C. and Wetzel S. 2002. Effect of rainfall patterns on soil surface CO₂ efflux, soil moisture, soil temperature and plant growth in a grassland ecosystem of Northern Ontario, Canada: implications for climate change. *BioMed Central Ecology*. **2**: 10-16.
- LeCain, D.R., Morgan, J.A., Schuman, G.E., Reeder, J.D. and Hart, R.H. 2002. Carbon exchange and species composition of grazed pastures and exclosures in shortgrass steppe of Colorado. *Agriculture, Ecosystems and Environment*. **93**: 421-435.
- Leuning, R. and Judd, M.J. 1996. The relative merits of open and closed path analysers for measurement of eddy fluxes. *Global Change Biology*. **2**: 241-253.
- LI-COR, Inc., 2000. LI-7500 CO₂/H₂O Analyzer Instruction Manual, LI-COR, Inc., Lincoln, Nebraska.
- Longton, R.E., and Greene, S.W. 1979. Experimental studies of growth and reproduction in the moss *Pleurozium schreberi* (Brid.) Mitt. *Journal of Bryology*. **10**: 321–338.
- MacFarlane, A.K. 2003. Vegetation response to seismic lines: edge effects and on-line succession. MSc thesis. Department of Biological Sciences. University of Alberta.
- Mahrt, L. 1998. Flux sampling errors for aircraft and towers. *Journal of Atmosphere and Ocean Technology* **15**: 416–429.
- Marshall, I.B., Schut, P. and Ballard, M. (compilers). 1999. Canadian ecodistrict climate normals for Canada 1961–1990. A national ecological framework for Canada: Attribute Data. Environmental Quality Branch, Ecosystems Science Directorate, Environment Canada and Research Branch, Agriculture and Agri-Food Canada, Ottawa/Hull.
- Massman, W.J. 2000. A simple method for estimating frequency response corrections for eddy covariance systems. *Agricultural and Forest Meteorology* **104**: 185–198.

- McLaren, J. D., Arain, M.A., Khomik, M., Peichl, M. and Brodeur, J. 2008. Water flux components and soil water-atmospheric controls in a temperate pine forest growing in a well-drained sandy soil. *Journal of Geophysical Research*. 113: doi:10.1029/2007JG000653.
- McLeod, M.K., Daniel, H., Faulkner, R., and Murison, R. 2004. Evaluation of an enclosed portable chamber to measure crop and pasture actual evapotranspiration at small scale. *Agricultural Water Management*. 67: 15-34.
- McNabb, D.H., Startsev, A.D., and Nguyen, H. 2001. Soil wetness and traffic level effects on bulk density and air-filled porosity of compacted boreal forest soils. *Soil Science Society of America Journal*. 65: 1238–1247.
- McNaughton, K.G. and Jarvis P.G. 1991. Effects of spatial scale on stomatal control of transpiration. *Agricultural and Forest Meteorology*. 54: 279–301.
- Meinzer, F.C. and Grantz, D.A. 1991. Coordination of stomatal, hydraulic and canopy boundary layer properties: do stomata balance conductances by measuring transpiration? *Physiologia Plantarum*. 83: 324-329.
- Metcalf, R.A. and Buttle, J.M., 1999. Semi-distributed water balance dynamics in a small boreal forest basin. *Journal of Hydrology*. 226(1-2): 66-87.
- Moore, K.E., Fitzjarrald, D.R., Sakai, R.K. and Freedman, J.M. 2000. Growing season water balance at a boreal jack pine forest. *Water Resources Research*. 36: 483-493.
- National Wetlands Working Group, 1988. Wetlands of Canada, Ecological Land Classification Series No. 24, Ottawa.
- Nichols, D.S. and Brown, J.M. 1980. Evaporation from a sphagnum moss surface. *Journal of Hydrology*. 48: 289-302.
- Nijssen, B. and Lettenmaier, D.P. 2002. Water balance dynamics of a boreal forest watershed: White Gull Creek basin, 1994-1996. *Water Resources Research*. 38: doi: 10.1029/2001WR000699
- Nosetto, M.D., Jobbagy, E.G. and Paruelo, J.M. 2005. Land-use change and water losses: the case of grassland afforestation across a soil textural gradient in central Argentina. *Global Change Biology*. 11: 1101-1117.
- Oke, T.R. Boundary Layer Climates – 2nd Edition. University Press, Cambridge. 1987.
- Oren, R. and Pataki, D. 2001. Transpiration in response to variation in microclimate and soil moisture in southeastern deciduous forests. *Oecologia*. 127:549-559.
- Pawlowicz, J.G. and Fenton, M.M., 2002. Drift thickness of the Peerless Lake map area (NTS 84B), Map 253, Alberta Geologic Survey, Edmonton, Alberta, Canada.

- Peixoto, J.P. and Oort, A.H. 1992. *Physics of Climate*. American Institute of Physics. 520 pg.
- Peterson, E.B. and Peterson, N.M. 1992. Ecology, management, and use of aspen and balsam poplar in the Prairie Provinces, Canada. Forestry Canada, Northern Forestry Centre, Special Report 1.
- Petrone R.M. and Rouse W.R. 2000. Synoptic controls on the surface energy and water budgets in subarctic regions of Canada. *International Journal of Climatology*. **20**: 1149–1165.
- Petrone, R.M., Waddington, J.M. and Price, J.S., 2001. Ecosystem scale evapotranspiration and net CO₂ exchange from a restored peatland. *Hydrological Processes* **15**: 2839–2845.
- Petrone, R.M. 2002. Hydroclimatic factors controlling net CO₂ exchange in managed peatland ecosystems. PhD thesis. Department of Geography. University of Waterloo.
- Petrone R.M., Waddington J.M. and Price J.S. 2003c. Ecosystem-scale flux of CO₂ from restored vacuum peatland. *Wetlands Ecology and Management*. **11**(6): 419–432
- Petrone, R.M., Silins, U. and Devito, K.J., 2007. Dynamics of evapotranspiration from a riparian pond complex in the Western Boreal Forest, Alberta, Canada. *Hydrological Processes*. **21**(11): 1391-1401.
- Petrone, R.M., Devito, K.J., Silins, U., Mendoza, C., Brown, S., Kaufman, S.C. and Price, J.S. 2008. Transient peat properties in two pond-peatland complexes in the sub-humid Western Boreal Plain, Canada. *Mires and Peat*. **3**: Article 05.
- Phillips, N. and Oren, R. 2001. Intra- and inter-annual variation in transpiration of a pine forest. *Ecological Applications*. **11**: 385-396.
- Price, J.S., 1991. Evaporation from a blanket bog in a foggy coastal environment. *Boundary Layer Meteorology*. **57**: 391–406.
- Price, J.S. 1997. Soil moisture, water tension, and water table relationships in a managed cutover bog. *Journal of Hydrology*. **202**: 21 – 32.
- Price, J.S., Rochefort, L. and Campeau, S. 2002. Use of shallow basins to restore cutover peatlands: hydrology. *Restoration Ecology*. **10**: 259-266.
- Priestley, C.H.B. and Taylor, R.J. 1972. On the assessment of surface heat flux and evaporation using large scale parameters. *Monthly Weather Review*. **100**: 81-91.
- Putz, G., Burke, J.M., Smith, D.W., Chanasyk, D.S., Prepas, E.E. and Mapfumo, E. 2003. Modelling the effects of boreal forest landscape management upon streamflow and water quality: Basic concepts and considerations. *Journal of Environmental Engineering Sciences*. **2**: S87–S101.

- Redding, T.E. and Devito, K.J. 2006. Particle densities of wetlands soils in northern Alberta. *Canadian Journal of Soil Science*. **86**: 57–60.
- Redding, T.E. and Devito, K.J. 2008. Lateral flow thresholds for aspen forested hillslopes on the Western Boreal Plain, Alberta, Canada. *Hydrological Processes*. DOI: 10.1002/hyp
- Restrepo, N.C. and Arain, M.A. 2005. Energy and water exchanges from a temperate pine plantation forest. *Hydrological Processes*. **19**: 27-49.
- Roberts, J. 1983. Forest Transpiration – a Conservative Hydrological Process. *Journal of Hydrology*. **66**: 133-141.
- Roberts, J. 2000. The influence of physical and physiological characteristics of vegetation on their hydrological response. *Hydrological Processes*. **19**: 2885-2901.
- Rouse, W. R. 2000. The energy and water balance of high-latitude wetlands: controls and extrapolation. *Global Change Biology*. **6**: 59-68.
- Saxton, K.E., Rawls, W.J., Romberger, J.S. and Papendick, R.I. 1986. Estimating generalized soil-water characteristics from texture. *Soil Science Society of America Journal*. **50(4)**: 1031-1036.
- Schafer, K.V.R, Oren, R., Lai, C.T. and Katul, G.G. 2002. Hydrologic balance in an intact temperate forest ecosystem under ambient and elevated atmospheric CO₂ concentration. *Global Change Biology*. **8**: 895-911.
- Schuepp, P. H., M. Y. Leclerc, J. I. MacPherson and Desjardins, R.L. 1990. Footprint prediction of scalar fluxes from analytical solutions of the diffusion equation. *Bound.-Layer Meteorology*. **50**: 355–374.
- Schwartz, M.D., Ahas, R. and Anto, A. 2006. Onset of spring starting earlier across the Northern Hemisphere. *Global Change Biology*. **12**: 343-351.
- Skre, O., Oechel, W.C. and Miller, P.M. 1983. Moss water leaf content and solar radiation at the moss surface in mature black spruce forest in central Alaska. *Canadian Journal of Forest Research*. **13**: 860-868.
- Smerdon, B.D., Devito, K.J. and Mendoza, C.A., 2005. Interaction of groundwater and shallow lakes on outwash sediments in the sub-humid Boreal Plains of Canada. *Journal of Hydrology*. **314(1-4)**: 246-262.
- Smerdon, B.D., Mendoza, C.A. and Devito, K.J., 2007. Simulations of fully coupled lake-groundwater exchange in a subhumid climate with an integrated hydrologic model. *Water Resources Research*. **43(1)**: W01416, doi:10.1029/2006WR005137.

Soil Classification Working Group, 1998. *The Canadian System of Soil Classification*, 3rd edn. Agriculture and Agri-Food Canada: Ottawa, ON.

Solondz, D.S. 2007. Spatial Relationships of Carbon Dioxide Exchange in an Upland Forested Wetland Complex in the Western Boreal Plain, Alberta, Canada. M.S. Thesis. Department of Geography and Environmental Studies. Wilfrid Laurier University.

Solondz, D.S., Petrone, R.M. and Devito, K.J. 2008. Forest floor carbon dioxide fluxes within an upland-peatland complex in the Western Boreal Plain, Canada. *Ecohydrology* **1(4)**: 361 – 376.

Stagnitti, F., Parlange, J.Y. and Rose, C.W. 1989. Hydrology of a small wet catchment. *Hydrological Processes*. **3**: 137–150.

Stannard, D.I., 1988. Use of a hemispherical chamber for measurement of evapotranspiration. Open-File Report 88-452. United State Geological Survey, Denver, CO.

Tufekcioglu, A., Raich, J.W., Isenhardt, T.M. and Schultz, R.C. 2001. Soil respiration within riparian buffers and adjacent crop fields. *Plant and Soil*. **229**: 117–124.

Twine, T.E., Kustas, W.P., Norman, J.M., Cook, D.R., Houser, P.R., Meyers, T.P., Prueger, J.H., Starks, P.J. and Wesely, M.L. 2000. Correcting eddy-covariance flux underestimates over a grassland. *Agricultural and Forest Meteorology*. **103**: 279–300.

Unsworth, M.H., Phillips, N. and Link, T. 2004. Components and controls of water flux in an old-growth Douglas-fir-western hemlock ecosystem. *Ecosystems*. **7**: 468-481.

Viereck, L.A., Van Cleve, K., and Dryness, C.T. 1986. Forest ecosystem distribution in a taiga environment. *Ecological Studies*.

Vitt, D.H. 1990. Growth and production dynamics of Boreal mosses over climatic, chemical and topographic gradients. *Botanical Journal of the Linnean Society*. **104**: 35-39.

Vitt, D.H., Halsey, L.A., Bauer, I.E. and Campbell, C. 2000. Spatial and temporal trends in carbon storage of peatlands of continental western Canada through the Holocene. *Canadian Journal of Earth Sciences*. **37(5)**: 683–693.

Vogwill, R. 1978. Hydrogeology of the Lesser Slave Lake area, Alberta. Edmonton AB. Alberta Research Council.

Waddington, J.M., Griffis, T.J. and Rouse, W.R. 1998. Northern Canadian wetlands: net ecosystem CO₂ exchange and climatic change. *Climatic Change*. **40**: 267-275.

Waddington, J.M. and Roulet, N.T., 2000. Carbon balance of a boreal patterned peatland. *Global Change Biology*. **6**: 87–97.

Webb E.K., Pearman, G.I. and Leuning, R. 1980. Correction for flux measurements for density effects due to heat and water vapour transfer. *Quarterly Journal of the Royal Meteorological Society*. **106**: 85-100.

Whitson, I.R., Chanasyk, D.S., and Prepas, E.E. 2003. Hydraulic properties of Orthic Gray Luvisolic soils and impact of winter logging. *Journal of Environmental Engineering Sciences*. **2**.

Williams, P.J. and Smith, M.W. 1989. *The Frozen Earth: Fundamentals of Geocryology*. Cambridge University Press: Cambridge, UK.

Williams, T.G. and Flanagan, L.B. 1996. Effects of changes in water content on photosynthesis, transpiration and discrimination against $^{13}\text{CO}_2$ and $\text{C}^{18}\text{O}^{16}\text{O}$ in *Pleurozium* and *Sphagnum*. *Oecologia*. **108**: 38–46.

Wilson, K.B. and Baldocchi, D.D. 2000. Seasonal and interannual variability of energy fluxes over a broadleaved temperate deciduous forest in North America. *Agricultural and Forest Meteorology*. **100**: 1–18.

Winter, T.C. and Woo, M.-K., 1990. Hydrology of lakes and wetlands. In: M.G. Wolman and H.C. Riggs (Editors), *The Geology of North America Vol O-1: Surface Water Hydrology*. Geological Society of America, Boulder, Colorado.

Winter, T.C. 2001. The concept of hydrologic landscapes. *Journal of the American Water Resources Association*. **37(2)**: 335-349.

Wolfe, B.B., Hall, R.I., Last, W.M., Edwards, T.W.D., English, M.C., Karst-Riddoch, T.L., Paterson, A. and Palmi, R., 2006. Reconstruction of multi-century flood histories from oxbow lake sediments, Peace-Athabasca Delta, Canada. *Hydrological Processes*. **20(19)**: 4131-4153.

Woo, M.-K. and Winter, T.C., 1993. The role of permafrost and seasonal frost in the hydrology of northern wetlands in North America. *Journal of Hydrology*. **141(1-4)**: 5-31.

Wullschleger, S.D., Hanson, O.J. and Tschaplinski, T.J. 1998a. Whole-plant water flux in understory red maple exposed to altered precipitation regimes. *Tree physiology*. **18**: 71-79.

Wullschleger, S.D. and Hanson, P.J. 2006. Sensitivity of canopy transpiration to altered precipitation in an upland oak forest: evidence from a long-term field manipulation study. *Global Change Biology*. **12**: 97-109.

Chapter Six

Appendices

6.1 Water Vapour Absorption by IRGA

The EGM-4 IRGA used during the experiment operates by filtering sampled air through the central membrane of the system before it is analyzed by the central processing unit and IRGA cell of the system (PP Systems, 1999). Thus, the air that is sampled first passes through a volume ($\sim 706.5 \text{ mm}^3$) of Sofnolime Granules (Sodium Hydroxide) (Molecular Products, Essex, UK). In order to address this removal of moisture from the sampled air, calculations were conducted to account for the moisture reduction. The volume of chamber air cycled through the IRGA was determined by,

$$A = \frac{PR}{V} * 1000 \quad (6.1)$$

where A is the volume of air cycled through the IRGA ($\% \text{ vol min}^{-1}$), PR is the pump rate ($300 \text{ cm}^3 \text{ min}^{-1}$) and V is the chamber volume (0.016 m^3). Assuming a saturated parcel of air at 20°C , with a vapor density of 17.3 g m^{-3} is cycled through the IRGA, the volume of air passing through the IRGA can then be calculated over the 5 min sampling interval via,

$$B = \left(\left(\frac{\rho_v}{Area} \right) * V \right) * S_i \quad (6.2)$$

where B is the volume of water passing through the column ($\text{g H}_2\text{O}$) and ρ_v is the vapour density of the air parcel saturated at 20°C ($\text{g H}_2\text{O}$) and S_i is the sampling interval (5 min). Finally, the net effect (drying capacity) of the Sofnolime granules was calculated given the volume of H_2O passing the column of the IRGA. This results in a decrease of 0.039 g

H₂O in vapour content of the sampled air as a result of the drying effect of the Sofnolime granules. When multiplied by the volume of Sofnolime granules present within the column of the IRGA (150 g) there becomes a loss of vapour of 0.011 g H₂O per 5 min interval, which amounts to a potential error of approximately 4 %.

6.2 Eddy Covariance Pre-Analysis

The eddy covariance (EC) technique for determining fluxes from forested wetland complex systems requires that tests be conducted to ensure valid measurements are achieved and include;

1. Suitable response time of the sensors which ensures the capture of smaller higher frequency (~20 Hz) eddies and the averaging period over which the covariance's are calculated should be long enough to ensure the larger, lower frequency eddies are captured,
2. The orientation and placement of the windspeed sensors must be precise to ensure that the correlations involving one or more velocity components are accurate (Brutsaert, 1982),
3. The energy balance is properly assessed and closure is achieved so as to account for the available energy within the system accurately and,
4. Friction velocity (u^*) thresholds are accurately assessed to ensure that issues revolving around nocturnal stability of fluxes are addressed.

The vertical windspeed mean, which is separated from the short time fluctuations, is subject to larger time scale trends. Therefore, the averaging period should be as short as

possible to ensure that the time series remains stationary but long enough to cover even the slowest fluctuations of the turbulent spectrum (Brutsaert, 1982). The averaging period used in this study was 30 minutes, with sensors sampling every 0.01 seconds. To ensure that the sensor placement, sampling and averaging periods were capturing all of the eddies contributing to the actual flux spectral analysis of the flux measurements was conducted. The power spectral density of the vertical wind signal was calculated using Welch's method (Figure 6.1). Optimized sampling interval is obtained when the curve flattens out, which occurs at approximately 1200 seconds (20 minutes). The average flux calculations should be done when the eddy signal is producing a flat spectrum (white noise), commonly occurring at the 30 min interval (Petrone, 2002).

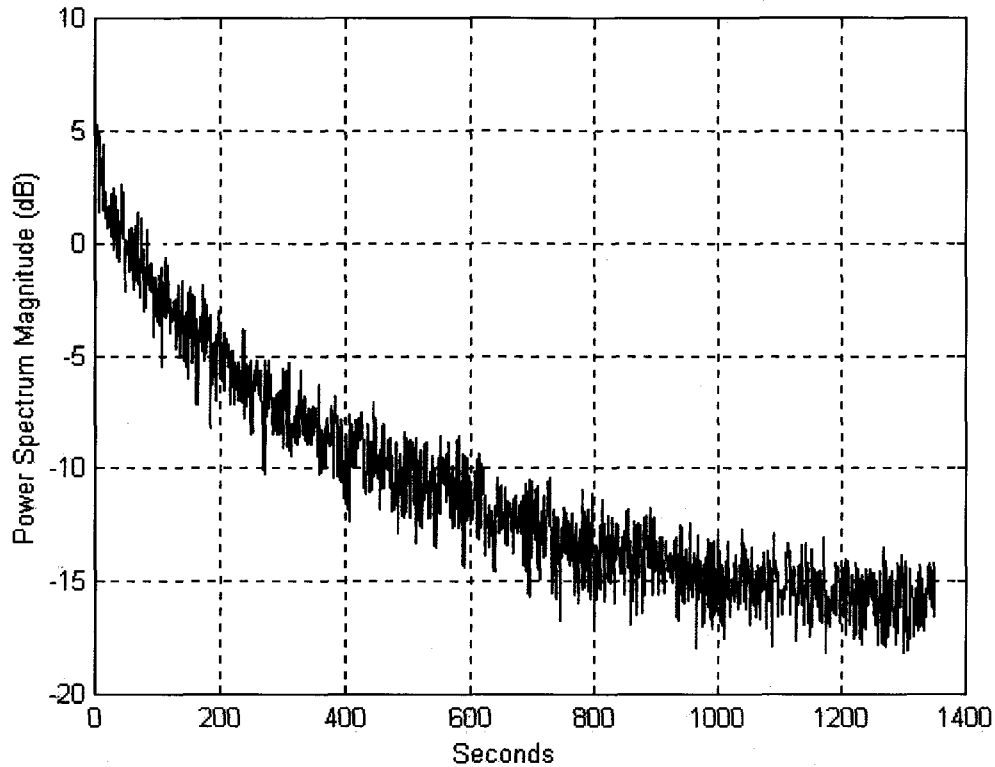


Figure 6.1 Power spectral density function of vertical windspeed using Welch's method. Data for spectral analysis was taken on August 18, 2005. Pond 40, Utikuma Region Study Area (URSA), Alberta, Canada.

The eddy covariance technique measures the flux of a constituent, mass or heat, past a point centered on the sampling volume of the instruments that are placed at a given height above the surface of interest. The validity of the measurements is dependent on the instruments having a large enough frequency response in order to measure all the turbulent eddies (large or small) contributing to the flux. This is dependent on the frequency response of the individual sensors as well as how they are positioned relative to each other along with the underlying surface being measured (Leuning and Judd, 1996). A correction factor for sensor separation placement can be defined as,

$$Q_{obs} = Q \times \frac{\int_{n_{min}}^{n_{max}} T_{wT}(n) S_{wT}(n) dn}{\int_{n_{min}}^{n_{max}} S_{wT}(n) dn} \quad (6.3)$$

where $S_{wT}(n)$ is the frequency cospectrum of the turbulence encountered, $T_{wT}(n)$ is the net system cospectral transfer function, n is the frequency of measurements (Hz) and Q_{obs} is observed flux (Moore, 1986; Blanford and Gay, 1992). The variables n_{min} and n_{max} refer to the lowest and highest frequencies, respectively, that contribute to the turbulent transport. Figure 6.2 shows the relationship of the correction factor to the horizontal windspeed and the relationship used to apply the correction factor to all flux data at URSA over the 2005 and 2006 measurement seasons.

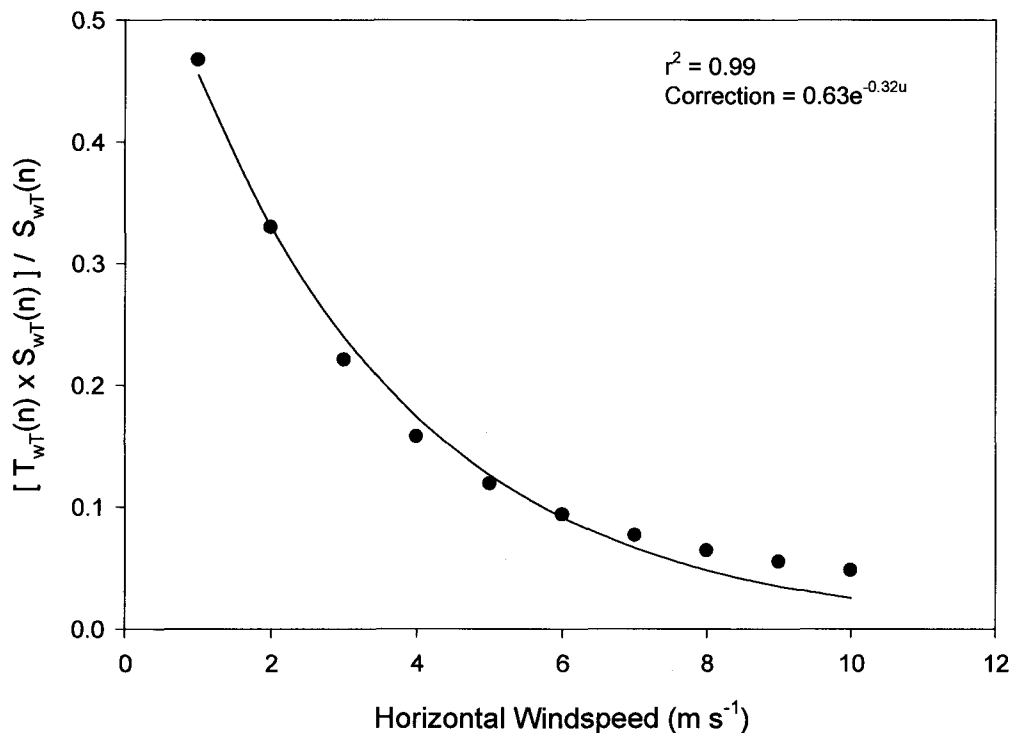


Figure 6.2 Blanford and Gay correction factor relative to horizontal windspeed for Pond 40, Utikuma Region Study Area (URSA), Alberta, Canada. Values are based on mean sensible heat flux and horizontal wind speed values from the 2005 and 2006 above canopy.

Another correction to the eddy covariance technique involves the closure of the energy balance for the study period (Barr et al., 1994; Blanken et al., 1997; Twine et al., 2000; Petrone et al., 2001). This method assumes that the fluxes of sensible and latent heat are measured correctly by the sensors and the individual magnitudes of the fluxes can be corrected using the closure ratio (CR) defined as,

$$CR = \frac{Q_H + Q_E}{Q^* - Q_G} \quad (6.4)$$

All flux results over both snow free seasons at URSA showed that prior to correction the closure ratio was 0.79.

Finally, thresholds for friction velocity (u^*) (m s^{-1}) from each site must be determined as a method of filtering out the data when stability issues arise, primarily during nighttime periods. Previous studies (Aubinet et al., 2000; Falge et al., 2001) correct nocturnal flux density measurements with values measured during windy periods using a regression between the flux density and friction velocity. It was determined that the critical friction velocity that produces ‘good’ nighttime fluxes is not universal and can range from 0.1 to 0.6 m s^{-1} (Baldocchi, 2003). For the purposes of this study, u^* was plotted against the energy balance closure for each site measured using the EC method over both seasons. The “critical” friction velocity point was determined by the point in each plot where the slope of the curve, or inflection point was altered (Petrone pers. comm.). Data were then filtered using this threshold (0.23 for wetland measurements and 0.1 for aspen canopy measurements). Figure 6.3 shows the u^* thresholds for the wetland measurements, Figure 6.4 shows the u^* thresholds for the aspen canopy measurements and Figure 6.5 shows the u^* thresholds for the within aspen canopy

measurements. Crosshairs were placed on each plot to show where the u^* threshold was inferred to be.

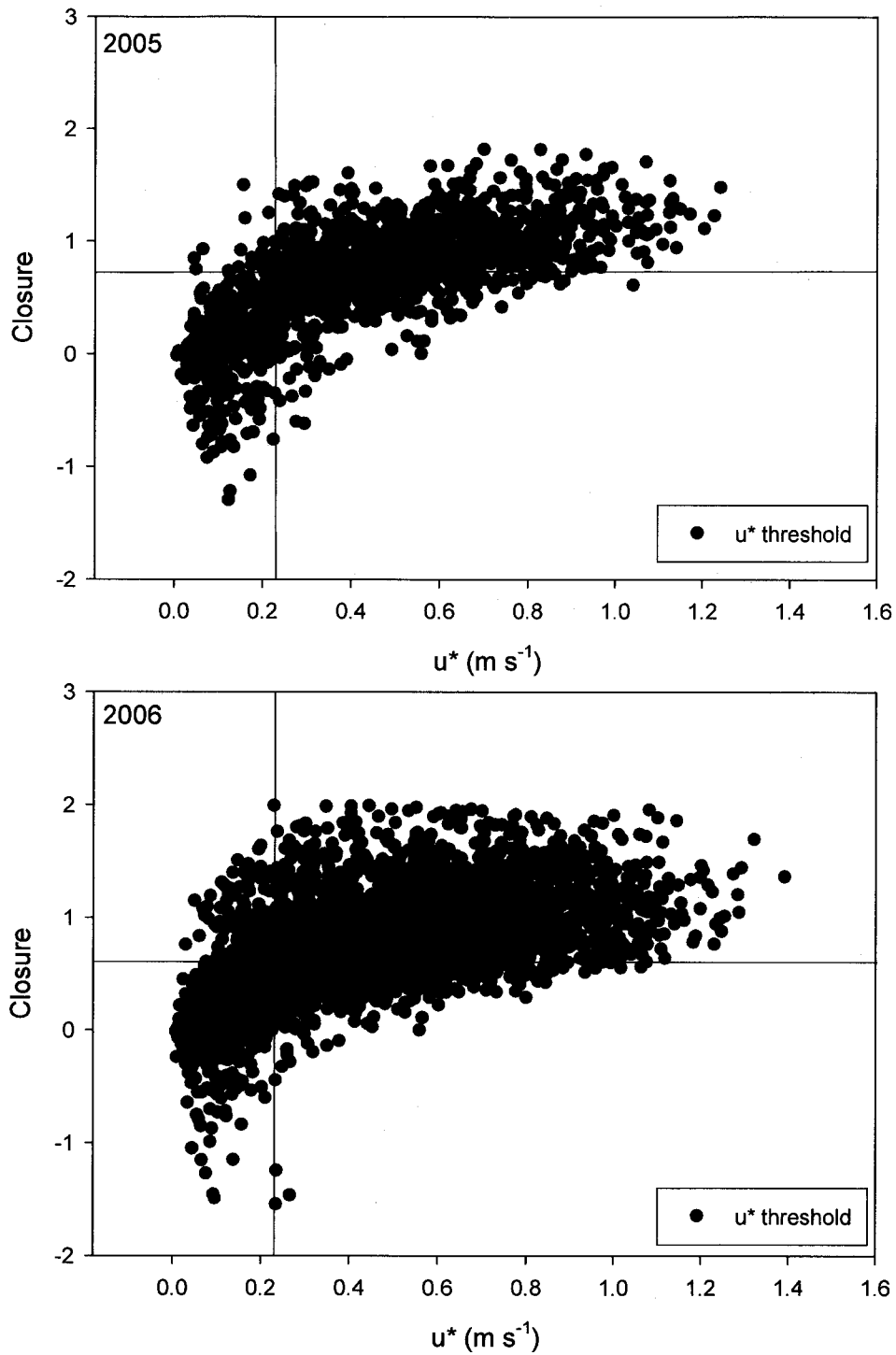


Figure 6.3 Wetland friction velocity (u^*) (m s^{-1}) thresholds plotted against energy balance closure for a) 2005 and b) 2006 for Pond 40, Utikuma Region Study Area (URSA), Alberta, Canada. Crosshairs in plots indicate the inferred threshold values. All fluxes were then filtered using the inferred thresholds (0.23 m s^{-1}).

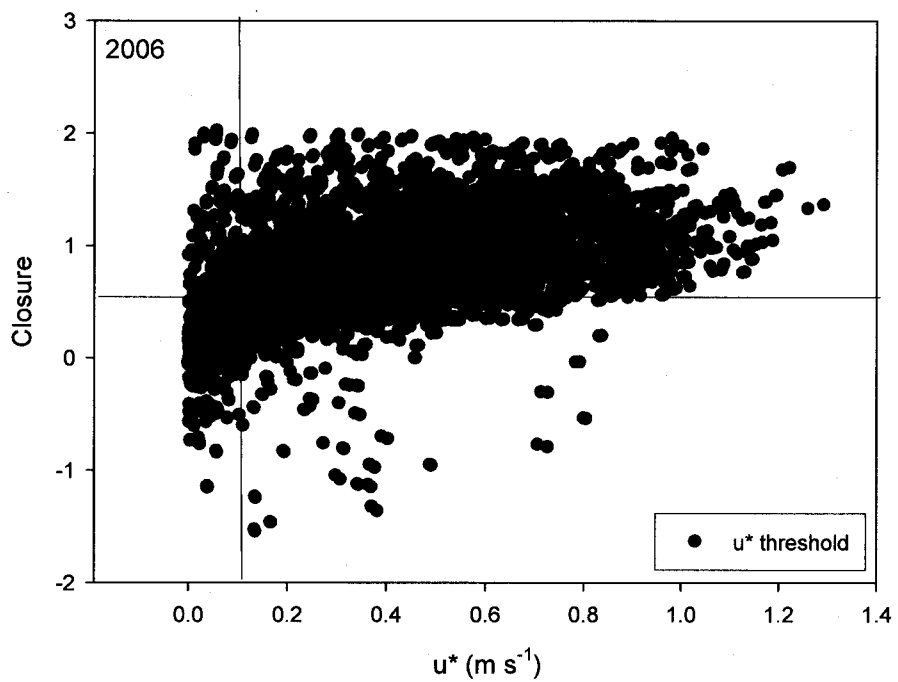
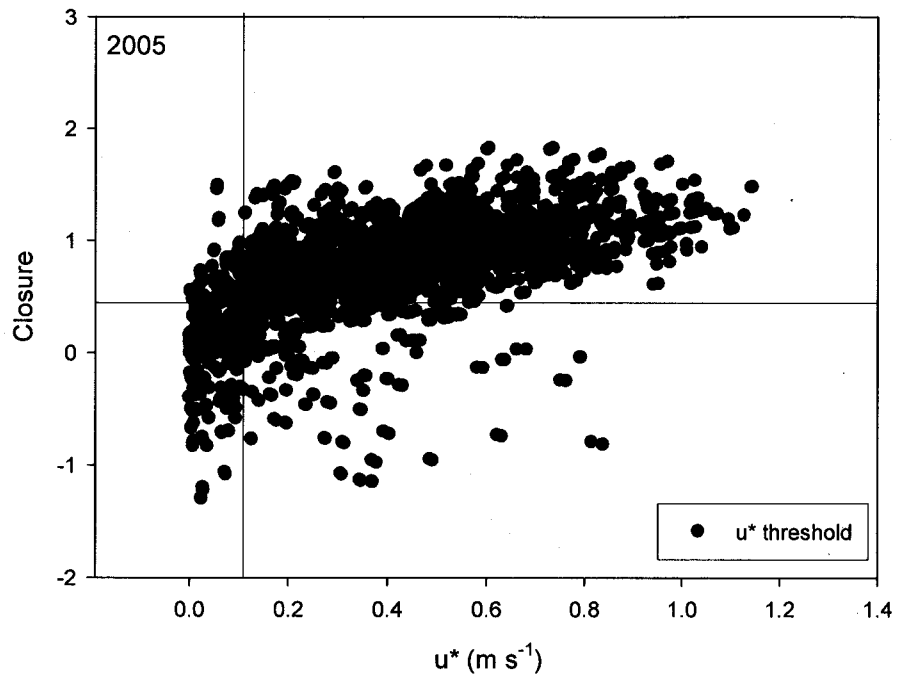


Figure 6.4 Aspen upland friction velocity (u^*) (m s^{-1}) thresholds plotted against energy balance closure for a) 2005 and b) 2006 for Pond 40, Utikuma Region Study Area (URSA), Alberta, Canada. Crosshairs in plots indicate the inferred threshold values. All fluxes were then filtered using the inferred thresholds (0.1 m s^{-1}).

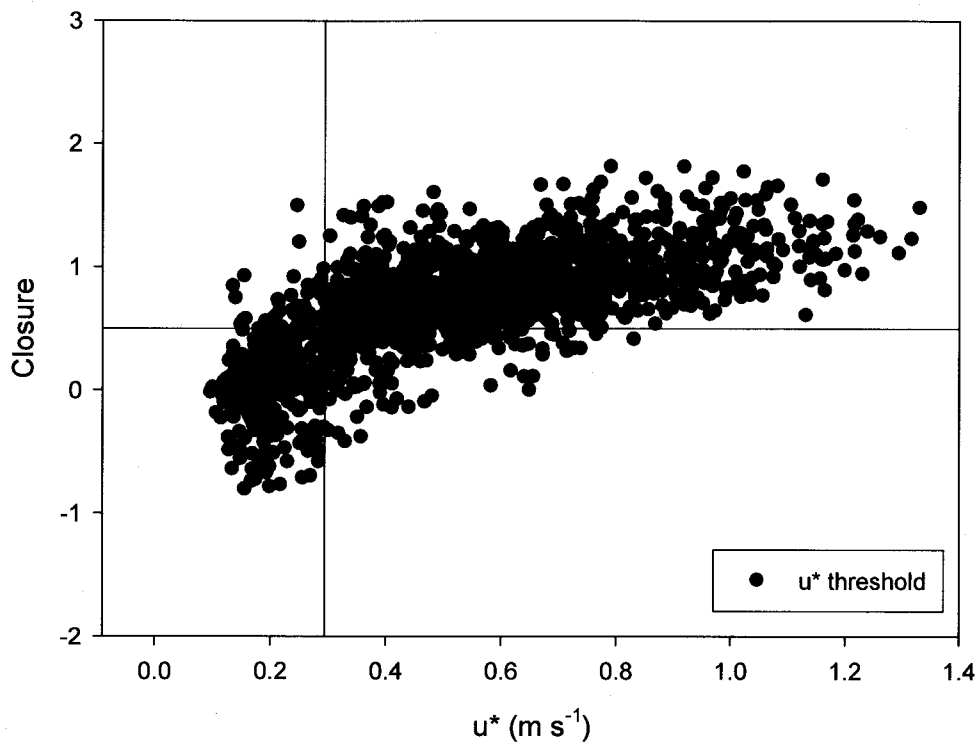


Figure 6.5 Within canopy upland friction velocity (u^*) (m s⁻¹) thresholds plotted against energy balance closure combined for the 2005 and 2006 snow-free seasons for Pond 40, Utikuma Region Study Area (URSA), Alberta, Canada. Crosshairs in plots indicate the inferred threshold values. All fluxes were then filtered using the inferred thresholds (0.29 m s⁻¹).